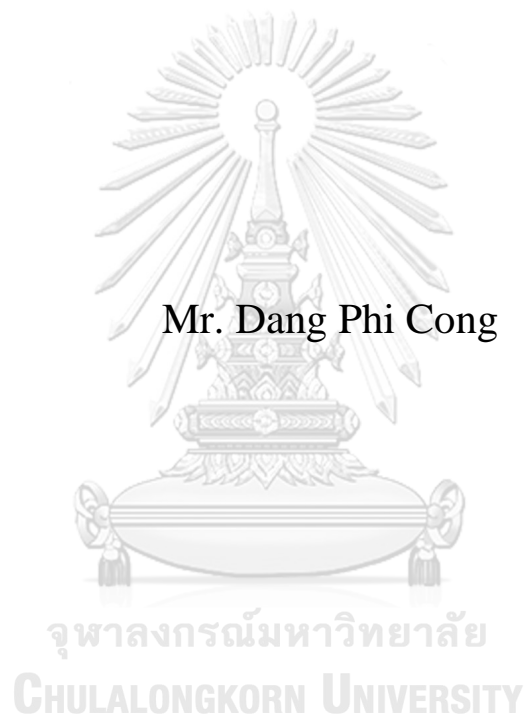


OVER-EXPRESSION OF MIR-223 INDUCES M2
MACROPHAGE THROUGH GLYCOLYSIS ALTERATION
AND ATTENUATES LIPOPOLYSACCHARIDE-INDUCED
SEPSIS MOUSE MODEL, A PROPOSAL SEPSIS CELL-
BASED THERAPY



Mr. Dang Phi Cong

A Dissertation Submitted in Partial Fulfillment of the Requirements
for the Degree of Doctor of Philosophy in Medical Microbiology
Medical Microbiology, Interdisciplinary Program
GRADUATE SCHOOL
Chulalongkorn University
Academic Year 2020
Copyright of Chulalongkorn University

การเพิ่มการแสดงผลของไมโครอาร์เอ็นเอ 223 เปลี่ยน เซลล์แมคโครเฟจ ให้มีลักษณะ M2
ผ่านทางการเปลี่ยนแปลงของกลไกไกลโคไลซิส สามารถลดการอักเสบของหนูที่ถูกกระตุ้นด้วยไล
โปโพลีแซคคาไรด์ ซึ่งอาจจะนำมาใช้ในการรักษาภาวะการติดเชื้อในกระแสโลหิต



วิทยานิพนธ์นี้เป็นส่วนหนึ่งของการศึกษาตามหลักสูตรปริญญาวิทยาศาสตรดุษฎีบัณฑิต
สาขาวิชาจุลชีววิทยาทางการแพทย์ สหสาขาวิชาจุลชีววิทยาทางการแพทย์
บัณฑิตวิทยาลัย จุฬาลงกรณ์มหาวิทยาลัย
ปีการศึกษา 2563
ลิขสิทธิ์ของจุฬาลงกรณ์มหาวิทยาลัย

Thesis Title OVER-EXPRESSION OF MIR-223 INDUCES M2
MACROPHAGE THROUGH GLYCOLYSIS
ALTERATION AND ATTENUATES
LIPOPOLYSACCHARIDE-INDUCED SEPSIS
MOUSE MODEL, A PROPOSAL SEPSIS CELL-
BASED THERAPY

By Mr. Dang Phi Cong

Field of Study Medical Microbiology

Thesis Advisor Associate Professor ASADA LEELAHAVANICHKUL,
MD., Ph.D

Accepted by the GRADUATE SCHOOL, Chulalongkorn University in
Partial Fulfillment of the Requirement for the Doctor of Philosophy

..... Dean of the GRADUATE
SCHOOL
(Associate Professor THUMNOON NHUJAK, Ph.D.)

DISSERTATION COMMITTEE

..... Chairman
(Associate Professor KANITHA PATARAKUL, MD,
Ph.D)

..... Thesis Advisor
(Associate Professor ASADA LEELAHAVANICHKUL,
MD., Ph.D)

..... Examiner
(Assistant Professor DIREKRIT CHIEWCHENGCHOL,
MD, Ph.D)

..... Examiner
(PIMPAYAO SODSAI, Ph.D.)

..... External Examiner
(Associate Professor Prapaporn Pisitkun, M.D., Ph.D)

ตั้ง พิ คง : การเพิ่มการแสดงออกของไมโครอาร์เอ็นเอ 223 เปลี่ยน เซลล์แมคโครเฟจ ให้มีลักษณะ M2 ผ่านทางการเปลี่ยนแปลงของกลไกไกลโคไลซิส สามารถลดการอักเสบของหนูที่ถูกกระตุ้นด้วยไลโปโพลีแซคคาไรด์ ซึ่งอาจจะนำมาใช้ในการรักษาภาวะการติดเชื้อในกระแสโลหิต. (OVER-EXPRESSION OF MIR-223 INDUCES M2 MACROPHAGE THROUGH GLYCOLYSIS ALTERATION AND ATTENUATES LIPOPOLYSACCHARIDE-INDUCED SEPSIS MOUSE MODEL, A PROPOSAL SEPSIS CELL-BASED THERAPY) อ.ที่ปรึกษาหลัก : อัยฎาศรี ลิฬหวนิชกุล

ภาวะติดเชื้อในกระแสเลือดเป็นผลทำให้เกิดกระบวนการอักเสบทั่วร่างกาย ซึ่งเกิดจากการเสียสมดุลของระบบภูมิคุ้มกัน โดยภาวะติดเชื้อในกระแสเลือดนี้ยังคงเป็นปัญหาสำคัญของระบบสาธารณสุขทั่วโลก เนื่องจากพบอัตราการเสียชีวิตจำนวนมากโดยเฉพาะอย่างยิ่งในผู้ป่วยภูมิคุ้มกันบกพร่อง โรคมะเร็ง รวมถึงโรคหลอดเลือดสมอง ในปัจจุบันมีการศึกษาเกี่ยวกับพยาธิสภาพของภาวะติดเชื้อในกระแสเลือดที่สัมพันธ์กับความผิดปกติของแมคโครเฟจ ซึ่งนำไปสู่การค้นพบการรักษาใหม่ๆ ที่มีประสิทธิภาพและตรงจุดมากขึ้น อย่างไรก็ตามแมคโครเฟจเป็นหนึ่งในเซลล์ภูมิคุ้มกันที่มี phenotype หลากหลายและมีหน้าที่แตกต่างกัน และหนึ่งในหน้าที่ที่สำคัญที่ยังไม่มีการศึกษาอย่างละเอียดคือ บทบาทของแมคโครเฟจในการควบคุมระบบเมตาบอลิซึมภายในร่างกาย ที่เกี่ยวข้องกับการควบคุมการอักเสบในภาวะติดเชื้อจึงยังเป็นที่น่าสนใจ ดังนั้นการศึกษานี้มีวัตถุประสงค์ที่จะศึกษารายละเอียดของแมคโครเฟจที่เกี่ยวข้องกับกระบวนการเมตาบอลิซึม โดยศึกษาทั้งประสิทธิภาพ กลไกและคุณสมบัติในการสร้างสมดุลของภูมิคุ้มกันในร่างกาย

จากการศึกษาครั้งนี้พบว่าการเหนี่ยวนำให้มีการแสดงออกของจีน miR-223 ในแมคโครเฟจสามารถกระตุ้นให้แมคโครเฟจเปลี่ยน phenotype เป็นชนิด M2 แมคโครเฟจ เป็นผลให้ยับยั้งการอักเสบผ่านกลไก Glycolytic activities ซึ่งนำไปสู่การศึกษาต่อในสัตว์ทดลองโดยการนำ miR-223 transfected macrophage ฉีดไปในหนูที่ถูกกระตุ้นด้วย LPS และพบว่าช่วยให้หนูมีอาการที่ดีขึ้น นอกจากนี้ยังพบว่ากระบวนการ Glycolysis และไมโทคอนเดรียที่มีบทบาทหลักในกระบวนการเมตาบอลิซึมและการตอบสนองของระบบภูมิคุ้มกัน โดยแมคโครเฟจมีการตอบสนองที่ลดลงหลังจากถูกกระตุ้นด้วย uncoupling agent ที่ส่งผลเปลี่ยนแปลงผนังเซลล์ของไมโทคอนเดรีย

ผลการวิจัยนี้สรุปได้ว่า กระบวนการยับยั้งการอักเสบผ่านกลไกของเมตาบอลิซึมสามารถควบคุมการตอบสนองที่มากเกินไปของระบบภูมิคุ้มกัน โดยกำเนิดในขณะที่มีการติดเชื้อทั้งการทดสอบในหลอดทดลองและสัตว์ทดลอง และสนับสนุนได้ว่าการควบคุมเซลล์ที่เกี่ยวข้องกับระบบเมตาบอลิซึมสามารถถูกพัฒนาและเป็นเป้าหมายหลักในการรักษาต่อไปในอนาคต

สาขาวิชา จุลชีววิทยาทางการแพทย์
ปีการศึกษา 2563

ลายมือชื่อนิสิต
ลายมือชื่อ อ.ที่ปรึกษาหลัก

6087767820 : MAJOR MEDICAL MICROBIOLOGY

KEYWOR sepsis infection macrophage innate immunity metabolism

D:

Dang Phi Cong : OVER-EXPRESSION OF MIR-223 INDUCES M2 MACROPHAGE THROUGH GLYCOLYSIS ALTERATION AND ATTENUATES LIPOPOLYSACCHARIDE-INDUCED SEPSIS MOUSE MODEL, A PROPOSAL SEPSIS CELL-BASED THERAPY. Advisor: Assoc. Prof. ASADA LEELAHAVANICHKUL, MD., Ph.D

Sepsis, a systemic infection with excessive inflammatory symptoms due to dysregulation of immune responses, remains the most concerned health-care problem worldwide with the mortality rate critically beyond the number of death cases in HIV, cancers or stroke. While it is well documented that pathogenesis of sepsis is intimately involved in dysregulation of macrophages, great effort has been made to discover efficacious therapy to control macrophage responses. However, macrophages are the most versatile immune cells with large spectrum of heterogeneous phenotypes and functions. Recently, collection of insights unravel the crucial role of metabolism as an orchestrator of immune regulation, intervention on macrophage metabolic pathway, therefore, is an interesting therapy to attenuate hyper-inflammation in infection. This work aims to investigate the efficacy and mechanism of recent immunomodulation strategies via targeting on metabolic pathway of macrophages. Herein, we report that the overexpression of miR-223 can induce M2 anti-inflammatory macrophage through downregulated glycolytic activities. This benefit paves the way for us to further test cell therapy in sepsis as the adoptive transfer of miR-223 transfected macrophages could ameliorate outcomes of LPS-injected mice. Beside glycolysis, mitochondria also play a crucial role as a central hub connecting metabolic activities and immune responses as demonstrating by reduction of immune response in macrophages after exposed to some mitochondrial uncoupling agents blunting mitochondrial membrane potential. Overall, our work demonstrated the anti-inflammatory effect of metabolic therapy for controlling excessive responses of innate immunity during infection both *in vitro* and *in vivo*, suggesting that cellular metabolism could be a promising target to develop effective strategy for better therapeutic treatment in sepsis.

Field of Study: Medical Microbiology

Student's Signature

Academic 2020

.....
Advisor's Signature

Year:

.....

ACKNOWLEDGEMENTS

“Everything will be okay.”

This work put a milestone in my life with great sense of gratitude to all occurring to me. Initiating, challenging, and accomplishing during the COVID 19 pandemic, this work stood as evidence witnessing my process of maturation, in which I learned to recognize and handle my negative feeling. After all, everything will be okay.

First of all, my sincerest gratefulness went to the inspiration and wisdom of my advisor - Ajarn Asada Leelahavanichkul. It is my great honor and merit to be a student under his guidance. His amazing intellect, formidable enthusiasm, and kind support have instilled my motivation in this tough academic life. Central to his encouragement is his belief in me, a student without any laboratory skills or knowledge from the very beginning. I have learned from him that our limitation can be unlocked if we really want to improve. Moreover, I also sincerely thank Ajarn Patcharee Ritprajak for her expertise and kindness. Her great patience to instruct me the experiences in meticulous techniques, goodness in working quality, and principles in research field helped me to gain achievement today.

This work is dedicated to my beloved family. Mom, I understand all of your wishes are for my happiness without any demand. As Dad passed away years ago, your love was the strong foundation for my effort through up and down, and sharing with you this achievement was my wish throughout the last 5 years. I also thank my sisters and brothers who are always there, listening to me whenever I am in need. I love you.

In addition, my great gratitude is for financial support by “the 100th Anniversary Chulalongkorn University Fund for Doctoral Scholarship” and “the 90th Anniversary Chulalongkorn University Fund (Ratchadaphiseksomphot Endowment Fund)”, which greatly facilitated my Ph.D. program in the Kingdom of Thailand.

Last but not least, I would like to express my deep gratitude for all of the mice I used in my experiments. I could not have completed this work without their meaningful sacrifice for science, and I strongly appreciate their lives.

Dang Phi Cong

TABLE OF CONTENTS

	Page
ABSTRACT (THAI)	iii
ABSTRACT (ENGLISH).....	iv
ACKNOWLEDGEMENTS.....	v
TABLE OF CONTENTS.....	vi
LIST OF TABLES	viii
LIST OF FIGURES	ix
SECTION I.....	1
Relationship amongst manuscripts	1
Background and rationales	3
Objectives	4
Conceptual framework.....	4
Benefits of study	6
SECTION II.....	7
Part I: Over-expression of miR-223 induces M2 macrophage through glycolysis alteration and attenuates LPS-induced sepsis mouse model, the cell-based therapy in sepsis	7
Part II: BAM15, a mitochondrial uncoupling agent, attenuates inflammation in LPS injection mouse model, an adjunctive anti-inflammation on macrophages and hepatocytes	33
Part III: Non-Thermal Atmospheric Pressure Argon-Sourced Plasma Flux Promotes Wound Healing of Burn Wounds and Burn Wounds with Infection in Mice through the Anti-Inflammatory Macrophages.....	60
SECTION III.....	85
Conclusion	85
Limitations.....	86
Further studies	86
REFERENCES	88

VITA.....101



จุฬาลงกรณ์มหาวิทยาลัย
CHULALONGKORN UNIVERSITY

LIST OF TABLES

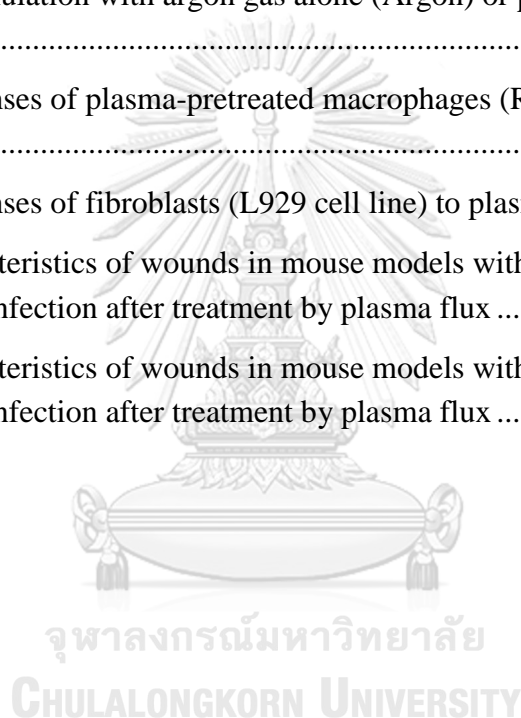
	Page
Table 1. List of primers for macrophage polarization and glycolysis pathway.....	15
Table 2. List of the primers for mitochondrial uncoupling protein macrophage polarization.	41
Table 3. List of the primers for macrophage polarization.	70



LIST OF FIGURES

	Page
Figure 1: Over-expression of miR-223 attenuates inflammation in macrophage through glycolysis reduction via targeting HIF-1 α	4
Figure 2: Cellular energy reduction via BAM15 mitochondrial uncoupling attenuate inflammation in macrophages and hepatocytes	5
Figure 3: Non-thermal atmospheric pressure Argon-sourced plasma flux attenuate inflammation in macrophages.....	5
Figure 4. Transfection efficiency of cell culture.....	13
Figure 5. Macrophage anti-inflammatory property after the over-expression of miR-223 is higher than miR-146a.....	18
Figure 6. Over-expression of miR-223 maintains IL-4 induced anti-inflammatory characteristics of macrophages after LPS-induction better than miR-146a over-expression.	19
Figure 7. Over-expression of miR-223 in LPS-activated macrophages reduces glycolysis activity and improves mitochondrial function as determined by extracellular flux analysis.	21
Figure 8. Over-expression of miR-223 in LPS-activated macrophages reduces HIF-1 α expression, while miR-223 over-expression in IL-4-activated macrophages decreases expression of PDK-1 and PFK.	23
Figure 9. Macrophages are demonstrated in kidney and liver at 2 h and 6 h after administration.	25
Figure 10. Administration of miR-223 over-expressed macrophages attenuates sepsis in LPS injection mouse model.	26
Figure 11. Administration of miR-223 over-expressed macrophages attenuates sepsis-induced lung injury in LPS injection mouse model.....	27
Figure 12. The transcriptome analysis in macrophages (RAW264.7) and UCP gene expression of in LPS-stimulated RAW264.7 and hepatocytes (Hepa 1-6).....	44
Figure 13. The in vitro optimization of BAM15 on macrophages (RAW264.7).	46
Figure 14. The anti-inflammatory effect of BAM15 in macrophages (RAW264.7). ..	47
Figure 15. The cell energy analysis of LPS-stimulated macrophages (RAW264.7) with BAM15 pre-treatment.....	48

Figure 16. The anti-inflammatory effect of BAM15 in hepatocytes (Hepa 1-6).....	50
Figure 17. The cell energy analysis of LPS-stimulated hepatocytes (Hepa 1-6) with BAM15 pre-treatment.....	51
Figure 18. BAM15 ameliorated the severity of LPS-administered mice.....	53
Figure 19. The increased abundance of activated AMPK in liver and flow cytometry analysis of LPS-administered mice with BAM15 pretreatment.	54
Figure 20. Schematic diagram of non-thermal atmospheric pressure plasma.	67
Figure 21. Characteristics of macrophages (RAW264.7 cells) without stimulation (Non) or after stimulation with argon gas alone (Argon) or plasma flux for 30 s (Plasma 30 s).....	73
Figure 22. Responses of plasma-pretreated macrophages (RAW264.7 cells) to plasma treatment	75
Figure 23. Responses of fibroblasts (L929 cell line) to plasma treatment.....	76
Figure 24. Characteristics of wounds in mouse models with burn injury with or without bacterial infection after treatment by plasma flux	79
Figure 25. Characteristics of wounds in mouse models with burn injury with or without bacterial infection after treatment by plasma flux	80



SECTION I

Relationship amongst manuscripts

Sepsis is characterized by excessively inflammatory symptoms due to systemic infection, leading to dilated vessel-induced hypotension then exhaustion of multiple organs and systems. In spite of the advance of modern medical treatment, sepsis perpetuates as a critically life-threatening cause in hospitals worldwide, especially with immunocompromised patient, which leads to high rate of mortality and huge burden of treatment cost. Currently, emerging research indicates a role of cellular metabolism in orchestrating immune response, especially macrophages response. Given that cellular metabolism includes two main pathways: oxidative phosphorylation and glycolysis, different phenotypes of macrophage require different characteristic of metabolic pathway. Our works aim to manipulate macrophages via targeting metabolic pathway to attenuate excessive immune response during infection. Here, we proposed 3 examples of macrophage manipulation that might be beneficial for the immune responses against infection through the induction of anti-inflammatory macrophages, including miR-223 transfection, BAM-15 administration and plasma flux stimulation.

Part I: *Over-expression of miR-223 induces M2 macrophage through glycolysis alteration and attenuates LPS-induced sepsis mouse model, a proposed cell-based therapy in sepsis*

As cellular metabolism plays an orchestrating role in immune responses as demonstrated by enhanced glycolysis in inflammatory M1 macrophage and intact OXPHOS in anti-inflammatory M2 macrophage, the regulation of macrophage

immune responses by glycolysis reduction via miR-223 overexpression could attenuate excessive immune response in LPS-injected mouse model

Part II: *BAM15, a mitochondrial uncoupling agent, attenuates inflammation in LPS injection mouse model, an adjunctive anti-inflammation on macrophages and hepatocytes*

Beside glycolysis as a well-known metabolic pathway associated with inflammation, mitochondrion also serves as a central hub with provision of cellular energy and metabolic mediators for inflammatory responses. This work aims to elucidate the role in another metabolic pathway, oxidative phosphorylation of mitochondrion, in immune regulation. Mitochondrial inhibition by BAM15, therefore, could attenuate inflammatory responses in macrophages as well as hepatocytes.

Part III: *Non-thermal atmospheric pressure Argon-sourced plasma flux promotes wound healing of burn wound in mice, regardless of bacterial infection, through anti-inflammatory macrophages*

Because i) the uncontrolled local infection results in systemic inflammation and sepsis and ii) macrophage is not only involved in the pathogenesis of systemic infection but also the microbial control at the site of infection, the imbalance of macrophage response also plays a critical role in local infection. While therapy treatment on local inflammatory site is still limited, reactive oxygen species/ reactive nitrogen species (ROS/RNS) from Argon-source non-thermal plasma flux might accelerate wound healing through macrophage manipulation. This work aim to establish a novel therapy to treat local infection through macrophage manipulation.

Three current manuscripts meet the demand of Doctor of Philosophy in Medical Microbiology Interdisciplinary Program, Graduate School, Chulalongkorn University.

Background and rationales

Part I: The immunometabolic and microRNA versus macrophage plasticity is a current topic on the researches of cancer but very less in sepsis. Here, we explored an impact of miR upon the anti-inflammatory characteristics of macrophages through the reduction of glycolysis possibly through the inhibition of HIF-1 α expression. In addition, miR-223 over-expressed macrophages reduced pro-inflammatory effect of LPS stimulation and attenuates LPS mouse model. Hence, these cells and the pattern of the study to have these cells for a discovery of a new candidate of sepsis treatment might be beneficial to the readers.

Part II: RNA sequencing analysis from LPS-stimulated macrophages demonstrated the down-regulation of several metabolism-related genes, especially the mitochondrial uncoupling proteins. Then, supplement of the uncoupling proteins might attenuate sepsis severity. Although the uncoupling agents have been demonstrated an anti-inflammatory effect in several models, the effect on sepsis has never been tested. Indeed, a proof of concept using “cell energy intervention” to manipulate macrophage functions by BAM15, a mitochondrial uncoupling agent, was demonstrated which might be a new strategic treatment for sepsis.

Part III: Although there are several publications on the therapeutic effect of plasma flux on wound healing, data of an impact of plasma flux upon macrophages and infected burn wound is still less. Here, we demonstrated that plasma flux improved burn wound, especially the infected wounds, through the activation of anti-

inflammatory macrophages by reactive oxygen species interference and NF- κ B downstream signaling.

Objectives

Part I: To investigate whether overexpression of miR-223 can attenuate inflammation in macrophages via glycolysis reduction

Part II: To investigate whether introduction of mitochondrial uncoupling BAM15 can alleviate inflammation in macrophages via OXPHOS inhibition

Part III: To investigate whether administration of ROS/RNS-enrich plasma flux can mitigate inflammation in macrophages via redox regulation.

Conceptual framework

Part I:

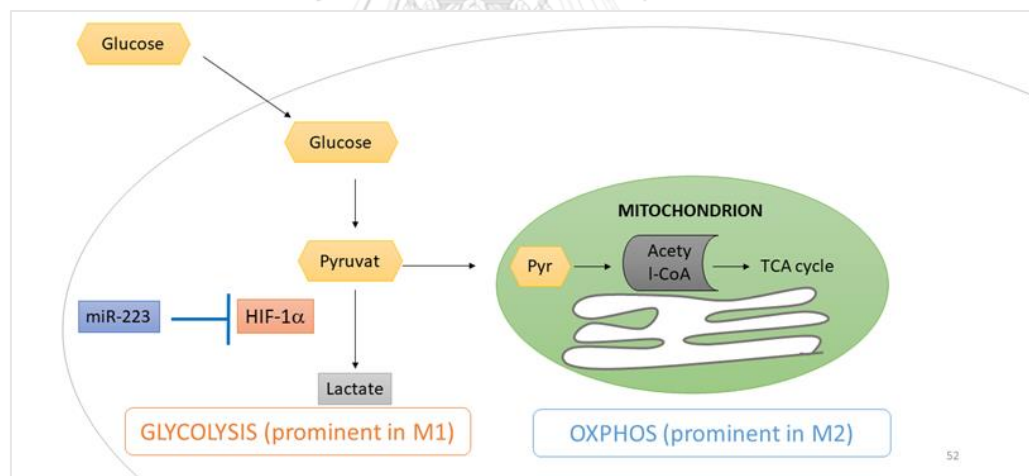


Figure 1: Over-expression of miR-223 attenuates inflammation in macrophage through glycolysis reduction via targeting HIF-1 α .

Part II:

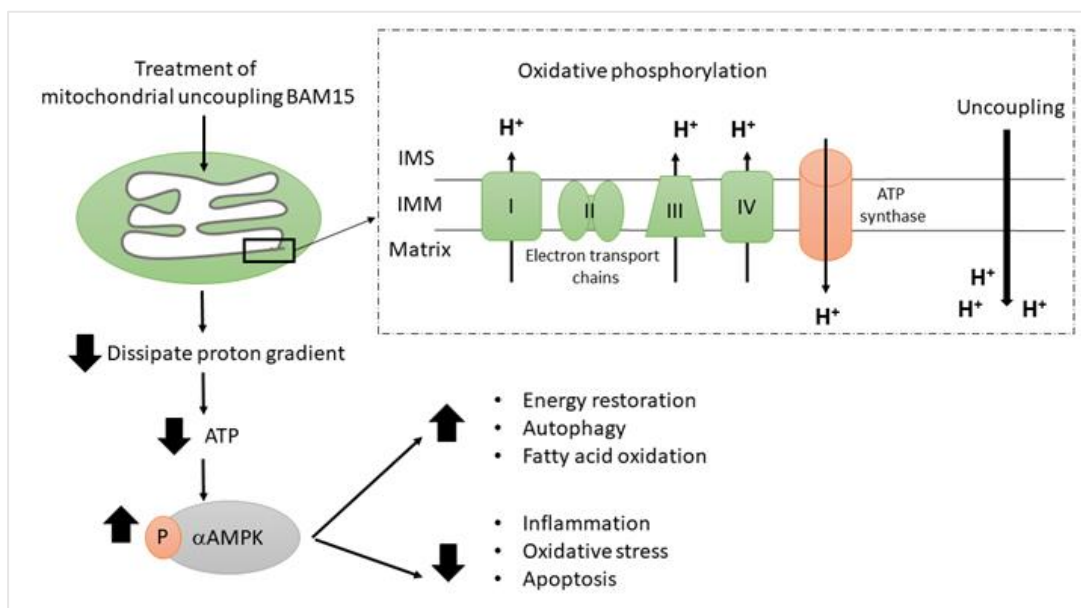


Figure 2: Cellular energy reduction via BAM15 mitochondrial uncoupling attenuate inflammation in macrophages and hepatocytes

IMS: intermembrane space, IMM: inter mitochondrial membrane.

Part III:

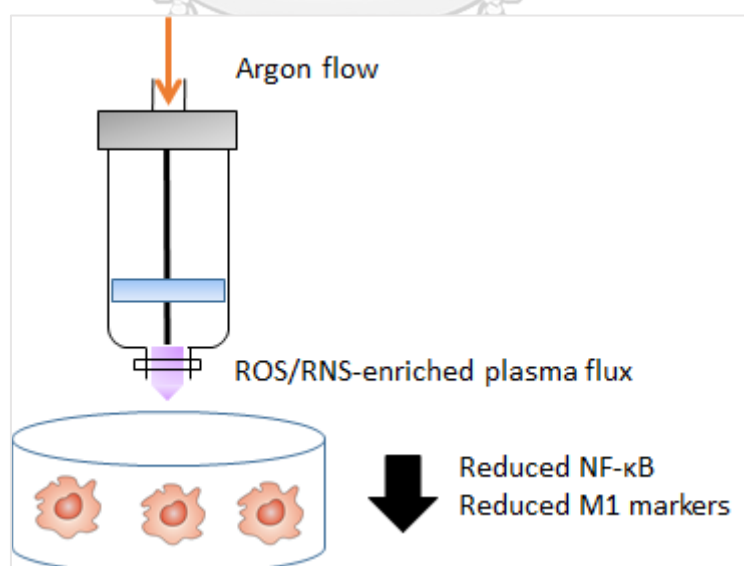


Figure 3: Non-thermal atmospheric pressure Argon-sourced plasma flux attenuate inflammation in macrophages

Benefits of study

Part I: This study could provide insights about role of miR-223 in enhancing anti-inflammatory macrophages via cellular metabolism modulations. Given that miR-223 is capable of controlling immune responses at the level of macrophage activation [1], adoptive transfer of miR-223-engineered cells into LPS-induced sepsis mouse model is expected to ameliorate outcome of sepsis. This understanding could pave the way for developing the more promising treatment of sepsis.

Part II: BAM15, a synthetic mitochondrial uncoupling agent, was identified as a promising candidate to apply in treatment. Unlike classical reagent (eg. FCCP), BAM15 exerts more specific functions on mitochondrial membrane without depolarization of cellular membrane [2]. Introduction of BAM15 into medical application is well mentioned in several models such as ischemic kidney injury [2], diet-induced obesity mouse model [3]. However, understanding of BAM15 in immune regulation is limited. This study firstly investigates the protective effect of BAM15 in sepsis mouse model with an aim to shed light on the role of BAM15 in reducing inflammation in macrophages and hepatocytes by sepsis mouse model.

Part III: Cold plasma (or non-thermal plasma) medicine is a novel method of treatment modality that taking an advantage of the energy from the gas ionization. Indeed, plasma application is well studied in a wide range of fields including dental hygiene, hematology, coagulation, microbial eradication, wound healing, and oncology therapy [4]. However, data on biological effect of plasma on immune regulation in burn wound is limited. This study provides a more insight about anti-inflammatory effect of plasma in macrophages in an augmentation of wound healing processes in burn mouse models.

SECTION II

Part I: Over-expression of miR-223 induces M2 macrophage through glycolysis alteration and attenuates LPS-induced sepsis mouse model, the cell-based therapy in sepsis

Published in PLOS ONE, 2020 Jul 13;15(7):e0236038. Doi: 10.1371/journal.pone.0236038.

Cong Phi Dang^{1,2}, Asada Leelahavanichkul^{2,3#}

¹Medical Microbiology, Interdisciplinary and International Program, Graduate School, Chulalongkorn University, Bangkok, Thailand.

²Department of Microbiology, Faculty of Medicine, Chulalongkorn University, Bangkok, Thailand

³Translational Research in Inflammation and Immunology Research Unit, Department of Microbiology, Chulalongkorn University, Bangkok, Thailand

Running Head :miR-223 over-expressed macrophages attenuated sepsis

Keywords: Sepsis, LPS model, M2 polarization, Micro-RNA

#Corresponding author: Asada Leelahavanichkul. Immunology Unit, Department of Microbiology, Chulalongkorn University, Bangkok 10330, Thailand Tel: +66-2-256-

4251, Fax: +66-2-252-6920 E-mail: aleelahavanit@gmail.com

Abstract (247 words)

The attenuation of hyper-inflammation in sepsis with the administration of anti-inflammatory macrophages is an interesting adjuvant therapy for sepsis. Because the induction of anti-inflammatory macrophages by microRNA (miR), a regulator of mRNA, has been mentioned, the exploration on miR-induced anti-inflammatory macrophages was performed.

The over-expression of miR-223 and miR-146a in RAW264.7 induced M2 macrophage-polarization (anti-inflammatory macrophages) as evaluated by the enhanced expression of *Arginase-1* and *Fizz*. However, miR-223 over-expressed cells demonstrated the more potent anti-inflammatory property against LPS stimulation as lesser *iNOS* expression, lower supernatant IL-6 and higher supernatant IL-10 compared with miR-146a over-expressed cells. Interestingly, LPS stimulation in miR-223 over-expressed cells, compared with LPS-stimulated control cells, demonstrated lower activity of glycolysis pathway and higher mitochondrial respiration, as evaluated by the extracellular flux analysis, and also down-regulated *HIF-1 α* , an important enzyme of glycolysis pathway. In addition, the administration of miR-223 over-expressed macrophages with IL-4 pre-conditioning, but not IL-4 stimulated control cells, attenuated sepsis severity in LPS injected mice as evaluated by serum creatinine, liver enzymes, lung histology and serum cytokines.

In conclusion, miR-223 interfered with the glycolysis pathway through the down-regulation of *HIF-1 α* , resulting in the anti-inflammatory status. The over-expression of miR-223 in macrophages prevented the conversion into M1 macrophage polarization after LPS stimulation. The administration of miR-223 over-expressed macrophages, with IL-4 preconditioning, attenuated sepsis severity in LPS model. Hence, a proof of concept in the induction of anti-inflammatory macrophages through the cell-energy interference for sepsis treatment was proposed as a basis of cell-based therapy in sepsis.

Introduction

Sepsis, a syndrome of organ dysfunction due to the dys-regulation of host responses to systemic infection, is a major cause of death in patients with clinically ill

conditions and has been recognized as an important world-wide healthcare problem [5]. The imbalance of pro- and anti-inflammatory immune-responses is one of the important causes of death in sepsis and the anti-inflammation is an interesting adjunctive treatment of sepsis, especially during the pro-inflammatory state [6-8]. Indeed, compelling evidences indicate that robust innate immune responses, including macrophages, mainly accounts for sepsis pathophysiology [9].

Macrophages, heterogeneous immune cells with pleiotropic functions [10], are fundamentally divided into classically M1 and alternative M2 polarization with pro- and anti-inflammatory property, respectively [11]. Interestingly, macrophages in sepsis hyper-inflammation are predominant in M1 polarization and are responsible for the production of inflammatory mediators [12]. As such, the induction or the administration of anti-inflammatory M2 macrophages during sepsis hyper-inflammation is mentioned [13, 14]. In addition, microRNA (miR), a small non-coding single-strand RNA [15], regulates post-transcriptional messenger RNA (mRNA) and inhibits protein-translation [16]. Because one miR is able to silence multiple targets that are responsible for numerous biological processes [17], the manipulation of macrophage-polarization with miR is interesting [18]. Accordingly, miR-223 is essential for M2 polarization [19] and the down-regulation of miR-223 in patients with severe sepsis possibly induces predominant M1 polarization [20]. In parallel, miR-146a is well documented as an anti-inflammatory miR, preferentially augments M2 polarization [21], that attenuates sepsis-induced cardiac injury in a mouse model [22].

Interestingly, cellular metabolism is essential for immune cells [23], including macrophages [24], as the metabolic signatures of M1 and M2 macrophage-

polarization are glycolysis and mitochondrial respiration, respectively [25]. Indeed, the induction of macrophage plasticity through the interference of cell energy and cell metabolism by miRs is mentioned as miR-33 augmented glycolysis and induced M1 macrophage-polarization in an atherosclerosis mouse model [26]. Although the impact of miRs upon malignant-cell metabolism is well-known [27], the information about influence of immune cells metabolism upon sepsis is still very little. Moreover, the anti-inflammatory potency of several miRs might be different, for example, miR-223 mediated anti-inflammation through HIF-1 α , PPAR γ and STAT3 [19, 28-30], while miR-146a inhibits IRAK1 and TRAF6 [31]. Here, the candidate miRs were over-expressed in macrophages and examined several cell characteristics, including cell energy, before using as a cell-based therapy in a sepsis LPS injection mouse model.

Materials and methods

Animal and animal model

Animal care and use protocol are based upon the National Institutes of Health (NIH), USA. The protocol was approved by the Institutional Animal Care and Use Committee of the Faculty of Medicine, Chulalongkorn University, Bangkok, Thailand. Male 8-wk-old mice on C57BL/6 background were purchased from Nomura Siam International (Pathumwan, Bangkok, Thailand) Mice were at rest for 1 wk in the animal facility before use and endotoxin (LPS) injection model was performed following previous publications [32-34]. Briefly, 4 mg/kg of endotoxin (LPS) from *Escherichia coli* 026:B6 (Sigma-Aldrich, St. Louis, USA) was administered intraperitoneum (ip) at 1 h after the tail vein injection by miR over-expressed RAW 264.7 preconditioning with IL-4 (detail later) at 1×10^6 CFU diluted in 0.3 ml phosphate

buffer solution (PBS) as previously described [35-38]. Blood collection through tail vein was performed at 3 days before-LPS-injection (0 h) and at 2 and 4 h post-LPS. Mice were sacrificed at 6 h post LPS-injection by cardiac puncture under isoflurane anesthesia. Of note, some mice were sacrificed at these time-points for organ collection. Serum creatinine (Cr) by QuantiChrom Creatinine-Assay (DICT-500, BioAssay, Hayward, CA, USA), serum aspartate transaminase (AST) by EnzyChrom AST assay (EASTR-100, BioAssay), serum alanine transaminase (ALT) by EnzyChrom ALT assay (EALT-100, BioAssay) and serum cytokines by ELISA assays (ReproTech, Oldwick, NJ, USA) were analysed. In addition, blood leukocyte determination was performed as previous published [39]. In short, blood was mixed with 3% acetic acid, a hemolytic solution, with a ratio of blood: acetic acid at 6:100 by volume before counting with a hemocytometer. In parallel, Wright-stained blood smear was examined for the percentage of polymorphonuclear cells (PMN) and lymphocyte. The total number of these cells was calculated by the total count from hemocytometer multiplied by the percentage of cells from the Wright-stained slide.

Cell tracker and histological analysis

Macrophages (RAW 264.7) at 3×10^6 cells per plate were incubated with cell-labeling Carboxy-fluorescein diacetate succinimidyl ester (CFDA-SE; Sigma-Aldrich), at 25 μ M in PBS, for 30 minutes at 37 °C according to the manufacturer's instructions. Then the buffer was gently aspirated and further incubated with warm media for 15 minutes before collecting the cells. Passively-diffused CFDA-SE in cytoplasm is cleaved by intracellular-esterase to form carboxyfluorescein succinimidyl ester with the fluorescent activity. CFDA-SE - labeled cells are confirmed under fluorescent microscope before the intravenous (iv) injection with

1×10^6 cells/ mouse. Then, mice were sacrificed with cardiac puncture under isoflurane anesthesia with organ collection in the optimal cutting temperature compound (OCT) at -80°C before cutting into $4 \mu\text{m}$ -thick slides and DAPI (4', 6-diamidino-2-phenylindole) (Thermo fisher Scientific) was incubated for 10 min at room temperature for nuclear counter stain. Each slide was observed with fluorescein microscope at 10 random 200X fields for the enumeration of fluorescent-positive tracked-cells per field as the representatives for cell burden in organs.

For organ injury analysis, the organs were fixed in 10% formalin before Hematoxylin and Eosin (H&E) staining process and the semi-quantitative analysis of organ injury. As such, lung injury was analyzed in accordance with previous publications [40, 41] through the evaluation of the area of the injury as determined by alveolar hemorrhage, alveolar congestion, neutrophil infiltration and alveolar wall thickness. Semi-quantitative scores were given in each observed field at 200x magnifications according to the following: 0 points, no injury in the observed field; 1 point, injury up to 25%; 2 points, injury up to 50%; 3 points, injury up to 75%; 4 points, injury to the entire field. The scores from 20 fields of each slide were calculated and were presented as the representative lung injury parameter.

Micro-RNA transfection and the preparation of IL-4 preconditioning cells

Murine macrophage cell line (RAW 264.7) were cultured in DMEM supplemented with 10% heat-inactivated fetal bovine serum (FBS) and Penicillin-Streptomycin (Thermo fisher Scientific, Waltham, MA, USA) in 5% carbon dioxide (CO_2) at 37°C . Then the microRNA (miR) was transfected into 1.5×10^6 / well of macrophages in 24-well plate following a previous protocol [42]. Briefly, the transfection mixture consisted of 5 pmol of miR (miR146a, miR223 or mimic control)

(Ambion, Austin, TX, USA) and 1.5 μ l Lipofectamin RNAiMax reagent (Invitrogen, Carlsbad, CA, USA) in Opti-MEM (Gibco, Thermo Fisher Scientific) for one reaction was incubated with cells for 2 days before the verification of transfection-efficiency by quantitative polymerase chain reaction (qPCR) as demonstrated in fig 4. In addition, M1 or M2 polarization was activated by LPS (10 ng/ml) or IL-4 (20 ng/ml), respectively, before cell collection and supernatant cytokines were measured by ELISA (Reprotech). For preparation of adoptive transfer, miR over-expressed RAW 264.7 were treated with IL-4 (20 ng/ml) to activate M2 macrophage polarization, washed 2 times by PBS and intravenously administered into mice at 1 hour prior to LPS intra-peritoneal injection (4 mg/kg).

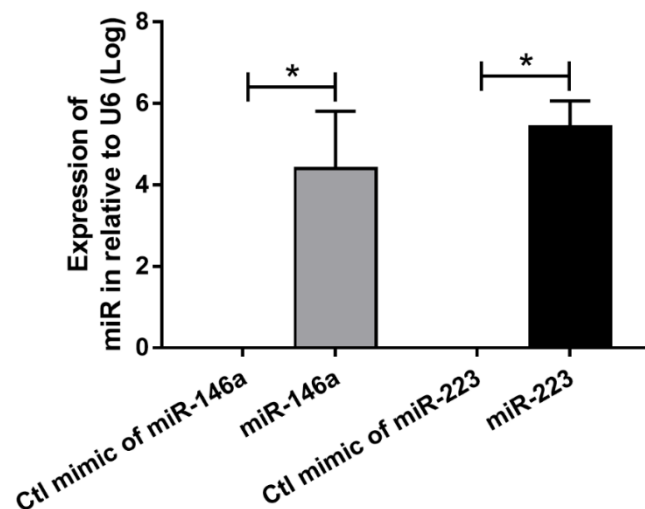


Figure 4. Transfection efficiency of cell culture.

Transfection efficiency of RAW264.7 cell with miR-146a and miR-223 was determined by quantitative polymerase chain reaction using Taqman probe in relative to the expression of housekeeping gene U6.

The determination of macrophage polarization by quantitative polymerase chain reaction (qPCR)

The qPCR was performed following previous publications [33]. Briefly, total RNA was prepared from the cell culture by Trizol (Thermo fisher Scientific) and quantified by Nano drop ND-1000 (Thermo fisher scientific). The ratio of absorbance at optical density (OD) 260 divided by OD 280 more than 1.8 indicated the adequate purity for further testing. After that, RNA was converted into cDNA by Reverse Transcription System and quantitative polymerase chain reaction (qPCR) was performed using SYBR Green master mix (Applied biosystem, Foster city, CA, USA), cDNA template and target primers based on $\Delta\Delta\text{CT}$ method with β -actin as a housekeeping gene. Primers of miR-146a, miR-223 were hsa-miR-146a-5p (Ambion, Cat.4464066, ID.MC10722); mmu-miR-223, ID (Ambion, Cat.4464066, ID.MC14755). In addition, the nucleotide sequences of primers for the analysis of M1 macrophage polarization (*iNOS*, *TNF- α* and *IL-1 β*), M2 macrophage polarization (*Arginase-1*, *IL-10* and *TGF- β*) and glycolysis pathway (Integrated DNA Technologies, Coralville, IA, USA) are demonstrated in table 1.

Primers

Macrophage polarization

β -actin	Forward	5'-CGGTTCCGATGCCCTGAGGCTCTT-3'
	Reward	5'-CGTCACACTTCATGATGGAATTGA-3'
Inducible nitric oxide synthase (<i>iNOS</i>)	Forward	5'-CCCTTCCGAAGTTTCTGGCAGCAGC-3'
	Reward	5'-GGCTGTCAGAGCCTCGTGGCTTTG-3'
Arginase 1 (<i>Arg-1</i>)	Forward	5'-CAGAAGAATG GAAGAGTCAG-3'
	Reward	5'-CAGATATGCA GGGG GTCACC-3'
Tumor necrosis factor α (<i>TNF-α</i>)	Forward	5'-CCTCACACTCAGATCATCTTCTC-3'
	Reward	5'-AGATCCATGCCG TTGGCCAG-3'
Interleukin-1 β (<i>IL-1β</i>)	Forward	5'-GAAATGCCACCTTTTGACAGTG-3'
	Reward	5'-TGGATGCTCTCATCAGGACAG-3'
Interleukin-10 (<i>IL-10</i>)	Forward	5'-GCTCTTACTGACTGGCATGAG-3'
	Reward	5'-CGCAGCTCTAGGAGCATGTG-3'
Transforming growth factor- β (<i>TGF-β</i>)	Forward	5'-CAGAGCTGCGCTTGCAGAG-3'
	Reward	5'-GTCAGCAGCCGGTTACCAAG-3'

Glycolysis pathway		
Solute carrier family 2, facilitated glucose transporter member 10 (<i>SLC2a10</i>)	Forward	5'-CAGTTCGGCTATAACACTGGTG-3'
	Reward	5'-GCCCCCGACAGAGAAGATG -3'
Lactate dehydrogenase A (<i>ldhA</i>)	Forward	5'-CATTGTCAAGTACAGTCCACACT -3'
	Reward	5'-TTCCAATTACTCGGTTTTTGGGA -3'
Phosphofruktokinase (<i>PFK</i>)	Forward	5'-GGAGGCGAGAACATCAAGCC -3'
	Reward	5'-CGGCCTTCCCTCGTAGTGA -3'
Pyruvate dehydrogenase kinase-1 (<i>PDK1</i>)	Forward	5'-GGACTTCGGGTCAGTGAATGC -3'
	Reward	5'-TCCTGAGAAGATTGTCGGGGA -3'
Hypoxia-inducible factor 1 α (<i>HIF-1α</i>)	Forward	5'-AGCTTCTGTTATGAGGCTCACC -3'
	Reward	5'-TGACTTGATGTTTCATCGTCCTC -3'

Table 1. List of primers for macrophage polarization and glycolysis pathway.

Mitochondrial DNA (mtDNA), total cellular ATP and extracellular Flux

Analysis

Total DNA from cells was extracted by Tissue Genomic DNA extraction mini kit (Favorgen Biotech, Wembley, WA, Australia) as previously published [43]. Briefly, DNA quantification was determined by Nano drop ND-100 (Thermo scientific) and mtDNA copy number was measured by qPCR with cellular DNA template, Mastermix 1xKAPA fast SYBR Green (KAPA Biosystems, Wilmington, MA, USA) and primers of mitochondrial encoded mtDNA (Favorgen Biotech). Quantification of mtDNA was analyzed by $\Delta\Delta CT$ method normalized by the expression of house-keeping gene $\beta 2$ -microglobulin ($\beta 2M$) with the following sequence, forward, 5'-TTCTGGTGCTTGTCTCACTGA-3', reverse, 5'-CAGTATGTTTCGGCTTCCCATTC-3'. In addition, ATP content in 2×10^4 cells/ well was determined by the Luminescent ATP Detection Assay (Abcam, Cambridge, UK) according to the manufacturer's protocol [43]. In addition, energy metabolism profiles with estimation of glycolysis and mitochondrial oxidative phosphorylation with

extracellular acidification rate (ECAR) and oxygen consumption rate (OCR) were performed, respectively, by Seahorse XFp Analyzers (Agilent, Santa Clara, CA, USA) upon the miR-transfected RAW 264.7 at 1×10^4 cells/ well by Seahorse Wave 2.6 software as previously described [33]. Glycolysis and mitochondrial parameters was calculated using the generator program report of XF Glycolysis stress test and XF Cell mito stress test, respectively, based on these following equations; Glycolysis = ECAR between glucose and oligomycin – ECAR before glucose administration, glycolysis capacity = ECAR between oligomycin and 2-Deoxy-d-glucose (2-DG) – ECAR before glucose administration, glycolysis reserve = ECAR between oligomycin and 2-DG - ECAR between glucose and oligomycin, basal respiration = OCR before oligomycin – OCR after antimycin A/ rotnone, respiratory capacity (maximal respiration) = OCR between Carbonyl cyanide-4-(trifluoromethoxy)-phenylhydrazone (FCCP) and antimycin A/ rotnone – OCR after antimycin A/ rotnone and respiratory reserve = OCR between FCCP and antimycin A/ rotnone – OCR before oligomycin.

Statistical analysis

GraphPad Prism 5.0 (GraphPad Software, Inc., San Diego, CA, USA) was used for all statistical analyses. Differences between groups were calculated by Student's t-test or one-way analysis of variance (ANOVA) followed by Tukey's analysis for the comparison of two or more experimental groups, respectively. *In vitro* data were based on independent triplicate experiments and represented by mean \pm standard error (SE). A p value less than 0.05 was considered as statistically significant.

Results

The over-expression of miR-223 facilitated M2 macrophage polarization in macrophages (RAW 246.5) through the inhibition of several genes in glycolysis pathway. In addition, the adoptive transfer of miR-223 over-expressed macrophages with IL-4 pre-conditioning attenuated LPS-induced sepsis mouse model.

The over-expression of miR-223 in macrophages reduced the characteristics of M1 polarization and decreased pro-inflammatory cytokines in cell-supernatant

Because of the known anti-inflammatory effect of both miR-223 and miR-146a in macrophages [31], both miRs were transfected in RAW 264.7 before the induction of M1 and M2 polarization by LPS and IL-4, respectively. As such, the overexpression of miR-223 down-regulated the gene expression of M1 biomarkers including *iNOS* and *IL-1 β* , but not *TNF- α* , while the over-expressed miR-146a down-regulated only *IL-1 β* (fig 5A-C). In parallel, the overexpression of miR-223 induced M2 polarization as demonstrated by the up-regulation of *Arg-1* and *Fizz*, but not *TGF- β* , and the over-expressed miR-146a up-regulated only *TGF- β* (fig 5D-F). However, the expression of both miRs did not further enhance the characteristics of IL-4 activated M2 polarization, as determined by the expression of several biomarkers, in comparison with IL-4 induced control mimic cells (fig 5D-F). In addition, the anti-inflammatory property of miR-223 was demonstrated by i) the reduction of supernatant IL-6, but not TNF- α , after LPS activation (fig 5G, H) and ii) the induction of supernatant IL-10 after IL-4 stimulation (fig 5I). On the other hand, the over-expression of miR-146a did not demonstrate an anti-inflammatory effect as evaluated by supernatant cytokines (fig 5G-I). Because the conversion from IL-4 activated M2 polarization into pro-inflammatory macrophages by LPS was previously mentioned

[44, 45], the property to maintain M2 polarization after IL-4 stimulation in miR-223 overexpressed macrophages was tested. Accordingly, while IL-4 stimulation alone induced very low expression of *iNOS*, *TNF- α* and *IL-1 β* compared with LPS stimulation (fig 5A-C), LPS activation in IL-4 pre-conditioning macrophages (IL-4/LPS) demonstrated a similar level of these genes in comparison with LPS stimulation alone (media/ LPS) (fig 6A-C). However, miR-223 over-expressed macrophages with IL-4 pre-conditioning (IL-4/ LPS) enhanced only some pro-inflammatory characteristics but still demonstrated lower *iNOS* expression, higher *Arg-1* expression and lower supernatant IL-6 (fig 6) compared with the miR-146a over-expressed cells.

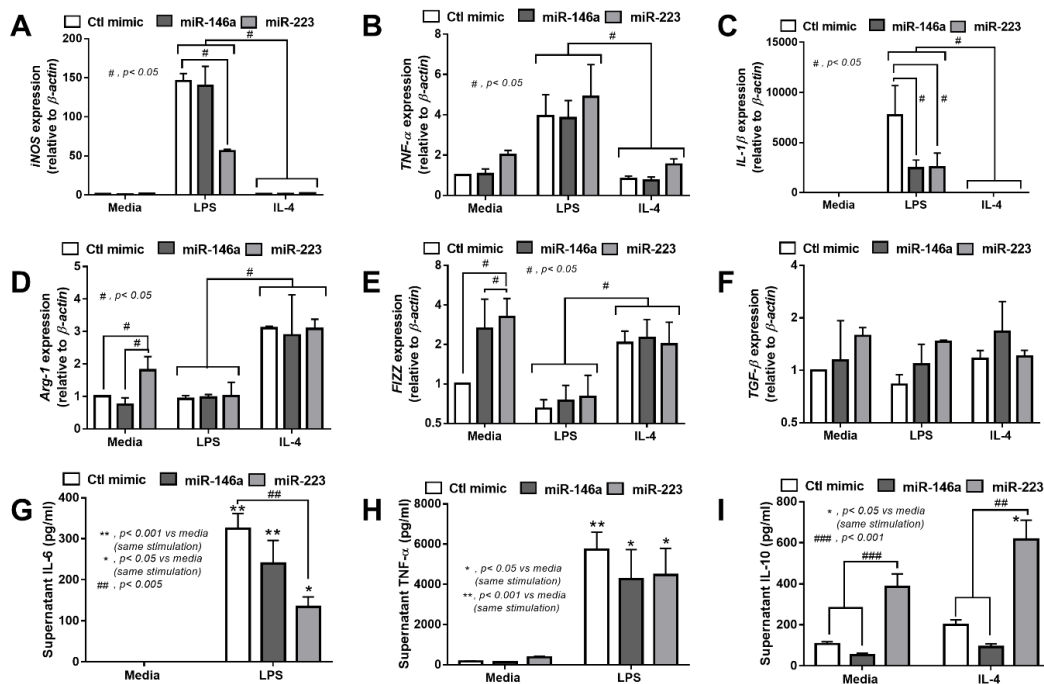


Figure 5. Macrophage anti-inflammatory property after the over-expression of miR-223 is higher than miR-146a.

The characteristics of M1 macrophage polarization as determined by the expression of *iNOS*, *TNF- α* and *IL-1 β* (A-C), and M2 macrophage polarization as evaluated by the expression of *Arg-1*, *Fizz* and *TGF- β* (D-F), of macrophages with the over-expression of control mimic (Ctl mimic), miR-146a and miR-223 after the stimulation

with LPS and IL-4, the stimulator of M1 and M2 macrophage polarization, respectively, are demonstrated. In addition, the supernatant pro-inflammatory cytokines, IL-6 and TNF- α (G, H), after LPS stimulation and an anti-inflammatory cytokine, IL-10 (I), after IL-4 activation, from these macrophages are demonstrated.

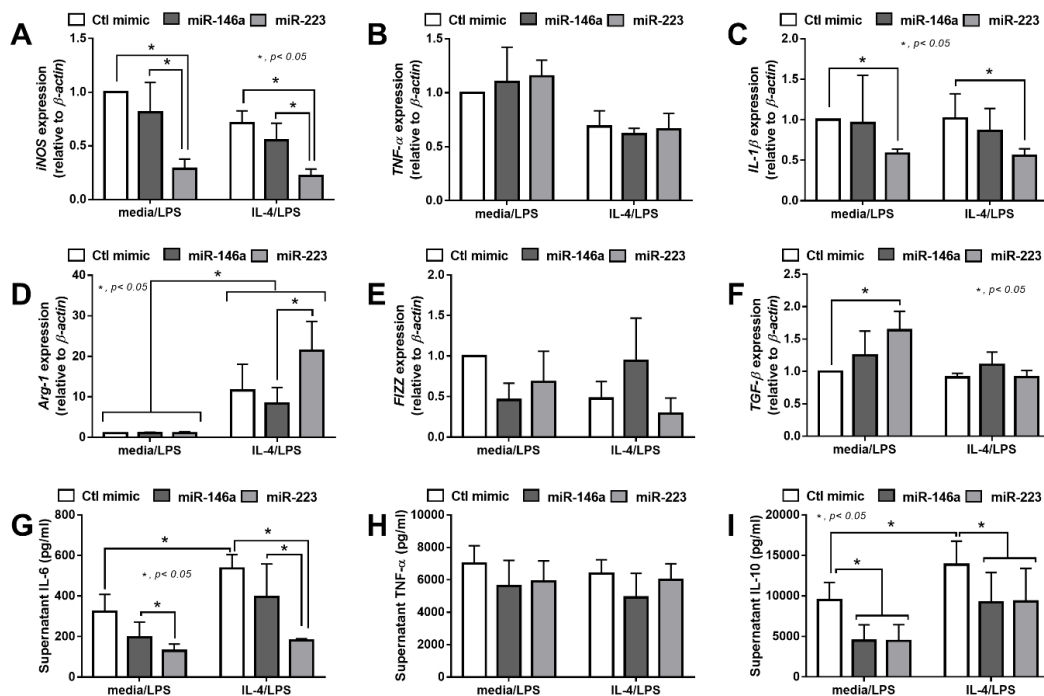


Figure 6. Over-expression of miR-223 maintains IL-4 induced anti-inflammatory characteristics of macrophages after LPS-induction better than miR-146a over-expression.

The characteristics of M1 macrophage polarization as determined by the expression of *iNOS*, *TNF- α* and *IL-1 β* (A-C), and M2 macrophage polarization as evaluated by the expression of *Arg-1*, *Fizz* and *TGF- β* (D-F), of macrophages with the over-expression of control mimic (Ctl mimic), miR-146a and miR-223 that stimulated with IL-4, the M2 macrophage polarization stimulator, prior to the stimulation with LPS, M1 macrophage-polarization stimulator, (IL-4/LPS) or control media prior to LPS (media/LPS) are demonstrated. In addition, the supernatant cytokines, IL-6, TNF- α and IL-10 (G-I), of these macrophages are demonstrated.

The inhibition of enzyme in glycolysis pathway by the miR-223 over-expression induced resistance against LPS-enhanced M1 polarization

Because the alteration of immunometabolism is, at least in part, responsible for the expression of pro- or anti- inflammatory characteristics of macrophages [46], the metabolism profiles are explored by the extracellular flux analysis. As such, LPS induced the glycolysis pathway as indicated by increased glycolysis area, glycolysis capacity and glycolysis reserve (fig 7A; Ctl mimic-LPS vs. Ctl mimic-media; E-G). In parallel, LPS reduced the mitochondrial pathway as indicated by reduced basal respiration, respiratory capacity and respiratory reserve (fig 7B; Ctl mimic-LPS vs. Ctl mimic-media, H-J). However, the patterns of glycolysis and mitochondrial responses in miR-223 over-expressed macrophages after LPS stimulation was similar to control (fig 7A, B; Ctl mimic-media vs. miR-223-LPS, E-J) implying the resistance of miR-223 over-expressed cells against the direction of LPS stimulation. On the other hand, IL-4 (Ctl mimic IL-4) also increased glycolysis activity compared with control (Ctl mimic-media) (fig 7C, E-G) without the alteration in mitochondrial activity (fig 7D, H-J). Moreover, LPS also reduced mitochondrial number, as determined by mitochondrial DNA analysis, and decreased total ATP while IL-4 did not change these parameters (fig 7K, L). Interestingly, mitochondrial DNA and ATP production in miR-223 over-expressed cells with LPS stimulation did not differ from the control macrophages (fig 7K, L). Of note, the profile of extra-cellular flux analysis in miR-223 over-expressed macrophages without LPS (miR-223-media) did not differ from the control mimic (Ctl mimic-media). These data supported that LPS induced glycolysis, suppressed mitochondrial function and reduced ATP production in macrophages but were attenuated by miR-223 over-expression.

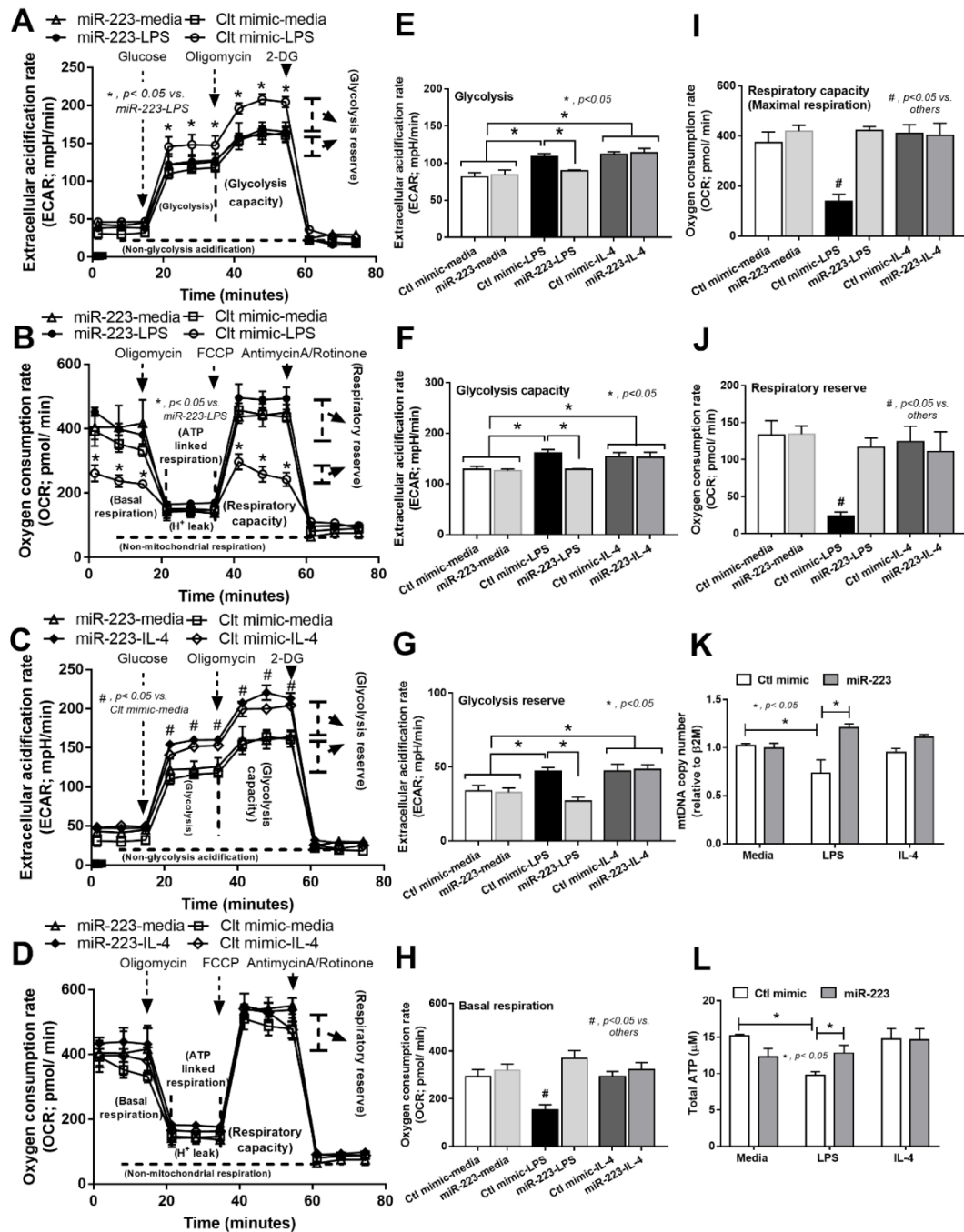


Figure 7. Over-expression of miR-223 in LPS-activated macrophages reduces glycolysis activity and improves mitochondrial function as determined by extracellular flux analysis.

The extracellular flux analysis pattern of macrophages over-expressed by miR-223 or control mimic (Ctl-mimic) as evaluated by extracellular acidification rate of glucose stress test for glycolysis pathway analysis and oxygen consumption rate of mitochondrial stress test for mitochondrial pathway analysis after the stimulation by LPS versus control media (A, B) or IL-4 versus control media (C, D) with the comparison in column bar graph of glucose stress test parameters (glycolysis, respiratory capacity and glycolysis reserve) (E-G) and

mitochondrial stress test parameters (basal respiration, respiratory capacity and respiratory reserve) (H-J) are demonstrated. In addition, the mitochondrial content as analyzed by the copy number of mitochondria (mtDNA) (K) and the ATP production (L) of macrophages over-expressed with Ctl-mimic or miR-223 after the stimulation with LPS, IL-4 or control media are demonstrated. Of note, the extracellular flux analysis pattern of miR-223-media is not showed due to the similarity to Ctl-mimic-media.

Due to the inhibitory property of miR against the mRNA functions [16], we hypothesize that miR-223 might inhibit some mRNAs in glycolysis pathway. Accordingly, hypoxic inducible factor-1 α (HIF-1 α) is an enzyme responsible to enhance glycolysis pathway through several mediators including Solute carrier family 2, facilitated glucose transporter member 10 (SLC2a10), phosphofructokinase (PFK), Lactate dehydrogenase A (ldhA) [47] (fig 8A). Furthermore, HIF-1 α also reduces the mitochondrial function through the expression of pyruvate dehydrogenase kinase (PDK1) [48]. Of note, increased PDK1 inhibited pyruvate dehydrogenase (PHD), an enzyme that converts pyruvate into acetyl CoA supplying for Krebs cycle, leads to the reduction of mitochondrial function [48]. As such, the exploration of glycolysis-related genes in macrophages demonstrated that LPS induced only *HIF-1 α* expression (fig 8B), while IL-4 enhanced the expression of several genes including; *HIF-1 α* , *SLC2a10*, *PDK1*, *PKF* and *ldhA* (fig 8C-F). Although miR-223 over-expression reduced only *HIF-1 α* in LPS-activated macrophages (fig 8A), the LPS-induced glycolysis was inhibited (fig 7A), implying the major role of *HIF-1 α* in the glycolysis pathway. In contrast, miR-223 inhibited both *PDK-1* and *PFK* in IL-4 stimulated-cells (fig 8E, F) without any impact upon extracellular flux pattern (fig 7C, D), suggesting less importance of these enzymes in glycolysis pathway.

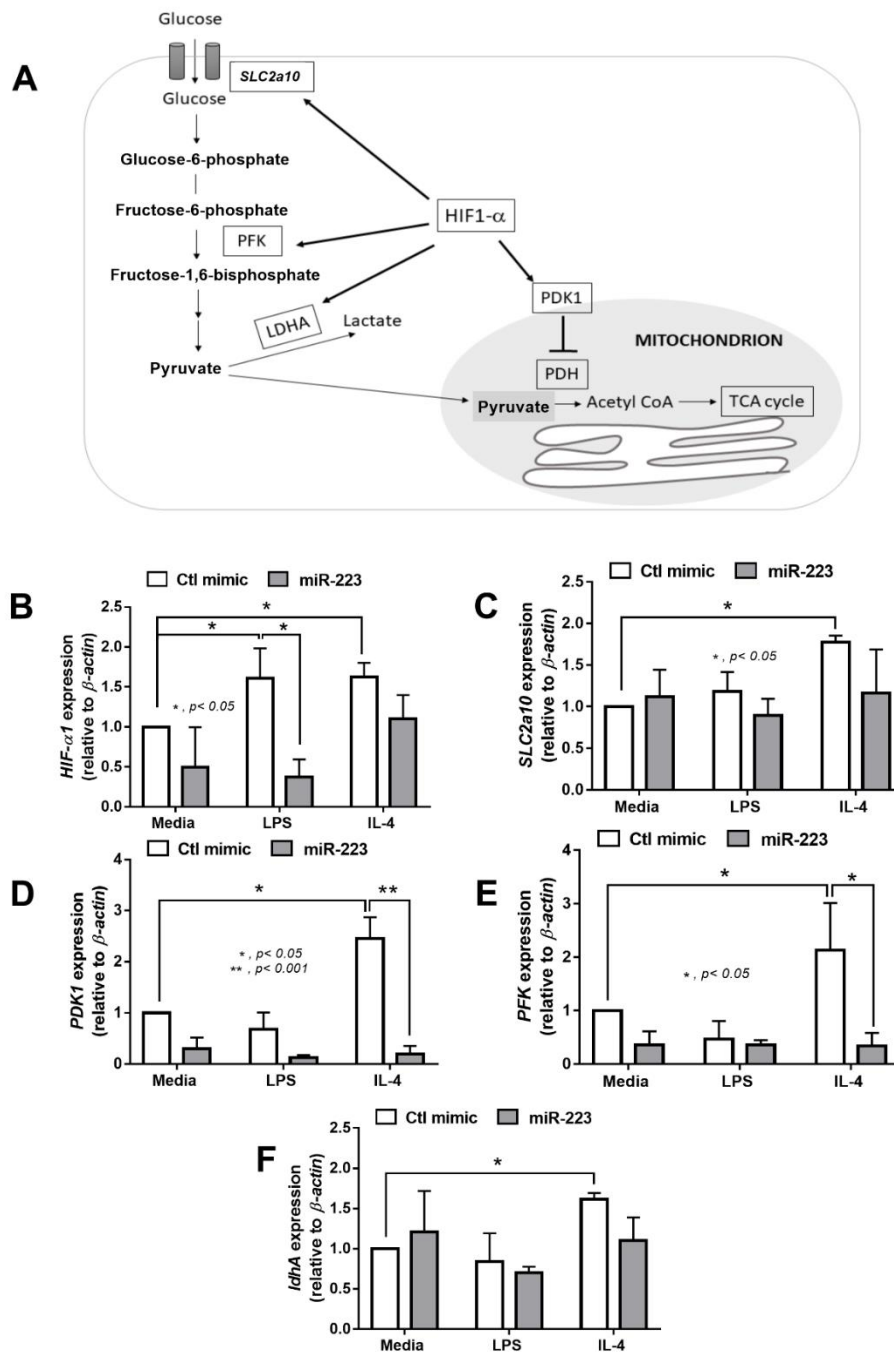


Figure 8. Over-expression of miR-223 in LPS-activated macrophages reduces HIF-1 α expression, while miR-223 over-expression in IL-4-activated macrophages decreases expression of PDK-1 and PFK.

The diagram demonstrates enzymes that associated with glycolysis pathway (A) and the gene expression of these enzymes in macrophages with the over-expression of miR-223 or control mimic (Ctl mimic) after the stimulation with LPS or IL-4 (B-F) are demonstrated. HIF-1 α , hypoxia-inducible factor-1 α ; *SLC2a10*, solute carrier family 2, facilitated glucose transporter member 10; PFK, phosphofructokinase; LDHA, lactate dehydrogenase A; PDK1, pyruvate

dehydrogenase kinase 1, PDH: pyruvate dehydrogenase; Acetyl-CoA, Acetyl Coenzyme A; TCA cycle, tri-carboxylic acid cycle or Krebs cycle.

The administration of IL-4 preconditioning macrophages with miR-233 over-expression attenuated sepsis in LPS injection mice

Because preconditioning with IL-4 in miR-223 over-expressed macrophages demonstrated anti-inflammatory state (fig 5) that resisted the LPS induced pro-inflammation (fig 6) possibly through the interference of HIF-1 α (fig 7, 8), these cells were used *in vivo* following previous publications [35-38]. As such, the intravenous cells administration demonstrated the highest cell accumulation in kidney and in liver at 1 h and 6 h post-injection, respectively (fig 9). The administration of IL-4 preconditioning macrophages with miR-223 over-expression, but not IL-4 stimulated control cells, attenuated the severity of LPS injection model as determined by renal injury (serum creatinine), liver injury (aspartate transaminase and alanine transaminase) (fig 10A-C) without therapeutic effect on leukocyte count (fig 10D-F). In addition, treatment with miR-223-manipulated cells also reduced pro-inflammatory cytokine (TNF- α), but not IL-6, increased anti-inflammatory cytokine (IL-10) (fig 10G-I) and improved lung pathology (fig 11).

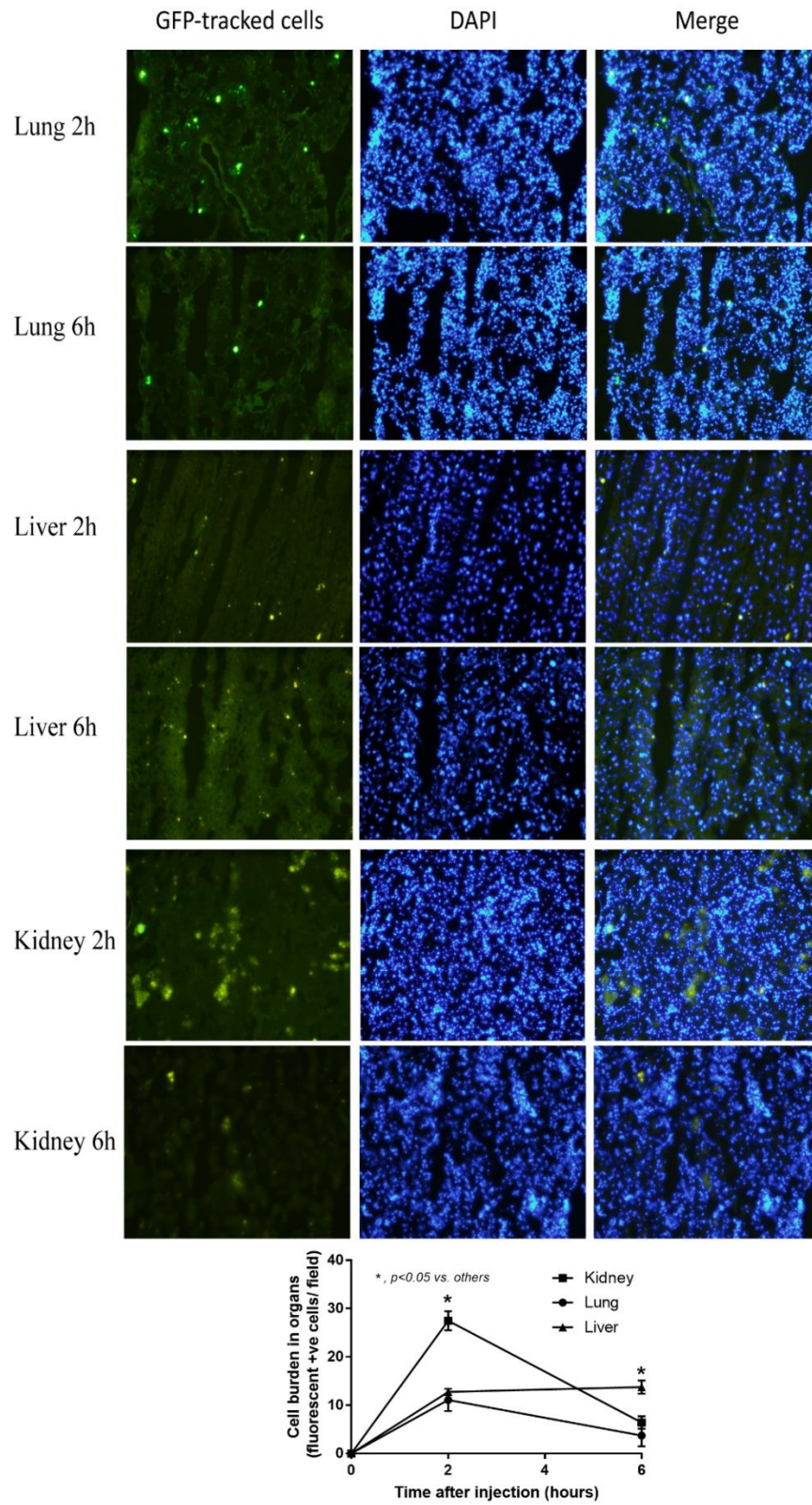


Figure 9. Macrophages are demonstrated in kidney and liver at 2 h and 6 h after administration.

The representative pictures of the kinetics of tagged green fluorescent protein (GFP) macrophages after intravenous injection in different organs at different time-points and the analysis of cells burdens in organs are demonstrated. DAPI, 4', 6-diamidino-2-phenylindole (a DNA fluorescence staining color).

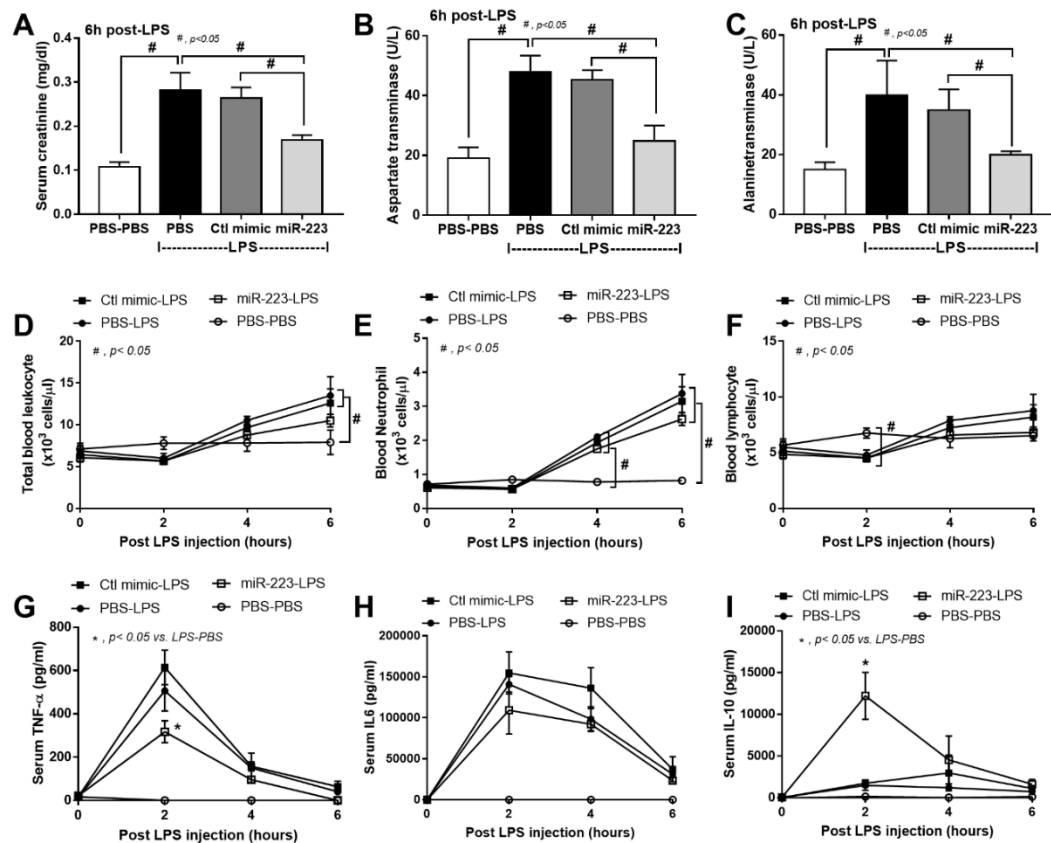


Figure 10. Administration of miR-223 over-expressed macrophages attenuates sepsis in LPS injection mouse model.

The characteristics of LPS injection mice after the administration with IL-4-activated-macrophages without gene over-expression (PBS-LPS) or with control mimic over-expression (Ctl mimic-LPS) or with miR-223 over-expression (miR-223-LPS) as evaluated by serum creatinine (A), aspartate transaminase (B), alanine transaminase (C), blood leukocyte evaluation (D-F) and serum cytokines (G-I) are demonstrated (n = 5-7/ group). Of note, only the control mice injected with phosphate buffer solution (PBS) group without LPS stimulation (PBS-PBS) is presented, but not Ctl mimic-PBS and miR-223-PBS, due to the similar values among these 3 control groups.

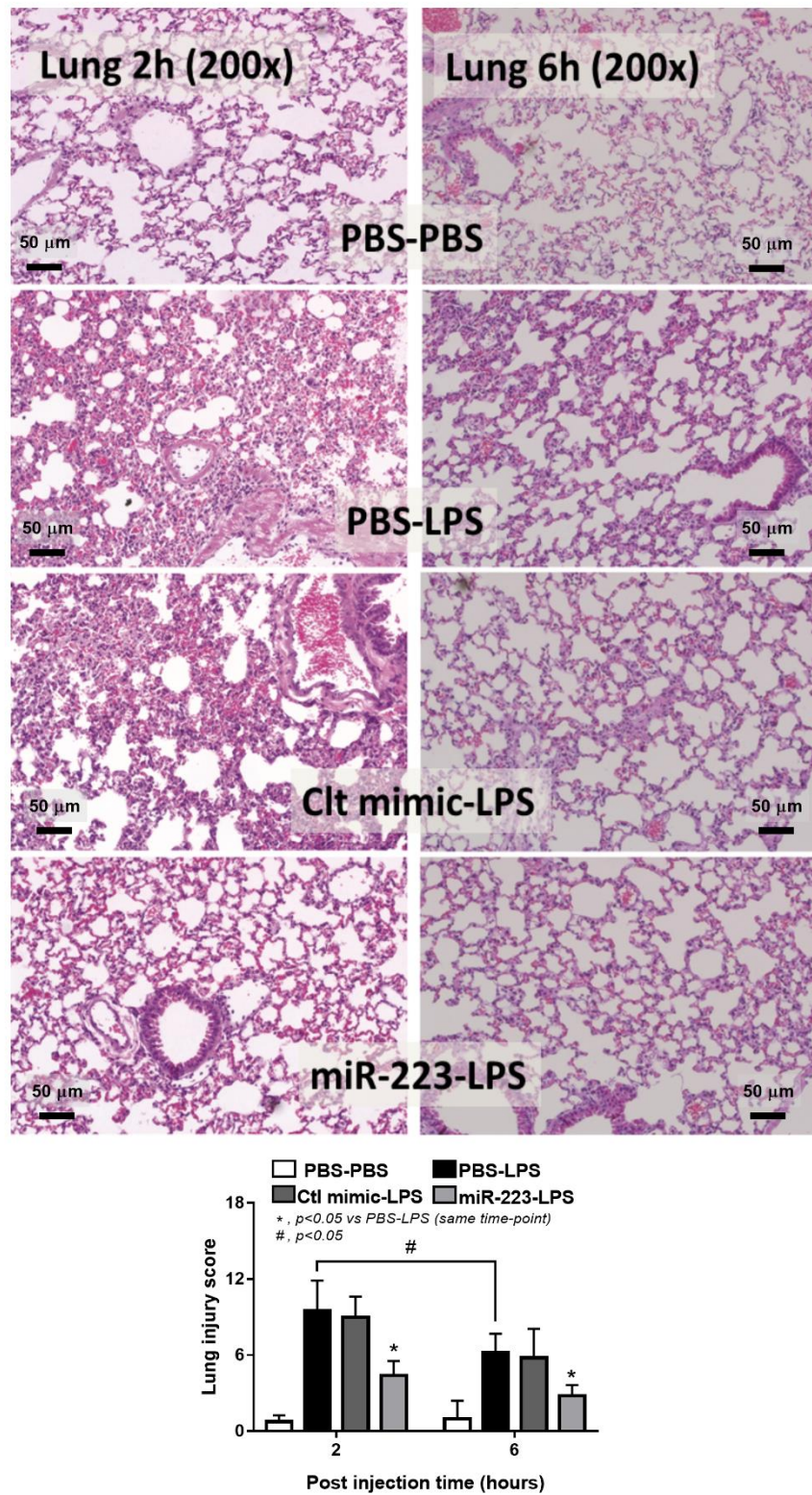


Figure 11. Administration of miR-223 over-expressed macrophages attenuates sepsis-induced lung injury in LPS injection mouse model.

The representative of lung histology (A) of LPS administered mice preconditioning with IL-4-activated-macrophages without gene over-expression (PBS-LPS) or with control mimic over-expression (Ctl mimic-LPS) or with miR-223 over-expression (miR-223-LPS) by the semi-quantitative histology score (B) are demonstrated (n = 5-7/ group). Of note, only the control mice injected with phosphate buffer solution (PBS) group without LPS stimulation (PBS-PBS) is presented, but not Ctl mimic-PBS and miR-223-PBS, due to the similar pictures among these 3 control groups.

Discussion

The over-expression of miR-223 in macrophages induced anti-inflammatory responses against LPS stimulation possibly due to the glycolysis interference through reduced *HIF-1 α* . The administration of IL-4 stimulated miR-223 over-expressed macrophages attenuated the severity of LPS injection sepsis mouse model.

Anti-inflammatory property of miR-223 over-expressed macrophages

The hyper-inflammatory responses induced sepsis mortality and the attenuation by anti-inflammatory macrophages are well-known [13, 14]. Due to the multiple inhibitory targets, either complementary or non-complementary sequence mRNA, is possible from a single miR [17], miR is an interesting method to induce anti-inflammatory macrophages. Indeed, both miR-223 and miR-146a (without IL-4) are associated with M2 macrophages polarization [49, 50] through, at least in part, targeting PPAR γ [19, 51]. With LPS stimulation, the anti-inflammatory property of miR-223 over-expressed macrophages was more potent than miR-146a over-expressed cells as determined by the reduced expression of *IL-1 β* and *iNOS* with decreased supernatant IL-6 and increased supernatant IL-10. Different effects of these miRs suggest the inhibition in different target-molecules. However, previous studies report that IL-4-primed macrophages are easily converted back into the pro-inflammatory macrophages after the subsequent LPS challenge due to the macrophage plasticity [44, 45]. Here, miR-223 over-expression prevented the conversion back into

the pro-inflammatory state with the subsequent LPS stimulation but miR-223 did not enhance the expression of IL-4 induced anti-inflammatory genes.

The interference of glycolysis pathway by miR-223 induced anti-inflammatory macrophages

The signatures of immunometabolic pathway of M1 and M2 polarized macrophages are glycolysis and mitochondrial oxidative phosphorylation, respectively [25]. As such, the induction of macrophage polarization by immunometabolic alteration using miRs is mentioned [26]. Here, LPS down regulated mitochondrial oxidative phosphorylation, along with the reduction of mtDNA and ATP production, with glycolysis enhancement while IL-4 stimulated only the glycolysis pathway supporting previous publications [52-54]. While glycolysis is not a major metabolic pathway in M2 macrophage polarization [55], glycolysis is required for the regular M2 macrophage functions [52] and the interference on glycolysis inhibits M2 macrophage polarization [53]. Because i) LPS increased only *HIF-1 α* while IL-4 enhanced *HIF-1 α* with other genes and ii) miR-223 over-expression, that mainly inhibited *HIF-1 α* , turned the immunometabolic characteristics of LPS-stimulated cells into the neutral state but no effect on IL-4-stimulated cells. These data implied a possible key role of *HIF-1 α* in glycolysis pathway after LPS activation [56]. Indeed, the impact of *HIF-1 α* upon glycolysis and M1 polarization is previously mentioned including; i) *HIF-1 α* expression up-regulates several enzymes in glycolysis [47], ii) *HIF-1 α* overexpression enhances glycolysis and increases inflammatory cytokine production in macrophages [57] and iii) *HIF-1 α* deficient macrophages did not produce cytokines after LPS stimulation [58]. Thus the

interference of *HIF-1 α* expression might be one of the important mechanisms of miR-223-induced anti-inflammatory macrophages.

In addition, from the previous reports, miR-223 also induced anti-inflammatory properties through the interference of other mechanisms such as STAT3, Nfat5 and PPAR γ [19, 30] implying the multiple targets of miR-223 for anti-inflammatory induction. On the other hand, miR-223 over-expression reduced the expression of *PFK* and *PDK-1*, but did not alter immunometabolic characteristics, of IL-4 stimulated cells implying that these enzymes are not the main enzymes used for cell-energy generation during IL-4 induced M2 macrophage polarization.

Of note, miR-223 regulation on *HIF-1 α* translation is nicely mentioned through the analysis of 3-prime un-translated region (3' UTR) [28, 29]. In addition, LPS and IL-4 possibly mediate *HIF-1 α* expression differently. Our working hypothesis is that while LPS enhances *HIF-1 α* through LPS-induced reactive oxygen species [59], IL-4 activates *HIF-1 α* via Akt-mTORC [52, 53], an upstream signaling of *HIF-1 α* [60]. As such, LPS and IL-4 enhanced glycolysis as demonstrated by extracellular flux analysis and genes of glycolysis pathway mainly through *HIF-1 α* and *HIF-1 α* with other several genes, respectively (fig 7). It seems that miR-223 targets only on *HIF-1 α* in LPS-enhanced glycolysis, but binds to *HIF-1 α* together with other several genes in IL-4-enhanced glycolysis. Indeed, the predicted-targets of miR-223 from the database of miRNAWalk 2.0 and TargetScan.org version 7.2, the comprehensive database on the predicted and validated targets of human and murine miR [61], was including both *HIF-1 α* and *PFK*. Here, we demonstrated that LPS increased *HIF-1 α* while IL-4 induced *HIF-1 α* , *PDK-1* and *PFK*. Hence, miR-223 blocked only *HIF-1 α* in LPS stimulation but targeted on *HIF-1 α* , *PDK-1* and *PFK* in IL-4 induction, resulted in the

higher inhibitory potency on LPS-derived *HIF-1 α* compared with IL-4 induced *HIF-1 α* . More studies in this topic are interesting.

The administration of IL-4 stimulated miR-223 over-expressed macrophages, a proof of concept for anti-inflammatory treatment in sepsis

Because of the potent anti-inflammatory property and the resistance against LPS induced macrophage-conversion of miR-223 over-expression, IL-4 stimulated miR-223 over-expressed macrophages were tested in LPS injection mouse model as a proof of concept for sepsis treatment. The injected cells distributed in lung, liver and kidney for at least 6 h after the administration. Immune-mediated rejection of C57BL/6 mice toward the administered Raw 264.7 cell, a cell line from BALB/c mice, might be responsible for the cell depletion which could be improved in the clinical translation. Nevertheless, the treatment attenuated the injury in several organs as evaluated by lung histology, liver enzymes and serum creatinine with decreased systemic inflammation as demonstrated by decreased TNF- α and increased IL-10 in serum at 6 h post LPS administration, a time-point with the highest injury of the model. Interestingly, administration of IL-4 stimulated macrophages without miR-223 over-expression did not demonstrate any beneficial effects in LPS injection model, perhaps due to the conversion back into pro-inflammatory state of the injected-cells by LPS stimulation as previously mentioned [44, 45, 62]. In addition, the higher pro-inflammatory responses by LPS stimulation in IL-4 pre-conditioning macrophages in comparison with LPS-stimulated control macrophages is demonstrated here (fig 7G) supporting several previous publications [44, 63, 64], possibly through IL-4 activated STAT-6 [45], which is a possible limitation of cell therapy in sepsis. Hence, the plasticity of macrophages in cell-based therapy in sepsis is an important issue for

further studies. In translational aspect, the injected cells that distribute in several organs might be responsible for direct local inflammatory control within the organs and is possibly an interesting adjunctive therapy in sepsis. Cell-based therapy has been currently developed for cancer treatment [65, 66] and some of these therapies might also be appropriated for use in sepsis. More studies are interesting.

In conclusion, miR-223 over-expression induced anti-inflammation through the inhibition of glycolysis pathway through the down-regulation of *HIF-1 α* . The anti-inflammatory induction by IL-4 in miR-223 over-expressed macrophages prevented the back-conversion into pro-inflammatory macrophage after LPS stimulation and these cells are proposed as a candidate for cell therapy for the pro-inflammatory phase of sepsis.

Part II: BAM15, a mitochondrial uncoupling agent, attenuates inflammation in LPS injection mouse model, an adjunctive anti-inflammation on macrophages and hepatocytes

Published in Journal of Innate Immunity, 2021 Jun 1;1-17. doi: 10.1159/000516348

Cong Phi Dang^{1,2}, Jiraphorn Issara-Amphorn², Awirut Chareonsappakit², Kanyarat Udompornpitak², Thansita Bhunyakarnjanarat², Wilasinee Saisorn², Kritsanawan Sae-Khow², Asada Leelahavanichkul^{2,3#}

¹Medical Microbiology, Interdisciplinary and International Program, Graduate School, Chulalongkorn University, Bangkok, Thailand.

²Department of Microbiology, Faculty of Medicine, Chulalongkorn University, Bangkok, Thailand

³Translational Research in Inflammation and Immunology Research Unit (TRIRU), Department of Microbiology, Chulalongkorn University, Bangkok, Thailand

Running Head : BAM15 attenuates inflammation in macrophages and hepatocytes

#Corresponding author: Asada Leelahavanichkul. Immunology Unit, Department of Microbiology, Chulalongkorn University, Bangkok 10330, Thailand Tel: +66-2-256-4251, Fax: +66-2-252-6920 E-mail: aleelahavanit@gmail.com

Number of Tables: 01

Number of Figures: 08

Word count: 4398

Keywords: BAM15, mitochondrial uncoupling, macrophage, inflammation, metabolism

Abstract (214 words)

Control of immune responses through the immunometabolism interference is interesting for sepsis treatment. Then, expression of immunometabolism-associated genes and BAM15, a mitochondrial uncoupling agent, was explored in a pro-inflammatory model using lipopolysaccharide (LPS) injection. Accordingly, the decreased expression of mitochondrial uncoupling proteins (*UCPs*) was demonstrated by transcriptomic analysis on metabolism-associated genes in macrophages (RAW246.7) and by polymerase chain reaction in LPS-stimulated RAW246.7 and hepatocytes (Hepa 1-6). Pre-treatment with BAM15 at 24 h prior to LPS in macrophages attenuated supernatant inflammatory cytokines (IL-6, TNF- α and IL-10), down-regulated genes of pro-inflammatory M1 polarization (*iNOS* and *IL-1 β*), up-regulated anti-inflammatory M2 polarization (*Arg1* and *FIZZ1*) and decreased cell energy status (extracellular flux analysis and ATP production). Likewise, BAM15 decreased expression of pro-inflammatory genes (*IL-6*, *TNF- α* , *IL-10* and *iNOS*) and reduced cell energy in hepatocytes. In LPS-administered mice, BAM15 attenuated serum cytokines, organ injury (liver enzymes and serum creatinine) and tissue cytokines (livers and kidneys), in part, through the enhanced phosphorylated α AMPK, a sensor of ATP depletion with anti-inflammatory property, in liver and the reduced inflammatory monocytes/macrophages (Ly6C⁺ve, CD11b⁺ve) in liver as detected by Western blot and flow cytometry, respectively. In conclusion, a proof of concept for inflammation attenuation of BAM15 through metabolic interference induced anti-inflammation on macrophages and hepatocytes was demonstrated as a new strategy of anti-inflammation in sepsis.

Introduction

Sepsis, a syndrome of organ dysfunction due to the imbalance of host responses against systemic infection [5], is an important world-wide healthcare problem that is a major cause of death in patients with clinically illness [5]. The shift in the balance toward pro-inflammatory immune-responses, referred to as “hyper-cytokine syndrome” or “systemic inflammatory response syndrome (SIRS)”, is an important cause of death in sepsis leading to the utilization of anti-inflammatory adjunctive treatment [6-8]. The robust responses of innate immune cells, including macrophages, mainly accounts for the sepsis pathophysiology [9].

The plasticity of macrophages, the important immune cells in response to infection [67], as classifies into a classical activated pro-inflammatory M1 macrophage polarization and an alternative anti-inflammatory M2 macrophage polarization is well-known [11]. An imbalance between M1 and M2 macrophage polarization is responsible for several abnormalities including the prominent M1 macrophage polarization in sepsis-induced hyper-inflammatory responses [9]. As such, the blockage of M1 polarization attenuates the exaggerated inflammation in systemic infection [13, 68]. Interestingly, the metabolic activities of immune cells, at least in part, depend on the status cell energy (Adenosine triphosphate; ATP) that derives from glycolysis and oxidative phosphorylation (OXPHOS) of mitochondria [23, 24]. Accordingly, glycolysis, but not OXPHOS, is important for the metabolism of M1 macrophages in hyper-inflammatory responses, possibly due to the reduced oxygen supply for the OXPHOS cycle [25]. The blockade of glycolysis induces anti-inflammatory status in sepsis [68-70]. Despite the less importance of OXPHOS during pro-inflammatory sepsis as previously mentioned [25], OXPHOS is important for inflammation in other models [71] as the decreased-OXPHOS reduces inflammation

in cord-blood macrophages [72] and blockade of ATP synthesis attenuates obesity-induced pro-inflammation [73].

Normally, OXPHOS is an effective process of ATP production in mitochondria using the electrochemical proton-gradient across mitochondrial inner membrane through ATP synthase [25]. However, some protons do not enter the ATP synthesis process but leak back into the mitochondrial matrix, referred to as “mitochondrial uncoupling”, which leads to the decrease in proton gradients and ATP production [74]. Then mitochondrial uncoupling proteins, a group of proteins with a capacity to transfer protons, enhance ATP synthesis and alter several cell metabolic profiles [75]. Nevertheless, the proton carrying by mitochondrial uncoupling agents enhance ATP synthesis only in a very short period of time after the administration but induce an impairment of mitochondrial membrane potential that dissipate proton gradient and reduce ATP synthesis [76-78]. Therefore, mitochondrial uncoupling agents are used for ATP production blockage that attenuate macrophage pro-inflammation [79-81]. Accordingly, the enhanced mitochondrial uncoupling protein 2 (UCP2) in transgenic mice attenuates inflammatory cytokines in an ischemic brain model [82] and UCP2 depletion amplifies inflammation through the accelerated I κ B kinase and NF κ B signaling [83]. In parallel, BAM15, a synthetic mitochondrial uncoupling agent, has been used as an interesting candidate of anti-inflammation in several models including ischemic kidney injury [2] and obesity-induced inflammation [84], but never been tested in sepsis. Due to the higher BAM15 distribution in liver, BAM15 attenuated fatty acid induced hepatocyte injury (steatohepatitis) in obesity model [3]. Because liver is also an important organ that is responsible for inflammatory responses in systemic infection [85], BAM15 might be

effectively attenuates sepsis-induced liver injury. Different from Carbonyl cyanide-4-phenylhydrazone (FCCP), a classical mitochondrial uncoupling agent, BAM15 is more specific to mitochondrial membrane without an adverse effect on cell membrane depolarization [2]. Here, BAM15 was tested *in vitro* (macrophages and hepatocytes) and in the lipopolysaccharide (LPS)-induced inflammation mouse model.

Materials and methods

Animal and animal model

The animal procedure, in accordance to the protocol of the National Institutes of Health (NIH; USA), was approved by the Institutional Animal Care and Use Committee of the Faculty of Medicine, Chulalongkorn University, Bangkok, Thailand. Male 6-week-old mice, purchased from Nomura Siam International (Pathumwan, Bangkok, Thailand), were housed in the animal facility for 1 week before performing the experiments. Systemic inflammation was induced by endotoxin (LPS) from *Escherichia coli* 026:B6 (Sigma-Aldrich, St. Louis, USA) as previously described [32, 33, 68] with BAM15 pre-treatment in a dose that modified from a previous publication [3]. Briefly, BAM15 (Sigma-Aldrich) at 1 mg/ kg in 10% of dimethyl sulfoxide (DMSO) (Sigma-Aldrich) or 10% DMSO alone was intraperitoneally (IP) administered at 3 hours prior to the IP injection of LPS (4 mg/kg) in phosphate buffer solution (PBS) or PBS alone. Because of the maximal injury at 2 h post-LPS injection in mouse model [68], all mice were sacrificed with cardiac puncture under isoflurane anesthesia with sample collections (blood and organs) at 2 h post-LPS. Organs (snap frozen on liquid nitrogen) and serum were kept in -70 °C until use.

Analysis of mouse samples and Western blotting

Systemic inflammation was determined by serum cytokines (IL-6, IL-10 and TNF- α) using ELISA assay (ReproTech, Oldwick, NJ, USA). Liver injury was evaluated by aspartate transaminase (AST) and alanine transaminase (ALT) by EnzyChrom AST (EASTR-100) and EnzyChrom ALT (EALT-100) (BioAssay, Hayward, CA, USA), respectively. Kidney injury was measured by creatinine (Cr) with QuantiChrom Creatinine-Assay (DICT-500) (BioAssay). Additionally, liver and kidney injury were also evaluated by tissue cytokines following a previous protocol [86]. Briefly, tissue samples were weighed, sonicated thoroughly and the supernatant from homogenous tissue preparation was collected for cytokine measurement by ELISA assay (Biolegend, San Diego, CA, USA) as the serum samples.

Furthermore, protein abundance of phosphorylated AMP-activated protein kinase in alpha isoform (p- α AMPK), a molecule for ATP-restoration [87], in liver was examined by Western blot analysis according to previous protocol [87]. Briefly, liver was homogenized and incubated in lysis buffer (radioimmunoprecipitation assay buffer; RIPA) complemented with protease and phosphatase inhibitor (Thermo-Scientific, Rockford, IL, USA). Quantification of protein concentration was performed via Bradford assay before the protein separation using polyacrylamide gel with 10% sodium dodecyl sulfate. Thereafter, protein from gel is transferring to PVDF membraned, followed by incubation of primary antibodies (Cell Signaling Technology Corporate, Danvers, MA) for i) Phospho- α AMPK (Thr172) (40H9) (p- α AMPK), ii) total α AMPK and iii) β -actin (a house-keeping protein) with a second antibody conjugated to horseradish peroxidase (HRP) and visualized by chemiluminescence (Thermo-Scientific). Notably, phospho- α AMPK (Thr172) detects

endogenous α AMPK only when phosphorylated at Threonine 172, but not at the phosphorylation at Threonine 183, that targeted both α 1 and α 2 isoform of the catalytic subunit, but not the β and γ regulatory subunit in accordance to the manufacturer's information.

Flow cytometry analysis of immune cells in liver

Flow cytometry analysis of liver macrophages were modified from the previous publication [88-90]. Briefly, at 2 hours following LPS injection, livers were minced, homogenized in Roswell Park Memorial Institute (RPMI) media, passed through cell strainers and incubated with red blood cell lysis (NH₄Cl) buffer before washing with PBS. Suspended hepatocytes were preincubated with bovine serum albumin (BSA) with 2% heat-inactivated fetal bovine serum (FBS) for 10 min at room temperature before incubated with antibodies against monocytes/macrophages including FITC-conjugated anti-Ly6G (BD Biosciences, Franklin Lakes, NJ, USA.), phycoerythrin (PE)-conjugated anti-F4/80 (Biolegend) and allophycocyanin (APC)-conjugated anti-CD11b (Biolegend) (at a dilution of 1:100). Then, cells were fixed with 4% paraformaldehyde (BD Biosciences) and determined absolute cell counts using absolute count bead (Beckman Coulter, Brea, CA, USA). Flow cytometry data were analyzed by BD LSRII cytometer (BD Biosciences) and analyzed using FlowJo software.

The *in vitro* experiments, RNA-sequencing analysis and quantitative polymerase chain reaction (qPCR)

The cell lines of murine macrophages (RAW264.7) (TIB-71TM; ATCC, Manassas, VA, USA) and murine hepatocytes (Hepa1-6) (CRL-1830TM, ATCC) were incubated in Dulbecco's Modified Eagle Medium (DMEM) with Penicillin-

Streptomycin and heat-inactivated fetal bovine serum (Thermo fisher Scientific, Waltham, MA, USA) at 37°C with 5% carbon dioxide (CO₂). Cells were seeded overnight before the pre-treatment with BAM15 (different concentrations and time-points) or DMSO control before the activation in macrophages or hepatocytes by LPS (100 ng/ mL) for 6 h or LPS (1 µg/ mL) for 1-6 h, respectively, prior to cell harvesting due to the different LPS-responses between these cells [91, 92]. For preparation of heat-killed microbes, *Escherichia coli* (ATCC 25922), *Staphylococcus aureus* (ATCC 25923), and *Candida albicans* (ATCC 14053) (the American Type Culture Collection, Manassas, VA, USA) were heat-inactivated at 65°C for 30 minutes and thoroughly sonicated as previous publication [93]. Then, RAW264.7 cells were stimulated with each of these heat-killed microbes with ratio between RAW264.7 cells: each organism (cells) at 1:10 for 6 h before the sample collection. Then, cytokines in supernatant were measured by ELISA assay (Biolegend) and cells were used for RNA extraction and extracellular flux analysis.

In macrophages, RNA sequencing analysis was performed to explore the downstream gene expression after LPS stimulation by the BGI Company. The differential gene expression using R package and the biological process and pathway analysis were performed by GO analysis and gene ontology pathway analysis, respectively [94]. In addition, several interesting molecules in both cell types were determined by qPCR as previously described [33]. Briefly, RNA extraction from cells was performed using Trizol (Thermo fisher Scientific). Amount of RNA was determined by Nano drop ND-1000 (Thermo fisher Scientific) before converted to cDNA by Reverse Transcription System. Gene expression was determined by qPCR using cDNA template, target primers, SYBR Green master mix (Applied biosystem,

Foster city, CA, USA) and β -actin was used as a housekeeping gene upon $\Delta\Delta CT$ method. The primers of target genes were listed in table 2.

Primers		
β -actin	Forward	5'-CGGTTCCGATGCCCTGAGGCTCTT-3'
	Reward	5'-CGTCACACTTCATGATGGAATTGA-3'
Uncoupling protein 2 (<i>UCP2</i>)	Forward	5'-GCCACTTCACTTCTGCCTTC-3'
	Reward	5'-GAAGGCATGAACCCCTTGTA-3'
Uncoupling protein 3 (<i>UCP3</i>)	Forward	5'-ACCTGGACTGCATGGTAAGG-3'
	Reward	5'-CTCGTTCTTGCCCTAAGGTG-3'
Inducible nitric oxide synthase (<i>iNOS</i>)	Forward	5'-CCCTTCCGAAGTTTCTGGCAGCAGC-3'
	Reward	5'-GGCTGTCAGAGCCTCGTGGCTTTG-3'
Arginase 1 (<i>Arg-1</i>)	Forward	5'-CAGAAGAATG GAAGAGTCAG-3'
	Reward	5'-CAGATATGCA GGA GTCACC-3'
Found in inflammatory zone (<i>Fizz</i>)	Forward	5'-GCCAGGTCCTGGAACCTTTC-3'
	Reward	5'-GGAGCAGGGAGATGCAGATGAG-3'
Tumor necrosis factor α (<i>TNF-α</i>)	Forward	5'-CCTCACACTCAGATCATCTTCTC-3'
	Reward	5'-AGATCCATGCCG TTGGCCAG-3'
Interleukin-1 β (<i>IL-1β</i>)	Forward	5'-GAAATGCCACCTTTTGACAGTG-3'
	Reward	5'-TGGATGCTCTCATCAGGACAG-3'
Interleukin-6 (<i>IL-6</i>)	Forward	5'-CTTCCATCCAGTTGCCTTCT-3'
	Reward	5'-CCTTCTGTGACTCCAGCTTATC-3'
Interleukin-10 (<i>IL-10</i>)	Forward	5'-GCTCTTACTGACTGGCATGAG-3'
	Reward	5'-CGCAGCTCTAGGAGCATGTG-3'

Table 2. List of the primers for mitochondrial uncoupling protein macrophage polarization.

Mitochondrial membrane potential assessment, extracellular flux analysis, cellular lactate and total cellular ATP

Mitochondrial membrane potential (MMP) was investigated using MitoTracker Red CMXRos (Thermo fisher Scientific) as red-fluorescent color on

mitochondria with active membrane potential in accordance to manufacture's protocol. Briefly, 200nM of MitoTracker Red was incubated into the cell culture at 37°C for 30 minutes before fixation with methanol at 20°C for 15 minutes. Cells were also stained with 4',6-diamidino-2-phenylindole DAPI (Sigma Aldrich), the blue-fluorescent color DNA staining. The fluorescent images were photographed by confocal microscopes ZEISS LSM 800 (Carl Zeiss, Germany) with the intensity analysis using Varioskan Flash microplate reader (Thermo Fisher Scientific). Oxygen consumption rate (OCR) and extracellular acidification rate (ECAR), a representative mitochondrial function (respiration) and glycolysis, respectively, were performed by Seahorse XFp Analyzers (Agilent, Santa Clara, CA, USA) as previous publication [95]. Briefly, cells were stimulated, as described above, in Seahorse cell culture plate before replacing by Seahorse media (DMEM complemented with glucose, pyruvate and L-glutamine) (Agilent, 103575-100) in pH 7.4 at 37°C for 1 h prior to the challenge with different metabolic interference compounds including oligomycin 1.5 μ M, carbonyl cyanide-4-(trifluoromethoxy)-phenylhydrazone (FCCP) 1 μ M and rotenone/antimycin A 0.5 μ M according to the protocol. The ECAR graph was calculated from OCR data and all data were analyzed by Seahorse Wave 2.6 software based on these following equations; basal respiration = OCR before oligomycin – OCR after rotenone/antimycin A, maximal respiration = OCR between FCCP and Rotenone/Antimycin A – OCR after rotenone/antimycin A and respiratory reserve = OCR between FCCP and rotenone/antimycin A – OCR before oligomycin. In addition, cellular lactate by colorimetric assay (BioVision, Milpitas, CA 95035 USA) and cellular ATP analysis by luminescent ATP detection assay (Abcam, Cambridge, UK) were performed upon manufacturers' protocol.

Statistical analysis

Graph establishment and data analysis was performed using GraphPad Prism 5.0 (GraphPad Software, Inc., San Diego, CA, USA) and demonstrated in mean \pm standard error (SEM). Student's t-test or one-way analysis of variance (ANOVA) upon Tukey's analysis was used to determine statistical significance between two or more groups, respectively. Statistical significance was marked with the p value less than 0.05.

Results

Pre-treatment with BAM15 reduced inflammatory responses in LPS-stimulated macrophages (RAW264.7) and hepatocytes (Hep1-6) and BAM15 attenuated the severity of LPS-injected mice.

The reduced mitochondrial uncoupling-related genes in LPS-activated macrophages, an association between cell energy and macrophage pro-inflammatory responses.

To investigate a possible association between cell energy and inflammatory responses in macrophages, the RNA-sequencing analysis of metabolism-associated genes in macrophages after stimulation by LPS or PBS control was performed. Accordingly, a reduction in most genes with an increase in a few genes were demonstrated in LPS-stimulated macrophages compared with the control (Fig 12A). The uncoupling proteins (*UCP1*, *UCP2* and *UCP3*), ATP synthesis associated molecules, were among the LPS-downregulated genes, indicating a reduced mitochondrial function after LPS stimulation (Fig 12A). Although most of the genes in respiratory electron transport and tricarboxylic acid cycle (TCA) was down-regulated, some genes including *LDHA*, *SLC16A3* and *PDK3*, pyruvate metabolism-associated genes [96], were up-regulated

suggesting an compensatory increased glucose consumption during LPS-induced mitochondrial dysfunction to restore cell energy status.

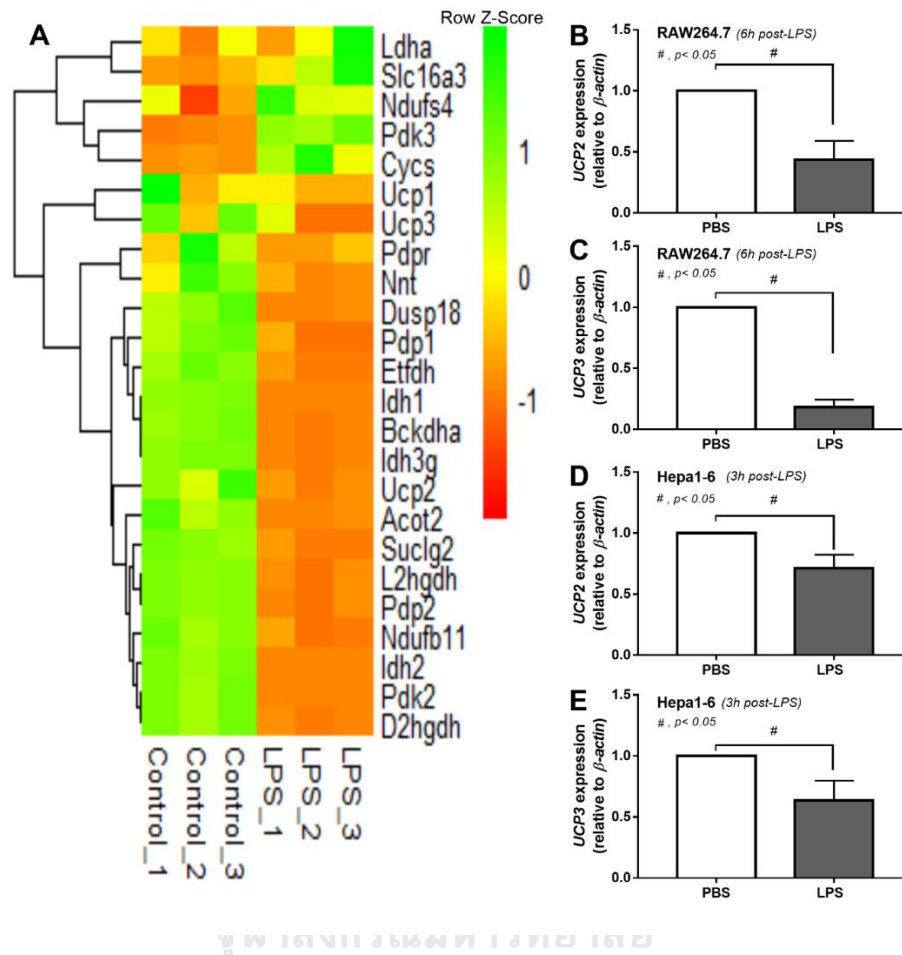


Figure 12. The transcriptome analysis in macrophages (RAW264.7) and UCP gene expression of in LPS-stimulated RAW264.7 and hepatocytes (Hepa 1-6).

The transcriptome analysis in macrophages (RAW264.7) presented by hierarchical clustering heat-map profiling groups focusing on oxidative phosphorylation and mitochondrial respiration-associated genes (A) and the gene expression of mitochondrial uncoupling proteins (UCP2 and UCP3) in macrophages and hepatocytes (Hepa1-6) (B-E) as determined by quantitative polymerase chain reaction (qPCR) in relative to expression of β -actin housekeeping gene are demonstrated (independent triplicate experiments were performed).

Due to the hepatic impacts in severe inflammatory responses [85, 97, 98] and the altered metabolic profiles in activated macrophages [95], LPS was stimulated in both macrophages and hepatocytes to further explore UCP gene expression. Indeed, a

down regulation of both *UCP2* and *UCP3* were also demonstrated in both macrophages and hepatocytes after LPS stimulation (Fig 12A-E). However, *UCP1* was non-detectable in both cells (data not shown). Due to the decrease expression of uncoupling proteins (*UCP2* and *UCP3*) during LPS stimulation, a supplement with mitochondrial uncoupling agents might be beneficial in the hyper-inflammatory status.

BAM15 reduced inflammatory responses (cytokines and pro-inflammatory M1 macrophage polarization) through the interference in macrophage metabolic profiles.

According to the cell viability assay using tetrazolium 3-(4, 5-dimethylthiazol-2-yl)-2,5-diphenyltetrazolium (MTT), BAM15 at the concentrations lower than 50 nM were non-toxic to macrophages (Fig 13A). Then BAM15 at 10 nM were further used in all of the *in vitro* experiments. The different incubation times of BAM15 were tested in RAW264.7 cells to investigate the kinetic effect of BAM15 on mitochondrial membrane potential (MMP) as determined by the staining with MitoTracker Red. As expected, BAM15 enhanced MMP at the early time point (0.5 and 1 hour post-BAM15) then downregulated at 24-hour post-BAM15 with the reduction of supernatant cytokines (Fig 13B-F). At 24 hours after BAM15, there were the reduction in supernatant cytokines (IL-6, TNF- α , IL-10) (Fig 14A-C) and pro-inflammatory markers of M1 polarization (*iNOS* and *IL-1 β*) with the enhancement in anti-inflammatory M2 polarization at 6 h post-LPS in macrophages (Fig 14E-H). Moreover, BAM15 also attenuated inflammatory responses after activation by the heat-killed microbes; including *Escherichia coli*, *Staphylococcus aureus* and *Candida albicans* despite the difference in pro-inflammatory activity (Fig 14I-K)

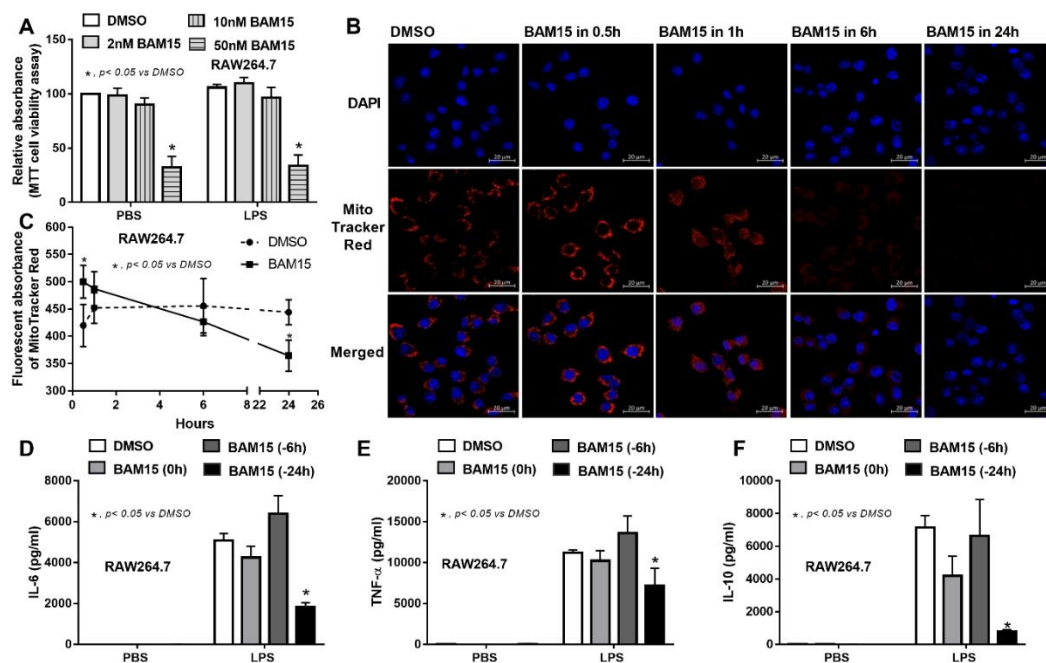


Figure 13. The *in vitro* optimization of BAM15 on macrophages (RAW264.7).

BAM15 or DMSO in the different concentrations were incubated with macrophages for 24 h before cell viability tested with tetrazolium 3-(4, 5-dimethylthiazol-2-yl)-2, 5-diphenyltetrazolium (MTT) assay (A). Mitochondrial membrane potential (MMP) measurement in different time of BAM15 incubation by MitoTracker Red CMXRos as demonstrated by the representative fluorescent pictures with the fluorescent absorbance score (B, C) and the supernatant cytokines from macrophages with the pre-treatment of BAM15 (10 nM) at the different time-points before LPS administration (D-F) are demonstrated (independent triplicate experiments were performed).

In parallel, 6 h LPS stimulation decreased mitochondrial functions (oxygen consumption rate; OCR) but enhanced glycolysis activity (extracellular acidification rate; ECAR) when compared with PBS negative control (Fig 15A, B) supporting the glycolysis-associated pro-inflammatory macrophages [69, 99]. The reduction of mitochondrial activity after LPS stimulation was also indicated by the decrease in several extracellular flux analysis parameters including basal respiration, maximal respiration (a short period of mitochondrial activity enhancement with FCCP) and respiratory reserve (an ability to enhance mitochondrial activity from the baseline

level) (Fig 15C-E). Due to the increased pro-inflammatory activities with decreased mitochondrial function in LPS-stimulated macrophages, mitochondrial ATP production and total ATP in macrophages were decreased (Fig 15F, G) along with a compensatory increased glycolysis as indicated by increased lactate (Fig 15H), an end product of glycolysis [100]. Then, BAM15 reduced cell energy in macrophages with LPS or PBS (Fig 15A-H) but BAM15 decreased cytokine production and pro-inflammatory features only in LPS-stimulated cells, but not control cells with PBS (Fig 14B-K).

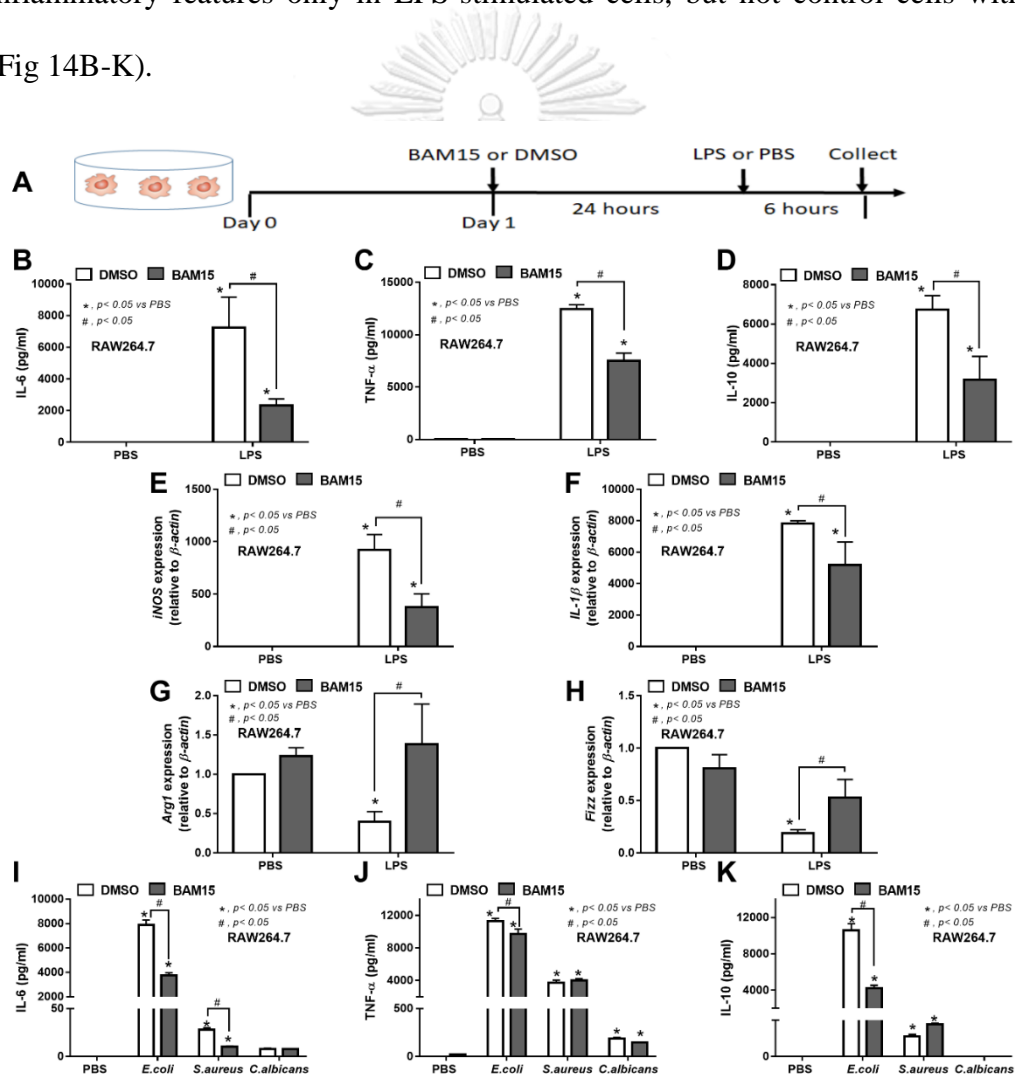


Figure 14. The anti-inflammatory effect of BAM15 in macrophages (RAW264.7).

The responses of macrophages (RAW264.7) with 24 h BAM15 (or DMSO control) pre-treatment prior to 6 h-LPS stimulation (or PBS) as displayed by schematic diagram (A) and

evaluated by supernatant cytokines (B-D) and gene expression of pro-inflammatory M1 (*iNOS* and *IL-1 β*) or anti-inflammatory M2 (*Arg-1* and *Fizz*) macrophage polarization using quantitative polymerase chain reaction (qPCR) in relative to expression of *β -actin* housekeeping gene (E-H) are demonstrated (independent triplicate experiments were performed). In similar experimental designs, the responses of macrophages against the heat-killed microbes including *Escherichia coli*, *Staphylococcus aureus* and *Candida albicans* (I-K) are also demonstrated (independent triplicate experiments were performed).

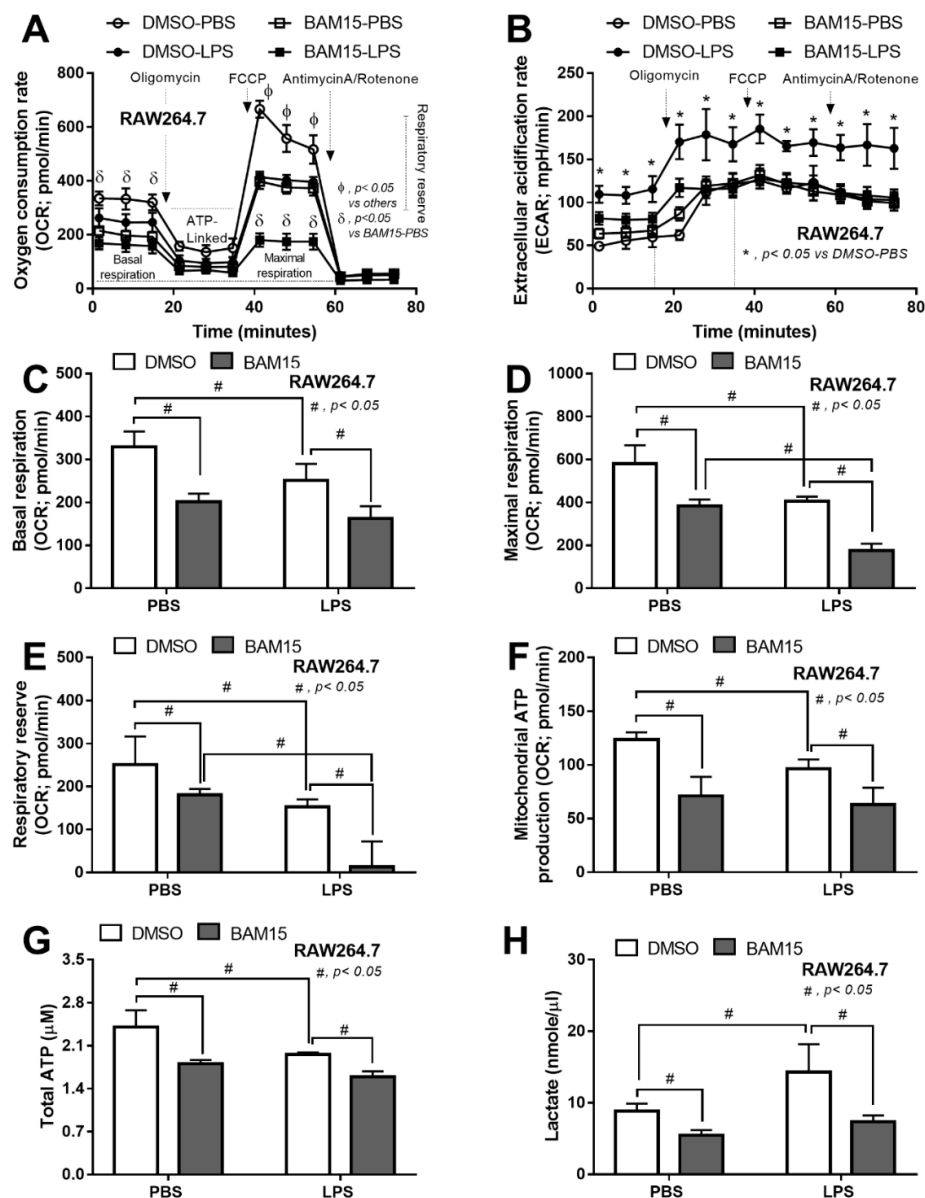


Figure 15. The cell energy analysis of LPS-stimulated macrophages (RAW264.7) with BAM15 pre-treatment.

The extracellular flux analysis pattern of macrophages (RAW264.7) with 24 h BAM15 (or DMSO control) pre-treatment prior to 6 h-LPS stimulation (or PBS) as evaluated by oxygen

consumption rate (OCR) of mitochondrial stress test for mitochondrial pathway analysis (A) and extracellular acidification rate (ECAR) of glucose stress test for glycolysis pathway analysis (B) with the parameters of mitochondrial activities including basal respiration, maximal respiration and mitochondrial reserve (C-E) are demonstrated (independent triplicate experiments were performed). Additionally, the mitochondrial ATP production using the extracellular flux analysis (F), total ATP production (chemiluminescent assay) (G) and supernatant lactate (colorimetric assay) (H) are indicated (independent triplicate experiments were performed).

BAM15 interfered hepatocyte metabolic profiles and attenuated septic severity in LPS injection mouse model, partly through an enhanced AMPK in liver.

Because of the liver accumulation of BAM15 [3] and the importance of hepatocytes in pro-inflammatory sepsis [85], effect of BAM15 on hepatocytes were evaluated. Indeed, LPS induced inflammatory cytokines and *iNOS* expression in hepatocytes (Fig 16A-C), supported the LPS inflammatory activation [92]. Then, BAM15 attenuated these parameters, but not an anti-inflammatory IL-10 (Fig 16A-C). In parallel, LPS reduced mitochondrial function (OCR) in hepatocytes (Fig 17A-E), similar to LPS-stimulated macrophages (Fig 15A-E), but LPS did not enhanced hepatic glycolysis activity (ECAR) (Fig 17A-E), different from LPS-stimulated macrophages (Fig 15A-E) perhaps due to hepatic glycogen storage. Additionally, LPS reduced basal respiration, maximal respiration, respiratory reserve and mitochondrial DNA production (Fig 17C-F) but did not decrease total hepatocyte ATP and lactate production (Fig 17G, H), different from LPS-stimulated macrophages (Fig 15G, H), possibly due to the prominent compensation by potent hepatic glycolysis [101, 102]. BAM15 partly reduced hepatocyte mitochondrial function (decreased glycolysis reserve but not basal and maximal respiration) and decreased other metabolic profiles (glycolysis activity, mitochondrial ATP production, total hepatocyte ATP and lactate

production) (Fig 17C-H). Hence, BAM15 attenuated inflammatory responses both in macrophages and hepatocytes through the cell-energy interference.

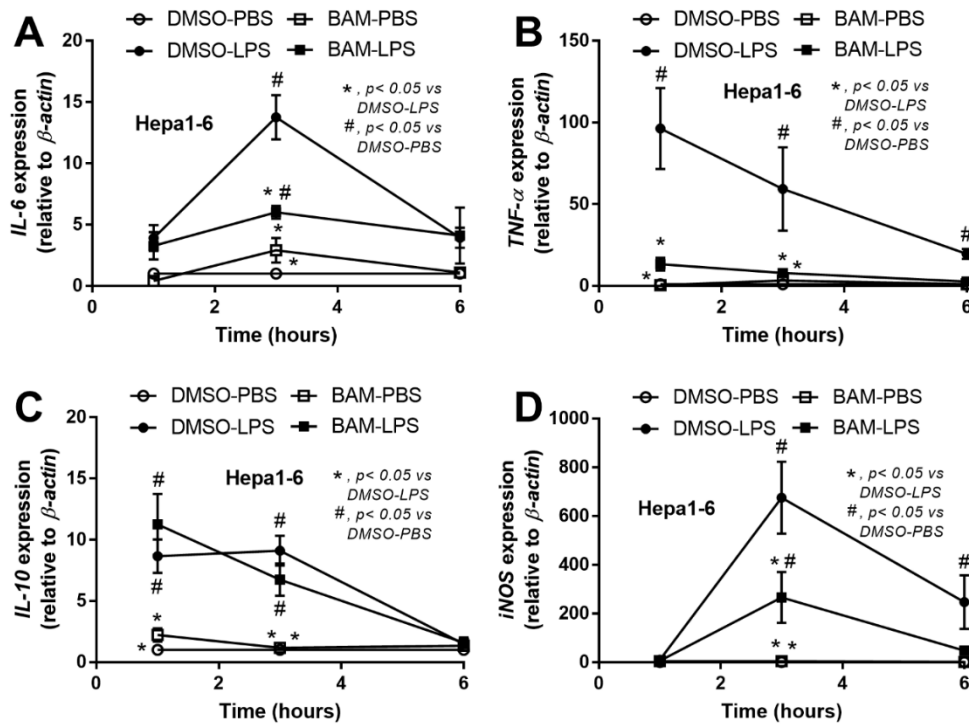


Figure 16. The anti-inflammatory effect of BAM15 in hepatocytes (Hepa 1-6).

The responses of hepatocytes (Hepa 1-6) with 24 h BAM15 (or DMSO control) pre-treatment prior to 6 h-LPS stimulation (or PBS) as evaluated by gene expression of cytokines (*IL-6*, *TNF- α* and *IL-10*) and inducible nitric oxide synthase (*iNOS*) using quantitative polymerase chain reaction (qPCR) in relative to expression of β -actin housekeeping gene are demonstrated (independent triplicate experiments were performed).

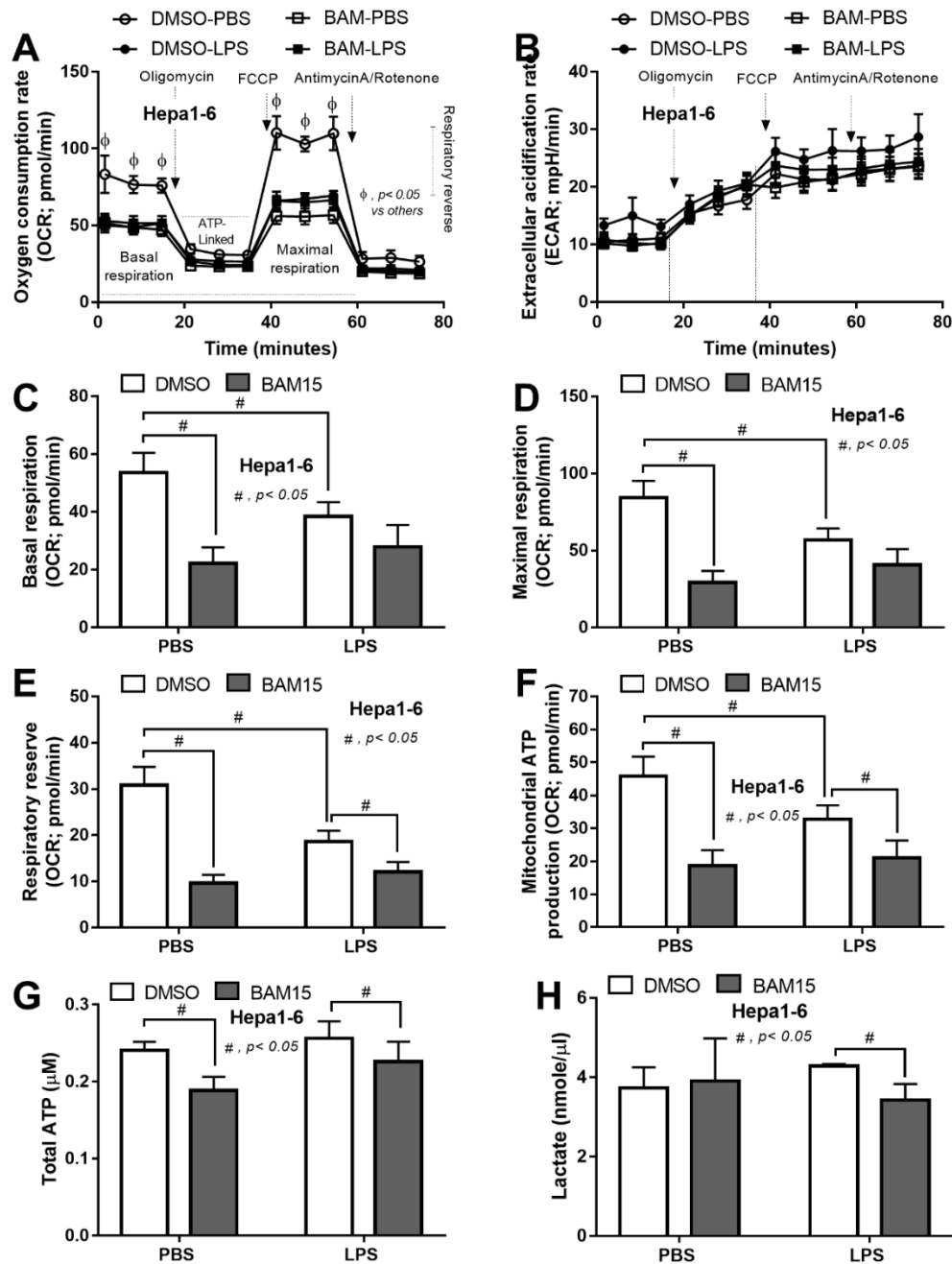


Figure 17. The cell energy analysis of LPS-stimulated hepatocytes (Hepa 1-6) with BAM15 pre-treatment.

The extracellular flux analysis pattern of hepatocytes (Hepa 1-6) with 24 h BAM15 (or DMSO control) pre-treatment prior to 6 h-LPS stimulation (or PBS) as evaluated by oxygen consumption rate (OCR) of mitochondrial stress test for mitochondrial pathway analysis (A) and extracellular acidification rate (ECAR) of glucose stress test for glycolysis pathway analysis (B) with the parameters of mitochondrial activities including basal respiration, maximal respiration and mitochondrial reserve (C-E) are demonstrated (independent triplicate

experiments were performed). Additionally, the mitochondrial ATP production using the extracellular flux analysis (F), total ATP production (chemiluminescent assay) (G) and supernatant lactate (colorimetric assay) (H) are indicated (independent triplicate experiments were performed).

In correspondence to the *in vitro* anti-inflammation, BAM15 attenuated systemic inflammatory cytokines (IL-6 and TNF- α but not anti-inflammatory IL-10) along with liver and kidney injury (liver enzymes and serum creatinine) (Fig 18A-F). Because BAM15 is accumulated in liver and excrete through kidney [3], the anti-inflammatory effect of BAM15 in these organs might be more prominent. Indeed, the reduced inflammatory cytokines (IL-6 and TNF- α) and increased anti-inflammatory IL-10 in liver and kidney were demonstrated (Fig 18G-L). Additionally, other systemic injury parameters such as aspartate transaminase, alanine transaminase and creatinine also significantly attenuated with BAM15. Because most of the cell-populations in liver is hepatocytes (liver parenchymal cells) with only 15% of Kupffer cells (immune cells) and other non-parenchymal cells (supporting cells) [103, 104], the lysate of liver tissue is used as a representative of hepatocytic protein expression. As such, LPS increased hepatic AMP-activated protein kinase (AMPK), an anti-inflammatory metabolic sensor of ATP depletion [105, 106] (Fig 19A), possibly counteracted against the LPS pro-inflammatory effect (Fig 16F, G). The higher liver AMPK (Fig 19A) was another mechanism of BAM15 anti-inflammation in systemic infection. Likewise, BAM15 also reduced hepatic accumulation of inflammatory macrophages (CD11b positive, Ly6C positive), but not the total macrophages (F4/80 positive), of LPS-administered mice (Fig 19B-D). Hence, BAM15 is an interesting candidate for anti-inflammatory adjunctive treatment in sepsis.

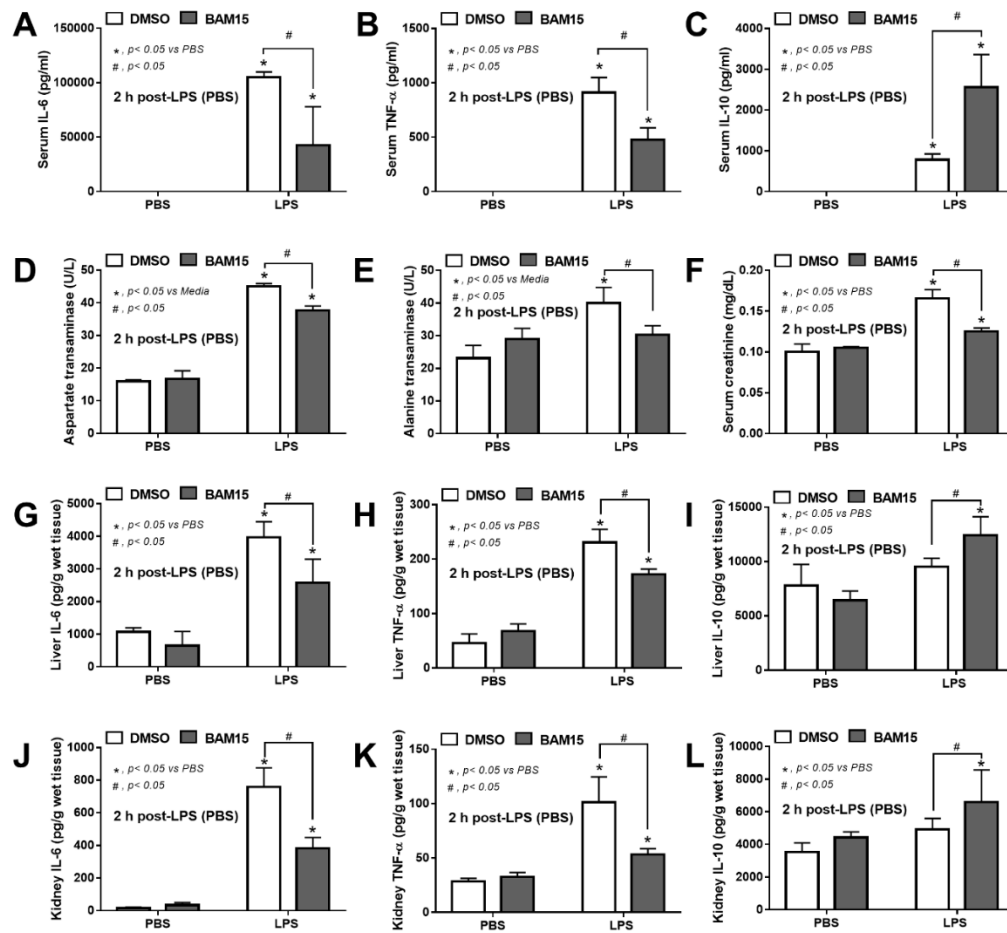


Figure 18. BAM15 ameliorated the severity of LPS-administered mice.

The severity of mice with intraperitoneal (IP) injection of BAM15 (1 mg/kg) or DMSO (10%) at 3 h prior to the intraperitoneal administration of LPS or PBS as evaluated by serum cytokines (A-C), liver enzymes (aspartate transaminase and alanine transaminase) (D, E), kidney injury (serum creatinine) (F) and cytokines in livers and kidneys (G-L) are demonstrated (n = 6-8 mice/group).

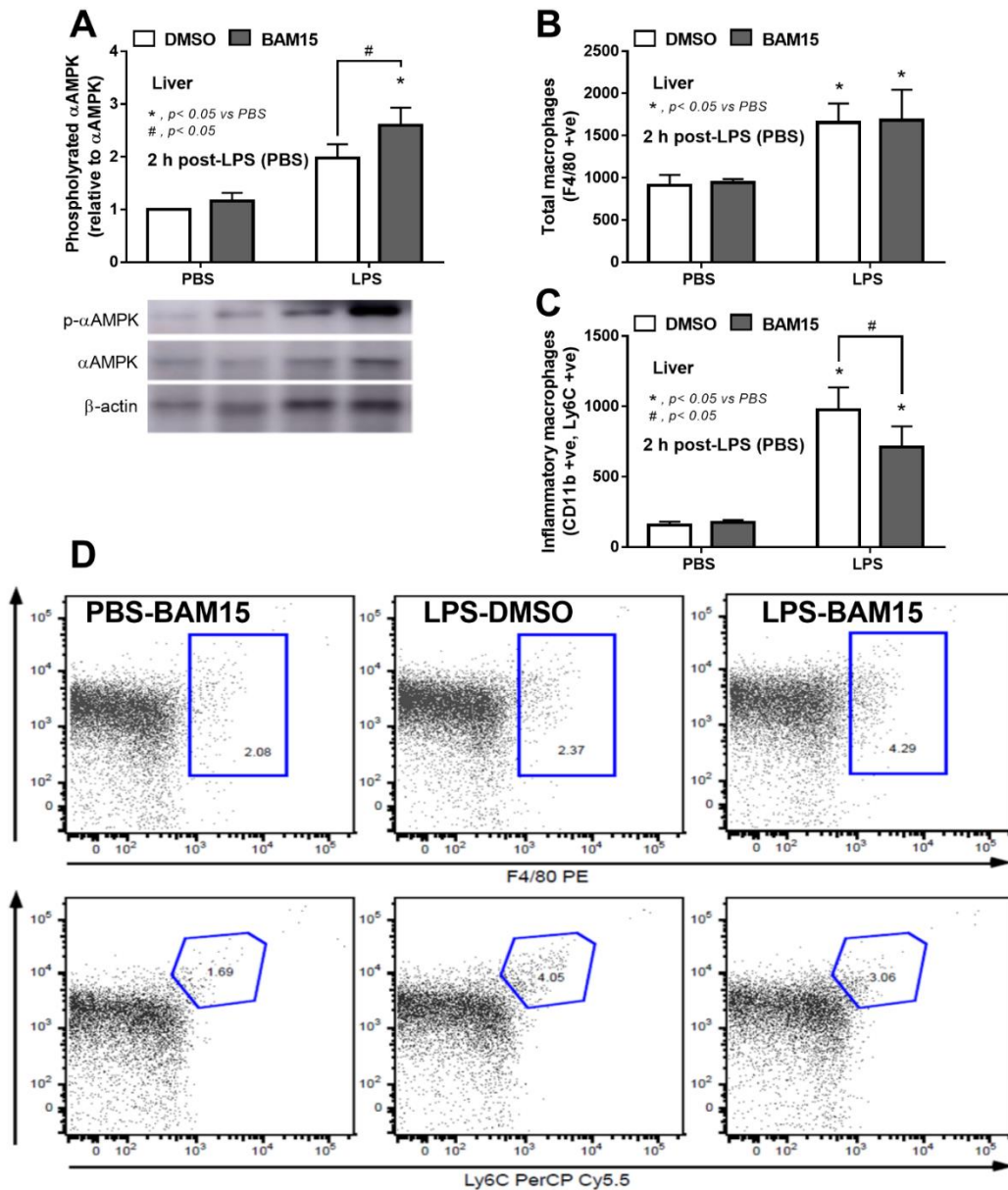


Figure 19. The increased abundance of activated AMPK in liver and flow cytometry analysis of LPS-administered mice with BAM15 pretreatment.

The abundance of hepatic phosphorylated AMP-activated protein kinase in alpha isoform (p- α AMPK) from mice with intraperitoneal (IP) injection of BAM15 (1 mg/kg) or DMSO (10%) at 3 h prior to intraperitoneal administration of LPS or PBS by Western blot analysis in relative ratio to total α AMPK along with the β -actin internal control with the representative blotting picture (A) and the flow cytometry analysis from liver for total and inflammatory monocytes/macrophages using F4/80 positive (F4/80+ve) and CD11b positive with Ly6C positive (Ly6C+ve, CD11b+ve), respectively, with the representative flowcytometry pattern

(B-D) are demonstrated (n=4-6 /group). The representative flowcytometry pattern of PBS-DMSO was not presented due to the similarity to PBS-BAM15.

Discussion

BAM15, a mitochondrial uncoupling agent attenuated the severity of LPS injection mouse model through the reduction of mitochondrial activity and cell energy status in macrophages and hepatocytes.

The downregulation of mitochondrial uncoupling proteins (UCP) after LPS stimulation, a possible natural balance against LPS-induced pro-inflammation.

Although mitochondria is an important source of the cellular ATP production through the electrochemical proton-gradient in oxidative phosphorylation process (OXPHOS), the dissipation (leakage) of proton away from the OXPHOS cycle reduces the effectiveness of ATP synthesis [107]. The leaked-protons also increase cell injury from increased reactive oxygen species [81]. Mitochondrial uncoupling proteins transfer the proton into OXPHOS cycle results in a quick boost-up of ATP synthesis but following by a rapid ATP reduction [76, 79, 108] leads to a reduction of cell responses [74]. As such, UCP2 depletion in the transgenic mice increased *IL-1 β* and *IL-6* [109] and *UCP2* over-expression suppresses *IL-6* and *Bcl-2* that attenuates cerebral ischemic injury [82]. Likewise, the decreased-cell energy status leads to the reduction in cytokine production in macrophages is also demonstrated [87].

Here, LPS downregulated *UCPs* (mitochondrial function), in either macrophages or hepatocytes, but enhanced glycolysis and reduced cell energy status only in macrophages but not in hepatocytes. While LPS could enhance glycolysis in macrophages (glycolysis-dependent macrophage pro-inflammation) [69, 99], LPS could not further increase hepatic glycolysis possibly because of the lower hepatic

cytokine production ability and the more dominant hepatic glycolysis when compared with macrophages [101, 102, 110]. Although the different LPS-activated metabolic responses between macrophages and hepatocytes is out of our scope, these data suggest the prominent role of mitochondrial uncoupling proteins in both cells which is a possible target for sepsis immune regulation.

BAM15, a synthetic mitochondrial uncoupling agent, attenuated inflammation in macrophages and hepatocytes by suppressing both mitochondrial function and glycolysis.

Hyper-inflammatory responses in sepsis is a main cause of the high mortality and the pro-inflammatory attenuation, especially against macrophages, are mentioned [13, 14]. Currently, the metabolism modification is an interesting strategy to harness macrophage responses as an alteration of the main energy metabolism from mitochondria to glycolysis in pro-inflammatory M1 macrophages is well-known [69, 99]. Not only energy generation and thermogenesis, an impact of mitochondria toward immune responses is well described [71]. Here, a mitochondrial uncoupling agent (BAM15) attenuated inflammation via the suppression on cell energy status on mitochondria and glycolysis activity supported previous publications [79, 111]. Our model demonstrated that BAM15 increased cell energy status at the early time point (less than 1 hour post-BAM15) similar to the previous report [3, 84]; however, the cell energy was reduced at 24 hours post-BAM15 resulting in the anti-inflammatory characteristics. Hence, this discrepancy might be explained by the difference in dose of BAM15, the activation time of BAM15 treatment and the cell type used in the studies. These data suggested an importance of the delivery methods for BAM15 administration in the clinical utilization. Perhaps, the theoretically enhanced

mitochondrial-functions (the energy boost-up) by proton transfer from uncoupling agents, might be very transient and, in contrast, the uncoupling agents might eventually result in mitochondrial energy-exhaustion and anti-inflammatory characteristics [72, 73, 112, 113]. Indeed, the increased pyruvate-influx into tricarboxylic acid cycle using dichloroacetate (DCA) results in a more sustainable enhanced-OXPHOS, in comparison with the uncoupling proteins, improves bactericidal activity [114] but does not improve clinical outcomes in patients with sepsis [115] possibly due to the increased cytokine production [116]. These data demonstrated the diverse responses between the different strategies on mitochondria. Notably, the organism control by antibiotics during sepsis adjunctive anti-inflammatory treatment is very important as the pro-inflammatory cytokines are necessary for organismal eradication [117]. Similar to our results with BAM15, the reduced mitochondrial function indirectly decreased glycolysis due to the compensatory increased pyruvate-influx into mitochondria which reduced pentose phosphate pathways of glycolysis as demonstrated by the reduced lactate after treatment with niclosamide ethanolamine (NEN) and oxyclozanide (the mitochondrial uncoupling agents) [118]. Because BAM15 attenuated inflammatory cytokines in both macrophages and hepatocytes and downregulates pro-inflammatory M1 macrophage polarization, BAM15 was interesting for anti-inflammatory treatment in the hyper-inflammatory status.

Administration of BAM15 attenuated the severity of LPS injection mouse model.

Despite BAM15 anti-inflammatory in several models [2, 3, 84], BAM15 has never been tested in LPS-induced inflammation. Here, BAM15 attenuates both systemic and local inflammation as indicated by pro-inflammatory cytokines in serum

and in organs (livers and kidneys), respectively, along with liver enzymes and serum creatinine. Additionally, BAM15 anti-inflammatory property was also demonstrated through the non-reduction of IL-10 both in serum and in organs, possibly due to the enhanced anti-inflammatory M2 macrophage polarization from BAM15. Likewise, an administration of UCP2, a natural mitochondrial uncoupling protein, also enhances IL-10 and facilitates M2 polarization in microglia and in RAW264.7 [119, 120]. Perhaps, the glycolysis reduction is not only down-regulate M1 macrophage polarization but also induced M2 polarization during inflammatory activation [68-70]. The prominent IL-10 in both kidneys and livers in LPS-administered mice was also possibly due the BAM15 accumulation in both organs [3], which demonstrated a potent anti-inflammatory local effect on both organs, the most common organ failure in severe infection [85, 121, 122]. Since liver is an important organ associated with sepsis pro-inflammation (producing acute phase proteins and complements) and thermoregulation [123], the reduced hepatic energy status might activate AMP-activated protein kinase (AMPK), a metabolic sensor for ATP depletion [105, 106]. Indeed, LPS slightly enhanced liver AMPK and BAM15 further increased liver AMPK which might amplify anti-inflammatory responses [124, 125]. Indeed, AMPK, an activated molecule during the depleted cell energy status, induces several processes to maintain the energy homeostasis and prevent cell damages in several models (sepsis, hepatic ischemic reperfusion, acute kidney disease) [126-128] through multiple mechanisms; including autophagy induction with apoptosis down-regulation, enhancement of the alternative sources for cell energy (lipolysis and fatty acid oxidation) and reduction in oxidative stress and inflammatory signaling [129-133]. Overall, AMPK anti-inflammatory effect is a cell adaptation to reduce the energy

utilization (decreased cytokine production) due to an energy in-sufficient condition [87]. Notably, we did not observe LPS induced hepatic lipid accumulation (data not shown) which was consistent with a previous publication [134]. Although the histological injury score of livers and kidneys along with survival rate in our LPS injection model did not improved by BAM15 possibly due to the non-lethality of the model, our result is a proof of concept supporting BAM15 as an interesting candidate for sepsis anti-inflammatory drug. More studies are warrant.

In conclusion, an anti-inflammatory property of a mitochondrial uncoupling agent (BAM15) was demonstrated as an example of anti-inflammatory induction through an interference of cell metabolic profile. BAM15 attenuated the severity of inflammation through the reduction of energy status in macrophages and hepatocytes. Further studies on the control of immune responses through cell metabolism in sepsis are interesting.

Part III: Non-Thermal Atmospheric Pressure Argon-Sourced Plasma Flux Promotes Wound Healing of Burn Wounds and Burn Wounds with Infection in Mice through the Anti-Inflammatory Macrophages

Published in Applied Science, 2021 Jun 9; vol.11(12), 5343.

Cong Phi Dang¹, Sirapong Weawseetong², Awirut Charoensappakit¹, Kritsanawan Sae-Khow¹, Decho Thong-Aram³ and Asada Leelahavanichkul^{1,4,*}

¹ Medical Microbiology, Interdisciplinary and International Program, Graduate School, Chulalongkorn University, Bangkok 10330, Thailand;

² Department of Microbiology, Faculty of Medicine, Chulalongkorn University, Bangkok 10330, Thailand;

³ Department of Nuclear Technology, Faculty of Engineer, Chulalongkorn University, Bangkok 10330, Thailand;

⁴ Translational Research in Inflammation and Immunology Research Unit (TRIRU), Department of Microbiology, Chulalongkorn University, Bangkok 10330, Thailand

*Correspondence: aleelahavanit@gmail.com; Tel.: +66-2-256-4251; Fax: +66-2-252-6920

Abstract:

Plasma medicine is the utilization of gas ionization that might be beneficial for the treatment of burn wounds, a healthcare problem with a significant mortality rate. Due to a lack of information on the impact of plasma flux in immune cells and a high prevalence of bacterial infection in burn wounds, non-thermal argon-based plasma flux was tested on macrophages (RAW246.7) and in mouse models of burn wounds with or without *Staphylococcus aureus* infection. Accordingly, plasma flux enhanced reactive oxygen species (ROS), using dihydroethidium assay, and decreased abundance of NF- κ B-p65 (Western blot analysis) in non-stimulating macrophages. In parallel, plasma flux upregulated IL-10 gene expression (an anti-inflammatory cytokine) in lipopolysaccharide (LPS)-induced inflammatory macrophages, while downregulating the pro-inflammatory cytokines (IL-1 β and IL-6). Additionally, plasma flux improved the migratory function of fibroblasts (L929) (fibroblast scratch assay) but not fibroblast proliferation. Moreover, once daily plasma flux administration for 7 days promoted the healing process in burn wounds with or without infection (wound area and wound rank score). Additionally, plasma flux reduced tissue cytokines (TNF- α and IL-6) in burn wounds with infection and promoted collagen in burn wounds without infection. In conclusion, plasma flux induced anti-inflammatory macrophages and promoted the burn-wound healing process partly through the decrease in macrophage NF- κ B. Hence, plasma flux treatment should be tested in patients with burn wounds.

Keywords: non-thermal plasma; inflammation; macrophage; burn wounds

1. Introduction

Plasma is a completely or partly ionized gas that is categorized as the fourth state of matter in addition to solid, liquid and gas [135]. A plasma is a state of matter that is similar to a gas in terms of its ability to change volume and shape, but unlike a gas, it is made up of groups of positively and negatively charged particles [135]. Plasma flux is utilized in medicine (plasma medicine) [135] and may be operated at normal atmospheric pressure with temperatures between 30 and 40 °C, which are appropriate for use on live organisms without toxicity and are referred to as “non-thermal plasma therapy” [136]. Generating plasma by ionization of gas can induce various active molecules, including reactive oxygen species (ROS) and reactive nitrogen species (RNS), without heat production [137]. Concentrations of the active molecules are adjustable by the different properties of plasma depending on different kinds of gas sources, power supply voltages and currents that are suitable for several specific purposes, ranging from enhanced cell proliferation to the induction of programmed cell death [138-141].

Non-thermal plasma does not destroy normal cells but selectively eliminates only severely injured cells or cancer cells, at least in part, due to the prominent stress-induced ROS in these cells [142-144]. Additionally, reactive species molecules of non-thermal plasma also demonstrate bactericidal activity, regardless of the antibiotic resistant properties of the organisms [145]. Plasma flux is used in numerous medical situations (malignancy, wound care, and organismal management) due to its ability for selective elimination and enhanced proliferation of abnormal and healthy cells, respectively, with additive bactericidal activity [136]. As such, plasma flux enhanced re-epithelialization, collagen synthesis, angiogenesis and the anti-inflammatory status in a rodent wound model [146], partly through the induction of several growth factors

in keratinocytes [147]. Hence, non-thermal plasma therapy is an emerging treatment strategy [1,2,12], especially for diabetic wounds [148] and burn injuries [149]. Indeed, a burn wound, a dermal injury from extreme insults (heat, erosive agents or electricity) is classified upon the depth of the wound damage (superficial, partial thickness and full thickness) and leads to several severe complications, including hypovolemia, hypermetabolism, gut permeability defect and opportunistic infections [150]. Unfortunately, the prevalence of burn wounds remains high, particularly among low- and middle-income households, with chronic wound care and treatment for sequelae having a disproportionately large economic cost [151]. In order to reduce burn injury mortality rates and country burdens, proper wound care is needed. Interestingly, secondary bacterial infection in burn wounds is one of the major complications, especially with a, currently, high prevalence of anti-microbial resistance [152]. Fortunately, the antibiotic resistant organisms are still vulnerable to microbial eradication with several physical strategies, including ultraviolet light, radiation and non-thermal plasma [153, 154]. Hence, the evaluation of plasma flux on infected burn wounds is interesting. Despite extensive evaluations of plasma flux in several models of traumatic wounds [155], data of non-thermal plasma on infected burn wounds are still lacking.

In parallel, macrophages are the immune cells responsible for either organismal control or the wound healing process, which can be manipulated by non-thermal plasma therapy as demonstrated in a solid cancer model [156]. As such, macrophages are immune cells with pleomorphic functions, referred to as “macrophage polarization”, that consist of pro-inflammatory M1 and anti-inflammatory M2 polarization [68]. The induction of macrophage polarization into a

proper direction for each situation might be beneficial. For example, an acceleration of M1 and M2 for the conditions with immune exhaustion (tumor micro-environments) and hyper-immune responses (infection), respectively, might improve clinical outcomes [13]. In wounds with infection, pro-inflammatory M1 polarization is necessary for organismal control but excessive pro-inflammation worsens the wound healing process [157]. With proper organismal control, M2 macrophages or anti-inflammatory macrophages enhance several processes (anti-inflammation, debris removal and matrix remodeling) and promote wound healing [157]. Because (i) non-thermal plasma can induce an anti-inflammatory wound status with bactericidal activity that might be beneficial for wound healing and (ii) due to the lack of data of the effect of plasma on macrophage function, plasma flux treatment in burn wounds with infection is interesting. Hence, non-thermal plasma was tested with *in vitro* experiments, using macrophages (RAW264.7 cell line) and fibroblasts (L929 cell line), and also evaluated *in vivo*, using burn wound mouse models with or without infection.

2. Materials and Methods

2.1. Animal Model and Plasma Flux Generator

C57BL/6 mice, purchased from Nomura Siam International (Pathumwan, Bangkok, Thailand), were used following an approved animal protocol from the Institutional Animal Care and Use Committee of the Faculty of Medicine, Chulalongkorn University, Bangkok, Thailand. The burn wound mouse models with and without infection were performed in accordance with the previous publications [158, 159]. Briefly, in burn wound models without infection, an aluminum rod 1 cm in diameter was heated to 100 °C, using a dry block heater (Thermo fisher Scientific,

Waltham, MA, U.S.A.) for 5 min before placing on a shaved area at the dorsal part of the mice under isoflurane anesthesia. After that, mice with the heated rod attached to the back were turned ventral upward to allow their own body weight to function as a controlled pressure on the heated rod for 20 s. In the infected wound model, the heated rod was placed with the same procedures of the non-infected wound model. Then, 1×10^7 CFU of *Staphylococcus aureus* (ATCC 25923, the American Type Culture Collection, Manassas, VA, U.S.A.) in 0.1 mL normal saline (NSS) was directly spread onto the wound 30 min after the injury, in accordance with a previous publication [26]. After 24 h, necrotic tissue at the burn wounds was removed in both wound models. Subsequently, treatment by non-thermal plasma flux for 30 s along with a visual evaluation of the wound was performed daily until the 7th day of experiments, when the mice were sacrificed via cardiac puncture under isoflurane anesthesia with sample collection (blood and tissue at the wound). For the in-house plasma generator, the machine was designed following the principle of atmospheric pressure plasma with alternating current (AC) electricity at 13 kHz in frequency, using argon gas flow to release the ionized, enriched gas [160] as demonstrated in the diagram (Figure 20A,B). In brief, the plasma jet was designed with two electrodes. The inner electrode was a tungsten rod with a diameter of 1 mm, while the outer electrode was a thin copper sheet in the shape of a ring, surrounding the borosilicate glass syringe as the dielectric material. To prevent arc generation during operation, the outer electrode was wrapped with a rubber band. The distance between the plasma source and substrate was 5 mm. The current of the output was approximately 0.5 mA with the square waveform. Argon flow was used during operation at a speed of 1.5 L/min.

2.2. Wound Injury Score and Gut Permeability Determination

The wound was macroscopically evaluated by direct visualization based on percentage of the injury area compared with the initial injury area at 24 h post-injury [161]. Due to the circular-shape of the wound, the wound area was calculated using wound diameters, which were measured by a Vernier caliper (Thermo fisher Scientific). Additionally, the wound rank score, a score for determination of inflammatory signs, was evaluated like a previous publication [161]. Briefly, the burn wound was assessed through 4 scoring criteria, including wound length and depth (wound closure assessment), wellness and redness (inflammatory degree evaluation), using a semi-quantitative scale of 0–3 for each characteristic. Because a gut permeability defect (gut leakage) in severe burn wounds is possible [162, 163], leaky gut was also tested in the models. As such, fluorescent isothiocyanate-dextran or FITC-dextran at 4.4 kDa (FD4, Sigma, St. Louis, MO, U.S.A.), a non-gastrointestinal absorbable substance, at 12.5 mg in 500 μ L sterile phosphate buffer solution (PBS) was orally administered at 3 h prior to the sacrifice. Then serum FITC-dextran was analyzed by fluorescent spectrometry with a Varioskan Flash microplate reader (Thermo Fisher Scientific). Presentation of an intestinal, non-absorbable substance in serum after oral administration demonstrated a gut permeability defect [95].

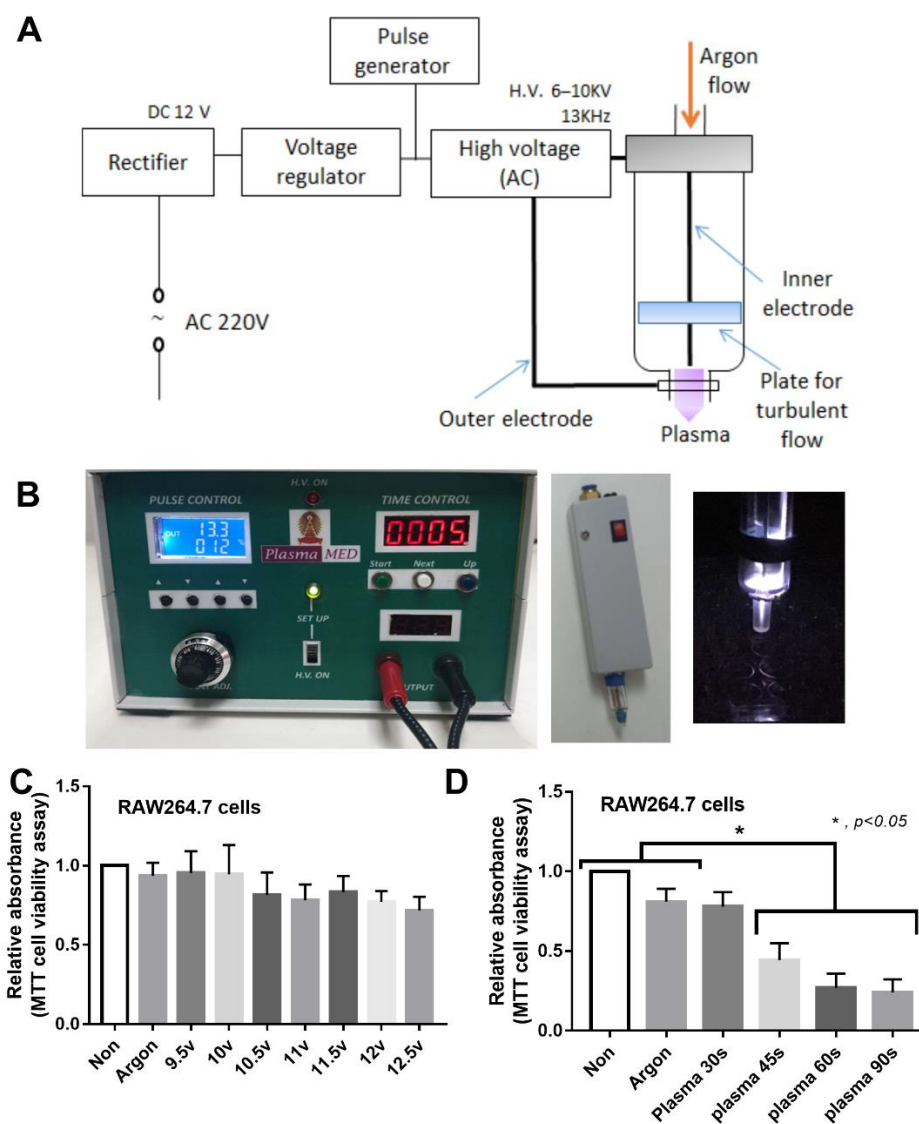


Figure 20. Schematic diagram of non-thermal atmospheric pressure plasma.

Component of plasma flux generator in schematic diagram (A) and the representative pictures of machine (B, left side) with an electrode-containing syringe (B, middle) and the electrode during plasma flux releasing (B, right side) are demonstrated. Cell viability test (MTT assay) in RAW264.7 cells after plasma flux treatment at 30 s at different voltage levels (C) and at 10 voltage with different exposure durations (in seconds) (D) compared with cells without stimulation (Non) or stimulation with argon gas alone without non-thermal plasma (Argon) are demonstrated. Independent triplicated experiments were performed.

2.3. Mouse Sample Analysis

The inflammatory cytokines in serum and in the wound tissue were evaluated, using Enzyme-linked Immunosorbent (ELISA) assay (Biolegend, San Diego, CA, U.S.A.). For cytokines in wound tissue, fresh skin samples were washed in PBS, weighted, homogenized and thoroughly sonicated. After that, a supernatant from the samples was used for cytokine evaluation. For bacterial burdens in the wound, tissue from the wound were weighed and minced into small pieces before being dissolved in PBS (1 g tissue per 1 mL PBS). After that, the samples were directly streaked onto a tryptic soy agar (TSA) plate (Oxoid, Thermo Fisher Scientific) in serial dilutions and incubated for 24 h at 37 °C before colony enumeration.

2.4. The In Vitro Experiments on Macrophages

Murine macrophages (RAW264.7) (TIB-71TM) (ATCC) were cultured in Dulbecco's Modified Eagle Medium (DMEM) supplemented with 10% heat-inactivated fetal bovine serum (FBS) (Thermo fisher Scientific) and Penicillin-Streptomycin in 5% carbon dioxide (CO₂) at 37 °C overnight. After that, the non-stimulated cells were used as a control group. Meanwhile, in the stimulated groups, macrophages at 2×10^5 cell/well were administered by plasma flux or argon gas alone (another control group) with different intensities and durations before cell collection. To determine the proper dose of plasma flux, the cell viability test after plasma flux administration was performed following a published protocol, using tetrazolium dye 3-(4, 5-dimethylthiazol-2-yl)-2, 5-diphenyltetrazolium (MTT) (Thermo Fisher Scientific) [33]. In brief, the cells in the 96-well plate at the indicated time-points were incubated with a MTT solution in the dark at 37 °C. After 2 h, the MTT solution was replaced by dimethyl sulfoxide (DMSO; Thermo Fisher Scientific) and the

dissolving purple color was measured by a Varioskan Flash microplate reader (Thermo Fisher Scientific) at OD 570 nm.

With the selected proper dose and duration of the plasma flux treatment, reactive oxygen species (ROS) in macrophages were determined by a dihydroethidium (DHE) fluorescent dye (Sigma-Aldrich, St. Louis, MS, U.S.A.) following a previous protocol [164]. In brief, DHE diluted in FBS free media at a concentration of 20 μ M was incubated with the cells at 37 °C for 20 min before analysis by the Varioskan Flash microplate reader (Thermo Fisher Scientific) at OD 520 nm. In parallel, the protein abundance of the possible downstream molecules of the ROS stimulation, including AMP-activated protein kinase (α AMPK) and nuclear factor kappa B (NF- κ B), was determined by Western blot analysis following a previous protocol [94]. Briefly, protein was extracted from the samples using a lysis buffer (radioimmunoprecipitation assay buffer; RIPA) in supplement with inhibitors of protease and phosphatase (Thermo Fisher Scientific). The protein concentration was measured via Bradford assay. Then, the samples were segregated in 10% SDS (sodium dodecyl sulfate) polyacrylamide gel and transferred into the nitrocellulose membrane. Thereafter, several primary antibodies against α AMPK, phosphorylated α AMPK, NF- κ B p65, phosphorylated NF- κ B p65 or the internal control β -actin (Cell signaling, Beverly, MA, U.S.A.) were incubated with the membrane prior to horseradish peroxidase (HRP)-conjugated second antibodies and visualized by chemiluminescence (Thermo Fisher Scientific). The qualification of the band intensity was calculated by Image Studio Lite Ver 5.2 software.

To test the effect of plasma flux on inflammatory responses, lipopolysaccharide (LPS), a potent inflammatory stimulator from Gram-negative bacteria, using LPS of

Escherichia coli 026: B6 (Sigma-Aldrich) at 100 ng/mL, or media control was added after plasma flux administration. The cell supernatant was used for cytokines measurement using ELISA assay (Biolegend) and the cells were collected to determine expression of several genes by quantitative polymerase chain reaction (qPCR) following a previous protocol [165], using Trizol and SYBR Green reagents. The list of primers is demonstrated in Table 3.

Primers	
<i>β-actin</i>	Forward 5'-CGGTTCCGATGCCCTGAGGCTCTT-3'
	Reward 5'-CGTCACACTTCATGATGGAATTGA-3'
Inducible nitric oxide synthase (<i>iNOS</i>)	Forward 5'-CCCTTCCGAAGTTTCTGGCAGCAGC-3'
	Reward 5'-GGCTGTCAGAGCCTCGTGGCTTTG-3'
Arginase 1 (<i>Arg-1</i>)	Forward 5'-CAGAAGAATG GAAGAGTCAG-3'
	Reward 5'-CAGATATGCA GGA GTCACC-3'
Found in inflammatory zone (<i>Fizz</i>)	Forward 5'-GCCAGGTCCTGGAACCTTTC-3'
	Reward 5'-GGAGCAGGGAGATGCAGATGAG-3'
Interleukin-1β (<i>Il-1β</i>)	Forward 5'-GAAATGCCACCTTTTGACAGTG-3'
	Reward 5'-TGGATGCTCTCATCAGGACAG-3'
Interleukin-10 (<i>Il-10</i>)	Forward 5'-GCTCTTACTGACTGGCATGAG-3'
	Reward 5'-CGCAGCTCTAGGAGCATGTG-3'
Transforming growth factor-β (<i>TGF-β</i>)	Forward 5'-CAGAGCTGCGCTTGCAGAG-3'
	Reward 5'-GTCAGCAGCCGGTTACCAAG-3'

Table 3. List of the primers for macrophage polarization.

2.5. The In Vitro Experiments on Fibroblasts

Murine fibroblasts (L929) (CCL-1™) (ATCC) were cultured in modified DMEM overnight, similar to RAW246.7 cells. For fibroblast scratch wound assay, the cells were seeded in a 24-well plate with 1×10^5 cell/well and incubated overnight to gain a monolayer with the cell confluence higher than 80%, following a previous publication [166]. The scratch in the culture plates was performed by gently scraping, using a 200 μ L pipette tip, on the cell layer. Then, the cell debris was washed with warm PBS and incubated with modified DMEM followed by plasma flux or argon gas without plasma. The gap between two edges of scratch was photographed over different time points to represent wound closure of the fibroblast.

In parallel, the impact of plasma on fibroblast proliferation was evaluated through the reduction in carboxy-fluorescein diacetate succinimidyl ester (CFDA-SE), a long-term fluorescent dye tracer of cells, in the daughter cells as previously published [167]. In brief, the fibroblasts were stained with 2 μ M CFDA-SE (Sigma-Aldrich) and diluted in warm PBS for 15 min at 37 °C in the dark. Then, the cells were washed twice by PBS and further incubated with warm media for 6 h prior to plasma flux treatment. The daughter cells were collected at 48 h after the plasma treatment for detecting fluorescent intensity by flow cytometry BD LSRII cytometer (BD Biosciences), using FlowJo software.

2.6. Statistical Analysis

GraphPad Prism 5.0 (GraphPad Software, Inc., San Diego, CA, U.S.A.) was used to generate graphs and statistical analysis of the experiments. The in vitro experiments were performed in three independent times and demonstrated by mean \pm standard error (SEM). Data analysis between two or more groups was assessed by

Student's t-test or one-way analysis of variance (ANOVA) with Tukey's analysis, respectively. The significance was determined by a p value of less than 0.05.

3. Results

The administration of non-thermal plasma flux promoted the healing process of burn wounds through several wound-healing promotion factors (anti-inflammatory macrophages and improved fibroblast migration).

3.1. Non-Thermal Plasma Flux Induced Anti-Inflammatory Macrophages and Fibroblast Migration, but Not Fibroblast Proliferation

An in-house non-thermal plasma flux generator, using argon gas in atmospheric pressure with adjustable plasma properties (electrical frequency and voltage), was developed (Figure 20A,B). Due to the importance of macrophages on the wound healing process, different plasma properties, titrated by voltages and durations, were applied on macrophages (RAW246.7 cell line) before the cell viability test (MTT assay, see method) to determine the proper dose of plasma flux. With the duration of the plasma treatment at 30 s, all of the selected input voltages, in a range between 9.5 and 12.5 volts (V), demonstrated a non-statistical difference on cell viability when compared with the control non-treatment (Non) or argon gas alone without non-thermal plasma (Argon) (Figure 20C). However, the power supply voltage below 10 V showed a tendency of more survived macrophages (Figure 20C). Input with 10 V (corresponding with the output of 10 kV) was applied in the different durations, from 30 s to 90 s, and a duration of less than 30 s demonstrated a decreased number of macrophage cell deaths (Figure 20D). Notably, argon gas alone did not affect the macrophages and only argon with 90 s is shown in Figure 20D. Subsequently, non-thermal plasma with 10 V input (10 kV output) for 30 s was

selected for further experiments. Because of the well-known enhanced ROS production by plasma flux [137], ROS in macrophages, using DHE fluorescent dye (see method), was measured. As expected, DHE in the plasma-treated macrophages was higher than the control conditions (Non and Argon) (Figure 21A).

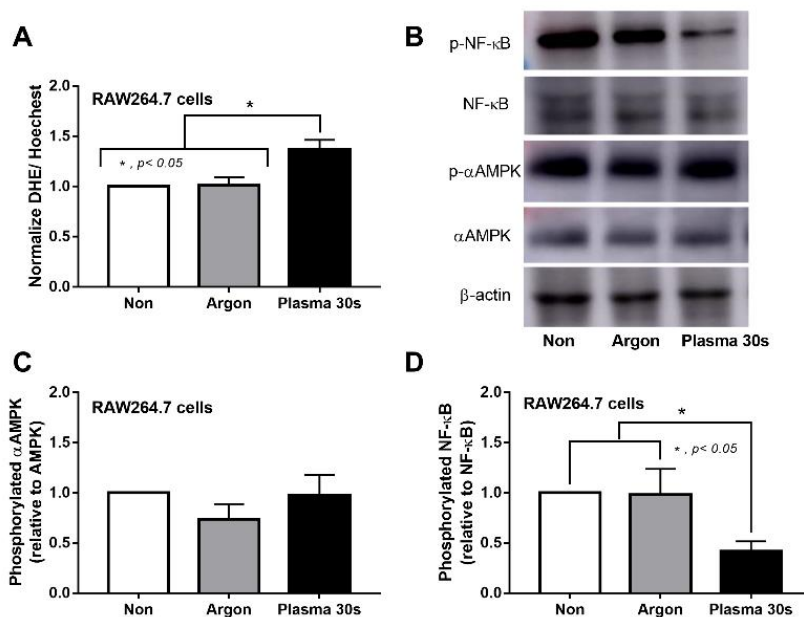


Figure 21. Characteristics of macrophages (RAW264.7 cells) without stimulation (Non) or after stimulation with argon gas alone (Argon) or plasma flux for 30 s (Plasma 30 s)

Characteristics of macrophages (RAW264.7 cells) without stimulation (Non) or after stimulation with argon gas alone (Argon) or plasma flux for 30 s (Plasma 30 s) as evaluated by intracellular reactive oxygen species (ROS) using dihydroethidium (DHE) fluorescent dye (neutralized by Hoechst nucleus staining dye) (A) and abundance of phosphorylated NF-κB-p65 (p-NF-κB) and phosphorylated-αAMPK (p-αAMPK) with the representative pictures of Western blot analysis (B–D) are demonstrated. Independently triplicated experiments were performed.

In parallel, the possible downstream signals of ROS, including AMPK (a protein sensing cell energy shortage and anti-inflammatory mediator) [87] and NF-κB

(a common proinflammatory transcriptional factor) [168] was determined. Accordingly, the abundance of activated NF- κ B (ratio of phosphorylated NF- κ B-p65/NF- κ B-p65), but not AMPK (ratio of phosphorylated α AMPK/total α AMPK), decreased after plasma flux administration (Figure 21B–D), implying a modulation of macrophage responses without cell energy alteration. Because of (i) an important transcriptional factor for cytokine production of NF- κ B [168] and (ii) a potent pro-inflammatory activating property of lipopolysaccharide (LPS), an organismal molecule [169], the effect of plasma flux on macrophages with or without LPS stimulation was tested. Accordingly, LPS induced pro-inflammatory cytokines (TNF- α and IL-6) with the peak levels at 24 h post-stimulation (Figure 22A,B). Meanwhile, LPS induced pro-inflammatory macrophage polarization as evaluated by expression of *IL-1 β* (peak level at 3–6 h post-LPS) and *iNOS* (peak level at 24 h Post-LPS) (Figure 22C,D). In parallel, LPS enhanced anti-inflammatory markers, including *IL-10* (similarly, between 3 and 24 h post-LPS) and *Arg-1* (peak level at 24 h post-LPS), but not *Fizz* and *TGF- β* (Figure 22E–H). Upregulation of anti-inflammatory *IL-10* was highest in LPS-stimulated macrophages with plasma flux (Figure 22E). Without LPS (PBS control), plasma flux mildly induced anti-inflammatory macrophages as determined by the upregulated *Fizz*, but not other genes (*IL-10*, *Arg-1* and *TGF- β*) (Figure 22E–H).

Due to the importance of fibroblasts in the wound healing process [143], the impact of plasma on fibroblasts (L929 cell line) was further tested. As such, wound closure as determined by fibroblast migration (the scratch wound assay), using the distance between each edge of fibroblast monolayer in cell culture plates, was lesser in the plasma treated group at 24 h post-treatment (Figure 23A,B). However, plasma

flux did not enhance fibroblast cell proliferation as evaluated by CFDA-SE fluorescent staining (Figure 23C,D).

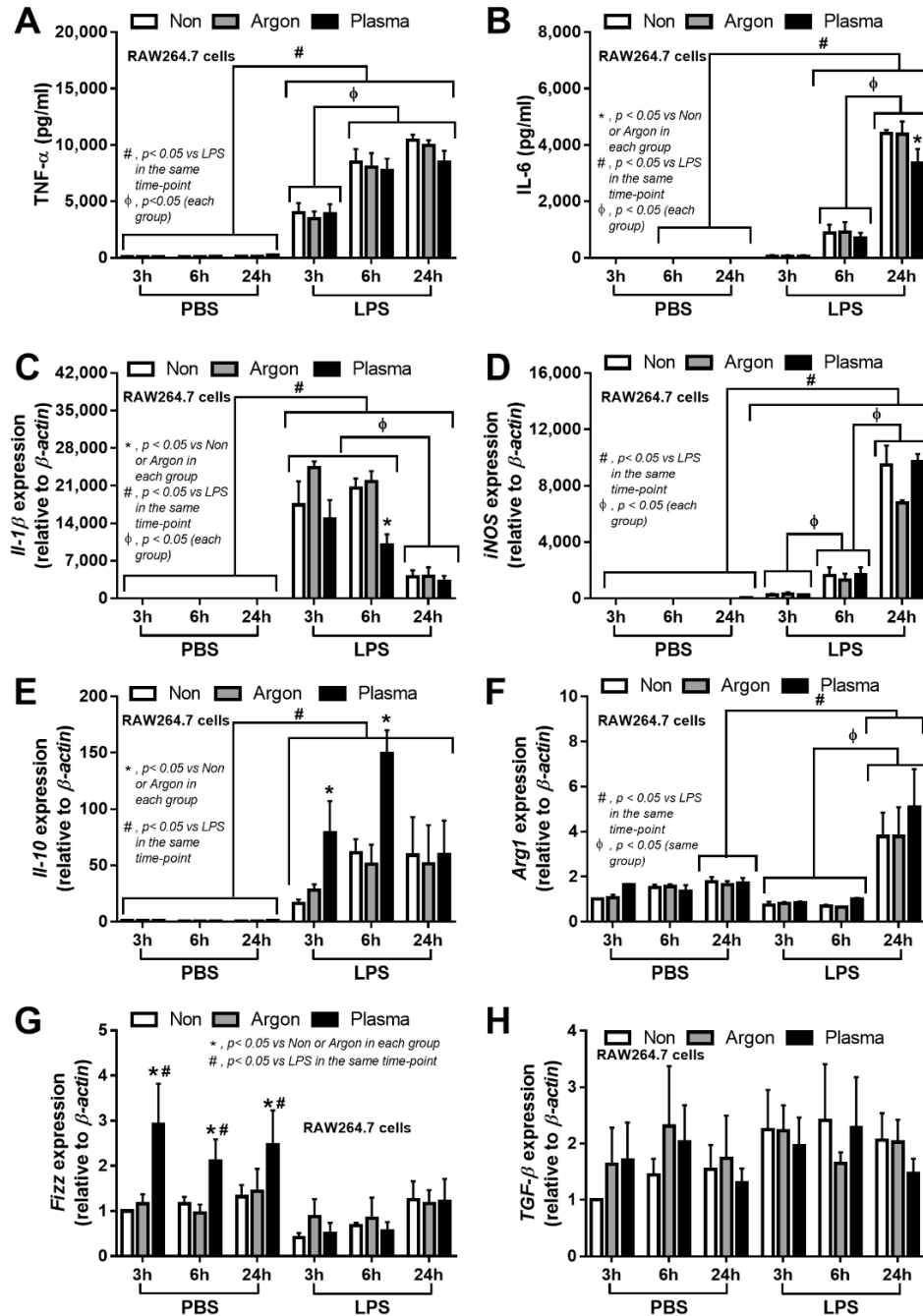


Figure 22. Responses of plasma-pretreated macrophages (RAW264.7 cells) to plasma treatment

Responses of plasma-pretreated macrophages (RAW264.7 cells) followed by stimulation with LPS or phosphate buffer saline (PBS) (negative control) at different time-points as evaluated by supernatant cytokines (TNF- α , IL-6) (A,B), gene expression of M1 macrophage polarization markers (*IL-1 β* and *iNOS*) (C,D) and M2 macrophage polarization markers (*IL-10*, *Arg1*, *Fizz* and *TGF- β*) (E-H) are demonstrated. Independently triplicated experiments were performed.

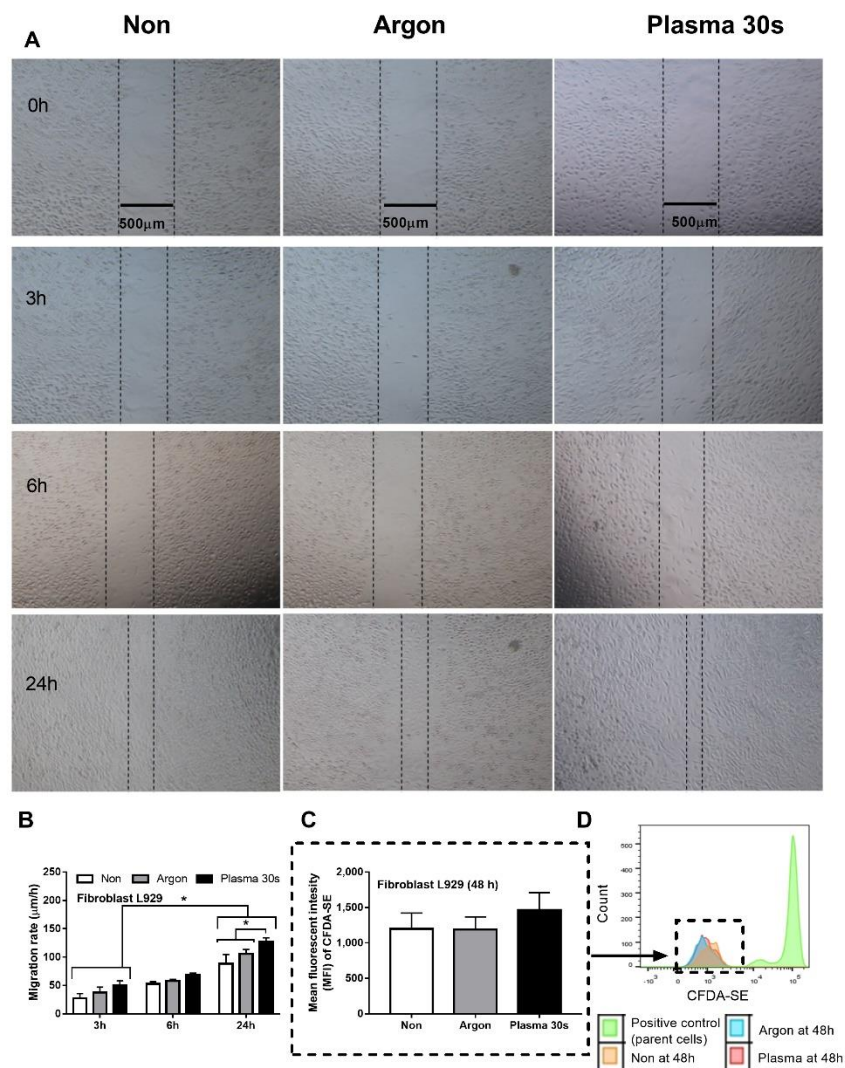


Figure 23. Responses of fibroblasts (L929 cell line) to plasma treatment

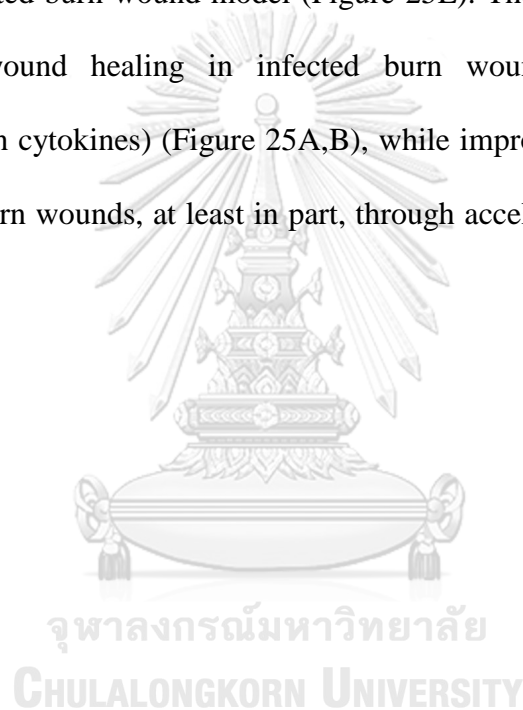
Responses of fibroblasts (L929 cell line) to plasma treatment (30 s), when compared with cells without stimulation (Non) or stimulated with argon gas alone (Argon) as evaluated by fibroblast migration (fibroblast scratch assay) with the representative microscopic photographs

at different time points and scoring comparison (A,B) with fibroblast proliferation, using carboxyfluorescein diacetate succinimidyl ester (CFDA-SE) fluorescent staining and the representative flow cytometry analysis for CFDA-SE (C,D) are demonstrated. Independently triplicated experiments were performed.

3.2. Plasma Flux Promoted Wound Healing in Burn Wounds of Mice, Regardless of Infection

For the in vivo experiments, two mouse models of burn wounds with and without infection by *Staphylococcus aureus*, the most common secondary infection in burn wounds [170], were used. Notably, the susceptibility against plasma flux of *S. aureus* and methicillin resistant *S. aureus* (MRSA) were non-different, as an approximately 30% reduction in colony count (by culture at 24 h) in both strains after a 30 s plasma flux exposure was found (data not shown). As such, the macroscopic wound monitoring at 7 days post-injury demonstrated a higher area of the wound with prominent inflammation (wound rank score, see method) in burn wounds with bacterial infection, compared with the non-infected wound (Figure 24A–C). With the plasma flux treatment, the wound area was smaller with fewer prominent inflammatory signs in the burn wound models either with or without bacterial infection (Figure 24A–C). However, our models were not severe enough to demonstrate the systemic effect of burn wounds or infected burn wounds as indicated by the non-difference in serum cytokines and the gut permeability defect when compared with the control group (Figure 24D–F), which is different from other publications [162, 171]. At 7 days, plasma flux attenuated tissue pro-inflammatory cytokines (TNF- α and IL-6), but not anti-inflammatory IL-10, in the bacterial infected burn wounds but not in the non-infected burn wounds (Figure 25A–C). These data support an anti-inflammatory effect of plasma during the wound healing process.

Despite the bactericidal activity of plasma flux in vitro [172], plasma flux did not reduce bacterial burdens in burn wounds with or without infection (Figure 25D). Moreover, the accumulation of collagen, an indicator of improved wound healing [173], as determined by Masson's trichrome staining, was higher in plasma-treated non-infected burn wounds compared with the control group (Figure 25E). However, the collagen deposition was not different between the plasma treatment and control group in the infected burn wound model (Figure 25E). These data imply that plasma flux promotes wound healing in infected burn wounds partly through anti-inflammation (skin cytokines) (Figure 25A,B), while improving the wound condition in non-infected burn wounds, at least in part, through accelerated collagen deposition (Figure 25E).



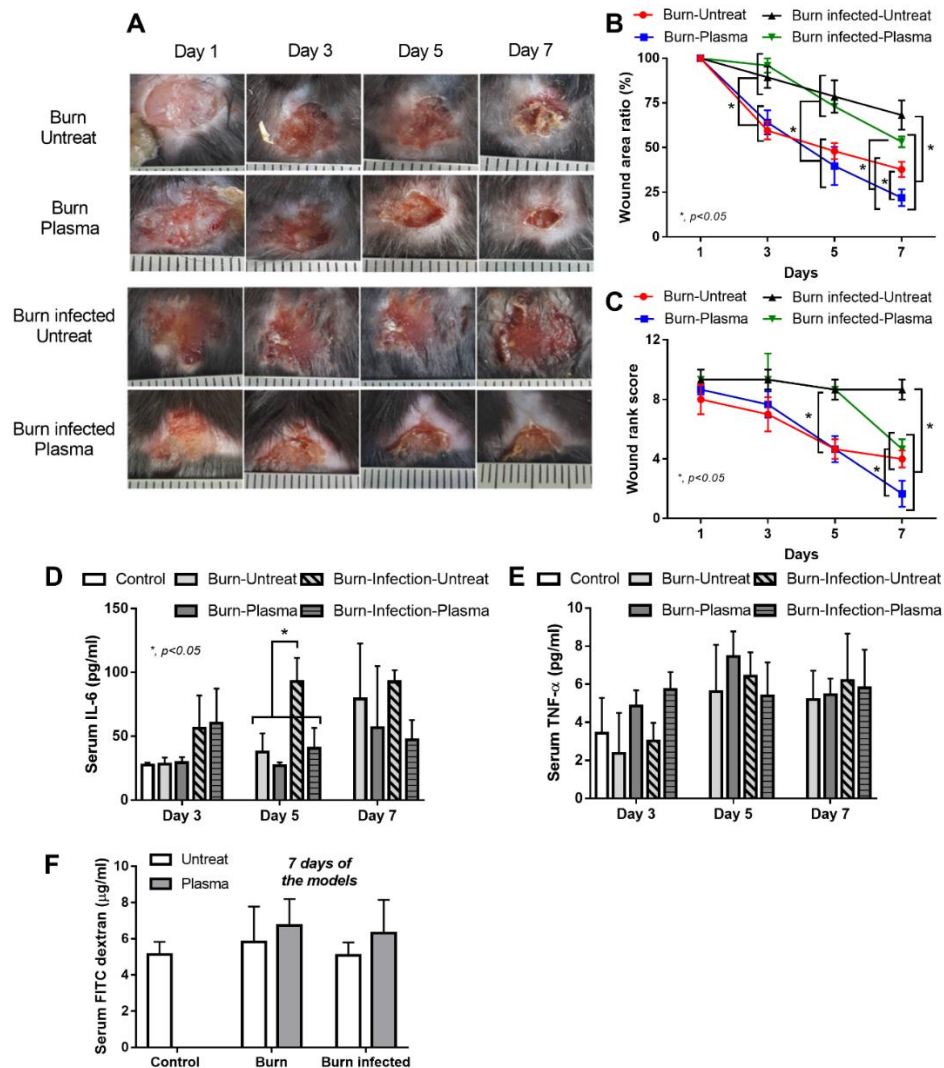


Figure 24. Characteristics of wounds in mouse models with burn injury with or without bacterial infection after treatment by plasma flux

Characteristics of wounds in mouse models with burn injury with or without bacterial infection after treatment by plasma flux (Plasma) or Argon gas alone (Untreat) as determined by wound area and wound rank score (see method) with the representative pictures (A–C), serum cytokines (IL-6 and TNF- α) (D,E) and gut permeability measurement (FITC-dextran assay) (F) (n = 5–7/time-point or group) are demonstrated.

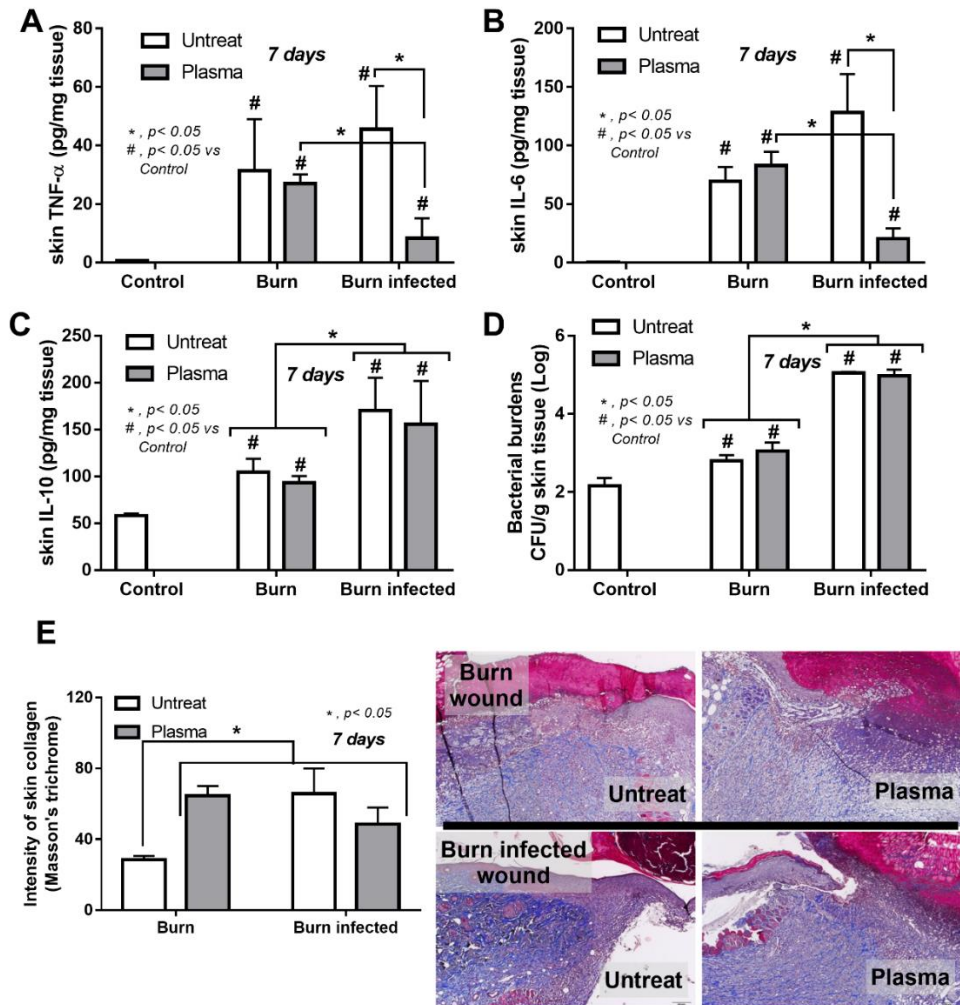


Figure 25. Characteristics of wounds in mouse models with burn injury with or without bacterial infection after treatment by plasma flux

Characteristics of wounds in mouse models with burn injury with or without bacterial infection after treatment by plasma flux (Plasma) or argon gas alone (Untreat) as determined by cytokines from skin tissue (TNF- α , IL-6 and IL-10) (A–C), bacterial burdens (D) and collagen in the lesions with the representative Masson's trichrome stained histological pictures (E) (n = 5–7/time-point or group) are demonstrated.

4. Discussion

Argon-sourced non-thermal plasma induced anti-inflammatory macrophages that promoted wound healing in burn wound models with and without infection.

4.1. Non-Thermal Plasma Flux Induced Anti-Inflammatory Macrophages and Fibroblast Migration

Non-thermal atmospheric pressure plasma might be beneficial in several health topics, including dentistry [174], hematology (coagulation) [175], microbiology (microbial eradication) [176], surgery (wound healing) [177] and oncology [178]. Interestingly, the effects of plasma flux on wound healing (in burns) and angiogenesis (in cancer) are dependent on the conditions and features of non-thermal plasma [179], which may cause varying intensities of bioactive molecules [4]. Indeed, plasma flux increased macrophage ROS, a mediator of several cell activities (apoptosis, proliferation and inflammation), inhibiting NF- κ B [180, 181] in a variety of cells, including epithelial cells (H9C2) [182] and T cells (Jurkat cell) [183]. Here, plasma flux enhanced ROS and reduced NF- κ B abundance in macrophages that might, at least in part, attenuate macrophage inflammatory responses. However, the reduced pro-inflammatory status of plasma-treated macrophages was not associated with the cell energy status, as the abundance of AMPK, a sensor of cell energy [87], was not different from control group.

Because (i) M2 polarized macrophages promote several processes of wound healing [157], (ii) excessive pro-inflammatory macrophages decelerate wound healing [184] and (iii) plasma flux could alter macrophage inflammatory responses [185], several genes are interesting to explore. Without LPS (an inflammatory activation), the macrophages in a neutral state did not produce inflammatory cytokines and plasma flux showed only a slight impact on macrophage as indicated by only the upregulation of *Fizz*, a biomarker of M2 macrophage polarization, but not other genes of M2 macrophages polarization. With LPS stimulation, plasma flux demonstrated a

greater anti-inflammatory effect as indicated by reduced IL-6 production (at 24 h post-LPS), *IL-1 β* downregulation (6 h post-LPS) and *IL-10* upregulation (3 and 6 h post-LPS). However, the expression of M2 associated genes was not different between the plasma flux treatment and the control group, implying that the plasma flux induced anti-inflammatory macrophages but did not profoundly activate M2 macrophage polarization. Nevertheless, the anti-inflammatory state could promote the wound healing process [157] and the wound healing promotion in our mouse models might partly have been due to the anti-inflammatory effect of plasma flux.

Due to the influence of fibroblasts in wound healing processes (fibrin clot lysis and production of extra cellular matrix and collagen [173]), the impact of plasma flux on fibroblasts was tested. Indeed, plasma flux induced fibroblast migration without enhanced fibroblast proliferation. Despite the promotion of both proliferation and migration in human fibroblast-like cells by helium plasma flux [167], our argon-based plasma flux could not induce fibroblast proliferation, possibly due to the difference in plasma sources. It was mentioned that argon-based plasma demonstrates a lower electron temperature than helium-based plasma [186]. Nevertheless, the enhanced fibroblast migration is one of the factors that promotes wound healing [187]. Notably, the non-different proliferation between the plasma-treated group and the control imply a safety of plasma flux on fibroblasts.

4.2. Non-Thermal Plasma Flux Promoted Healing Process of Burn Wounds, Regardless of Infection

Amongst the proposed plasma flux applications, wound healing enhancement is one of the most attractive treatment indications among the potential plasma flux applications [188], owing to the anti-inflammation action on epithelial cells

[38,62,63]. However, other cell types, including immune cells and fibroblasts, are also important in the wound healing process [189]. Unfortunately, data on the effects of plasma flux on non-epithelial cells are still limited. Because burn wounds are associated with a high mortality rate [190], partly through immune dysregulation-induced opportunistic infection [150, 191], burn wound models with and without *S. aureus* infection were used [192]. Although MRSA-infected burn wounds are the most important problem in clinical practice, a standard ATCC strain of *S. aureus*, but not clinical isolated MRSA, was used due to the concern of model reproducibility at this level of proof-of-concept experimentation.

Indeed, the plasma flux treatment attenuated burn wounds with and without infection as evaluated by the wound area and wound inflammatory score. Plasma flux might promote wound healing differently between burn wounds and infected burn wounds. There were no differences in cutaneous inflammatory cytokines between the plasma-treated and control groups in non-infected burn wounds. Plasma, on the other hand, improved wound healing in non-infected burn wounds, probably by increasing fibroblast migration and collagen formation. As such, the ability of fibroblasts to make collagen was enhanced by efficient cell migration [187]. On the other hand, plasma flux lowered pro-inflammatory cytokines in dermal tissue without affecting collagen formation in the infected burn wounds. These data imply promotion of the wound healing process through an anti-inflammatory effect in the infected burn wounds. Due to the activation by pathogen molecules, pro-inflammatory macrophages may be over-activated in infected burn wounds [193], and plasma flux adjusts the balance of the response. However, bacterial burdens in the total dermal tissue of the wound were not different between the plasma-treated and control groups. Perhaps the

bactericidal impact may be restricted primarily to the surface of the lesions due to the limited depth of penetration by plasma flux. A more proper method to determine bacterial burdens on the surface of lesions is needed. Nevertheless, our experiments support the utilization of plasma flux in burn wounds, which could be easily used in real clinical practice. More studies on patients would be interesting.

In conclusion, non-thermal atmospheric pressure argon-based plasma induced anti-inflammatory macrophages, possibly through (i) reduced NF- κ B by ROS and (ii) enhanced fibroblast migration, which were responsible for wound healing promotion in murine burn wound models.



SECTION III

Conclusion

Part I: Although it is well-known that miRNA largely impacts on metabolism of cancer cell but there is still less data about a role of miRNA in immunometabolism. This present study firstly demonstrates that miR-223 manipulates anti-inflammatory macrophages via glycolytic activity inhibition. Our study also proposes a cell therapy in which transplantation of anti-inflammatory macrophages into LPS-induced septic mice likely ameliorates the sepsis outcomes by attenuation of inflammation and organ injury.

Part II: BAM15, with a capacity to hamper both metabolic pathways (glycolysis and mitochondrial activity), attenuates inflammation in macrophages and hepatocytes. Protective effect of BAM15 against sepsis was well observed in the mouse model. Thus, this findings demonstrated the anti-inflammatory therapeutic strategy in sepsis through the interference of cellular metabolism by a mitochondrial uncoupling agent.

Part III: In conclusion, the therapeutic effect of non-thermal plasma flux from Argon was demonstrated by an induction of anti-inflammatory phenotype of macrophages possibly via mitigating NF κ B pathway. Plasma treatment on burn wound mouse models with either non-infection or infection facilitates the healing processes by decreasing excessive inflammation at the local site. More studies for exploring various effect of plasma are interesting.

Limitations

1. Regarding to metabolism, the present studies have some limitations in a lack of the investigation on the lipid pathway, which is one of the important energy-producing mechanisms. Because only a slight alteration in hepatic lipid accumulation has been mentioned in LPS injection model [194], we proposed that our model with 2 hours of LPS stimulation should have the similar results as a previous published paper, which show an insignificant change of lipid accumulation.

2. In some methods for tissue injury evaluation by histology, the measurement of injury remains limited in the accuracy due to the semi-quantitative scale. More quantitative experiments for support the degree of injury that are more sophisticated than the serum biomarkers (AST, ALT or Creatinine), such as the Western blot analysis, should be performed.

3. To mimic sepsis pathogenesis *in vivo*, the LPS injection model has some limitations in which immune responses trigger in only short term (within 6 hours) [195] without mortality rate, different from most of the patients with severe sepsis in the real clinical situations [196].

Further studies

1. The protective effect of cell therapy with miR-223 transfected macrophages should be investigated in sepsis model induced by other models (eg. cecum ligation and puncture). Moreover, more experiments should be performed to explore the appropriate administration time of the adoptive transfer.

2. Because of an impact of BAM15 in all immune cells and organs, more studies are necessary to understand the whole effect of BAM15 on different cell types,

such as neutrophils, B cells or pulmonary cells. Moreover, immunomodulatory effect of BAM15 should be tested in other sepsis models (eg. cecum ligation and puncture).

3. Due to the possible different effects on different cells with the variety of energy intensities, argon-sourced non-thermal plasma can be applied in various purposes. More studies investigate the microbial regulation effect such as microbiome analysis is also interesting.



REFERENCES

1. Zhou, H., et al., *MicroRNA-223 Regulates the Differentiation and Function of Intestinal Dendritic Cells and Macrophages by Targeting C/EBPbeta*. Cell Rep, 2015. **13**(6): p. 1149-1160.
2. Kenwood, B.M., et al., *Identification of a novel mitochondrial uncoupler that does not depolarize the plasma membrane*. Mol Metab, 2014. **3**(2): p. 114-23.
3. Alexopoulos, S.J., et al., *Mitochondrial uncoupler BAM15 reverses diet-induced obesity and insulin resistance in mice*. Nat Commun, 2020. **11**(1): p. 2397.
4. Smolkova, B., et al., *Critical Analysis of Non-Thermal Plasma-Driven Modulation of Immune Cells from Clinical Perspective*. Int J Mol Sci, 2020. **21**(17).
5. Singer, M., et al., *The Third International Consensus Definitions for Sepsis and Septic Shock (Sepsis-3)*. JAMA, 2016. **315**(8): p. 801-10.
6. Doi, K., et al., *Animal models of sepsis and sepsis-induced kidney injury*. J Clin Invest, 2009. **119**(10): p. 2868-78.
7. Rosen, D.A., et al., *Modulation of the sigma-1 receptor-IRE1 pathway is beneficial in preclinical models of inflammation and sepsis*. Sci Transl Med, 2019. **11**(478).
8. Riedemann, N.C. and P.A. Ward, *Anti-inflammatory strategies for the treatment of sepsis*. Expert Opin Biol Ther, 2003. **3**(2): p. 339-50.
9. Hotchkiss, R.S., et al., *Sepsis and septic shock*. Nat Rev Dis Primers, 2016. **2**: p. 16045.
10. Varol, C., A. Mildner, and S. Jung, *Macrophages: development and tissue specialization*. Annu Rev Immunol, 2015. **33**: p. 643-75.
11. Murray, P.J., *Macrophage Polarization*. Annu Rev Physiol, 2017. **79**: p. 541-566.
12. Hamidzadeh, K., et al., *Macrophages and the Recovery from Acute and Chronic Inflammation*. Annu Rev Physiol, 2017. **79**: p. 567-592.
13. Taratummarat, S., et al., *Gold nanoparticles attenuates bacterial sepsis in cecal ligation and puncture mouse model through the induction of M2 macrophage polarization*. BMC Microbiol, 2018. **18**(1): p. 85.
14. Nemeth, K., et al., *Bone marrow stromal cells attenuate sepsis via prostaglandin E(2)-dependent reprogramming of host macrophages to increase their interleukin-10 production*. Nat Med, 2009. **15**(1): p. 42-9.
15. Essandoh, K., et al., *MiRNA-Mediated Macrophage Polarization and its Potential Role in the Regulation of Inflammatory Response*. Shock, 2016. **46**(2): p. 122-31.
16. Gebert, L.F.R. and I.J. MacRae, *Regulation of microRNA function in animals*. Nat Rev Mol Cell Biol, 2019. **20**(1): p. 21-37.
17. Selbach, M., et al., *Widespread changes in protein synthesis induced by microRNAs*. Nature, 2008. **455**(7209): p. 58-63.
18. Wu, X.Q., et al., *Emerging role of microRNAs in regulating macrophage activation and polarization in immune response and inflammation*. Immunology, 2016. **148**(3): p. 237-48.
19. Ying, W., et al., *MicroRNA-223 is a crucial mediator of PPARgamma-regulated alternative macrophage activation*. J Clin Invest, 2015. **125**(11): p. 4149-59.

20. Wang, J.F., et al., *Serum miR-146a and miR-223 as potential new biomarkers for sepsis*. *Biochem Biophys Res Commun*, 2010. **394**(1): p. 184-8.
21. Taganov, K.D., et al., *NF-kappaB-dependent induction of microRNA miR-146, an inhibitor targeted to signaling proteins of innate immune responses*. *Proc Natl Acad Sci U S A*, 2006. **103**(33): p. 12481-6.
22. Gao, M., et al., *Attenuation of Cardiac Dysfunction in Polymicrobial Sepsis by MicroRNA-146a Is Mediated via Targeting of IRAK1 and TRAF6 Expression*. *J Immunol*, 2015. **195**(2): p. 672-82.
23. O'Neill, L.A., R.J. Kishton, and J. Rathmell, *A guide to immunometabolism for immunologists*. *Nat Rev Immunol*, 2016. **16**(9): p. 553-65.
24. Domblides, C., L. Lartigue, and B. Faustin, *Metabolic Stress in the Immune Function of T Cells, Macrophages and Dendritic Cells*. *Cells*, 2018. **7**(7).
25. Thapa, B. and K. Lee, *Metabolic influence on macrophage polarization and pathogenesis*. *BMB Rep*, 2019. **52**(6): p. 360-372.
26. Ouimet, M., et al., *MicroRNA-33-dependent regulation of macrophage metabolism directs immune cell polarization in atherosclerosis*. *J Clin Invest*, 2015. **125**(12): p. 4334-48.
27. Subramaniam, S., et al., *Emergence of MicroRNAs as Key Players in Cancer Cell Metabolism*. *Clin Chem*, 2019. **65**(9): p. 1090-1101.
28. Yang, L., et al., *Overexpression of miR-223 Tips the Balance of Pro- and Anti-hypertrophic Signaling Cascades toward Physiologic Cardiac Hypertrophy*. *J Biol Chem*, 2016. **291**(30): p. 15700-13.
29. Zhao, Z., et al., *Altered expression of microRNA-223 in the plasma of patients with first-episode schizophrenia and its possible relation to neuronal migration-related genes*. *Transl Psychiatry*, 2019. **9**(1): p. 289.
30. Chen, Q., et al., *Inducible microRNA-223 down-regulation promotes TLR-triggered IL-6 and IL-1beta production in macrophages by targeting STAT3*. *PLoS One*, 2012. **7**(8): p. e42971.
31. Vergadi, E., et al., *Akt2 deficiency protects from acute lung injury via alternative macrophage activation and miR-146a induction in mice*. *J Immunol*, 2014. **192**(1): p. 394-406.
32. Leelahavanichkul, A., et al., *Gastrointestinal Leakage Detected by Serum (1->3)-beta-D-Glucan in Mouse Models and a Pilot Study in Patients with Sepsis*. *Shock*, 2016. **46**(5): p. 506-518.
33. Ondee, T., et al., *Lipocalin-2 (Lcn-2) Attenuates Polymicrobial Sepsis with LPS Preconditioning (LPS Tolerance) in FcGR1b Deficient Lupus Mice*. *Cells*, 2019. **8**(9).
34. Ondee, T., et al., *Decreased Protein Kinase C-beta Type II Associated with the Prominent Endotoxin Exhaustion in the Macrophage of FcGR1b-/- Lupus Prone Mice is Revealed by Phosphoproteomic Analysis*. *Int J Mol Sci*, 2019. **20**(6).
35. Kong, X.N., et al., *LPS-induced down-regulation of signal regulatory protein {alpha} contributes to innate immune activation in macrophages*. *J Exp Med*, 2007. **204**(11): p. 2719-31.
36. Vinuesa, E., et al., *Macrophage involvement in the kidney repair phase after ischaemia/reperfusion injury*. *J Pathol*, 2008. **214**(1): p. 104-13.
37. Perske, C., et al., *Loss of inducible nitric oxide synthase expression in the mouse renal cell carcinoma cell line RENCA is mediated by microRNA miR-146a*. *Am*

- J Pathol, 2010. **177**(4): p. 2046-54.
38. Gerasimovskaya, E., et al., *Interplay of macrophages and T cells in the lung vasculature*. Am J Physiol Lung Cell Mol Physiol, 2012. **302**(10): p. L1014-22.
 39. Leelahavanichkul, A., et al., *High-dose ascorbate with low-dose amphotericin B attenuates severity of disease in a model of the reappearance of candidemia during sepsis in the mouse*. Am J Physiol Regul Integr Comp Physiol, 2015. **309**(3): p. R223-34.
 40. Gupta, N., et al., *Intrapulmonary delivery of bone marrow-derived mesenchymal stem cells improves survival and attenuates endotoxin-induced acute lung injury in mice*. J Immunol, 2007. **179**(3): p. 1855-63.
 41. Li, J., et al., *Human umbilical cord mesenchymal stem cells reduce systemic inflammation and attenuate LPS-induced acute lung injury in rats*. J Inflamm (Lond), 2012. **9**(1): p. 33.
 42. Tangtanatakul, P., et al., *Transcriptomic profiling in human mesangial cells using patient-derived lupus autoantibodies identified miR-10a as a potential regulator of IL8*. Sci Rep, 2017. **7**(1): p. 14517.
 43. Thim-Uam, A., et al., *Leaky-gut enhanced lupus progression in the Fc gamma receptor-IIb deficient and pristane-induced mouse models of lupus*. Sci Rep, 2020. **10**(1): p. 777.
 44. Rajaiyah, R., et al., *Dissociation of endotoxin tolerance and differentiation of alternatively activated macrophages*. J Immunol, 2013. **190**(9): p. 4763-72.
 45. Major, J., J.E. Fletcher, and T.A. Hamilton, *IL-4 pretreatment selectively enhances cytokine and chemokine production in lipopolysaccharide-stimulated mouse peritoneal macrophages*. J Immunol, 2002. **168**(5): p. 2456-63.
 46. Koelwyn, G.J., et al., *Regulation of macrophage immunometabolism in atherosclerosis*. Nat Immunol, 2018. **19**(6): p. 526-537.
 47. Li, X.B., J.D. Gu, and Q.H. Zhou, *Review of aerobic glycolysis and its key enzymes - new targets for lung cancer therapy*. Thorac Cancer, 2015. **6**(1): p. 17-24.
 48. Tan, Z., et al., *Pyruvate dehydrogenase kinase 1 participates in macrophage polarization via regulating glucose metabolism*. J Immunol, 2015. **194**(12): p. 6082-9.
 49. Curtale, G., M. Rubino, and M. Locati, *MicroRNAs as Molecular Switches in Macrophage Activation*. Front Immunol, 2019. **10**: p. 799.
 50. Tran, T.H., S. Krishnan, and M.M. Amiji, *MicroRNA-223 Induced Repolarization of Peritoneal Macrophages Using CD44 Targeting Hyaluronic Acid Nanoparticles for Anti-Inflammatory Effects*. PLoS One, 2016. **11**(5): p. e0152024.
 51. Huang, C., et al., *MiR-146a modulates macrophage polarization by inhibiting Notch1 pathway in RAW264.7 macrophages*. Int Immunopharmacol, 2016. **32**: p. 46-54.
 52. Covarrubias, A.J., et al., *Akt-mTORC1 signaling regulates Acly to integrate metabolic input to control of macrophage activation*. Elife, 2016. **5**.
 53. Huang, S.C., et al., *Metabolic Reprogramming Mediated by the mTORC2-IRF4 Signaling Axis Is Essential for Macrophage Alternative Activation*. Immunity, 2016. **45**(4): p. 817-830.
 54. Van den Bossche, J., L.A. O'Neill, and D. Menon, *Macrophage*

- Immunometabolism: Where Are We (Going)?* Trends Immunol, 2017. **38**(6): p. 395-406.
55. Wang, F., et al., *Glycolytic Stimulation Is Not a Requirement for M2 Macrophage Differentiation*. Cell Metab, 2018. **28**(3): p. 463-475 e4.
 56. Corcoran, S.E. and L.A. O'Neill, *HIF1alpha and metabolic reprogramming in inflammation*. J Clin Invest, 2016. **126**(10): p. 3699-3707.
 57. Wang, T., et al., *HIF1alpha-Induced Glycolysis Metabolism Is Essential to the Activation of Inflammatory Macrophages*. Mediators Inflamm, 2017. **2017**: p. 9029327.
 58. Li, C., et al., *HIF1alpha-dependent glycolysis promotes macrophage functional activities in protecting against bacterial and fungal infection*. Sci Rep, 2018. **8**(1): p. 3603.
 59. Nishi, K., et al., *LPS induces hypoxia-inducible factor 1 activation in macrophage-differentiated cells in a reactive oxygen species-dependent manner*. Antioxid Redox Signal, 2008. **10**(5): p. 983-95.
 60. Duvel, K., et al., *Activation of a metabolic gene regulatory network downstream of mTOR complex 1*. Mol Cell, 2010. **39**(2): p. 171-83.
 61. Dweep, H. and N. Gretz, *miRWalk2.0: a comprehensive atlas of microRNA-target interactions*. Nat Methods, 2015. **12**(8): p. 697.
 62. Fleming, B.D., et al., *The generation of macrophages with anti-inflammatory activity in the absence of STAT6 signaling*. J Leukoc Biol, 2015. **98**(3): p. 395-407.
 63. Roy, S., et al., *Interleukin-4 regulates macrophage interleukin-12 protein synthesis through a c-fos mediated mechanism*. Surgery, 2000. **128**(2): p. 219-24.
 64. D'Andrea, A., et al., *Stimulatory and inhibitory effects of interleukin (IL)-4 and IL-13 on the production of cytokines by human peripheral blood mononuclear cells: priming for IL-12 and tumor necrosis factor alpha production*. J Exp Med, 1995. **181**(2): p. 537-46.
 65. Brown, J.M., L. Recht, and S. Strober, *The Promise of Targeting Macrophages in Cancer Therapy*. Clin Cancer Res, 2017. **23**(13): p. 3241-3250.
 66. Kowal, J., M. Kornete, and J.A. Joyce, *Re-education of macrophages as a therapeutic strategy in cancer*. Immunotherapy, 2019. **11**(8): p. 677-689.
 67. Mosser, D.M., K. Hamidzadeh, and R. Goncalves, *Macrophages and the maintenance of homeostasis*. Cell Mol Immunol, 2020.
 68. Dang, C.P. and A. Leelahavanichkul, *Over-expression of miR-223 induces M2 macrophage through glycolysis alteration and attenuates LPS-induced sepsis mouse model, the cell-based therapy in sepsis*. PLoS One, 2020. **15**(7): p. e0236038.
 69. Palsson-McDermott, E.M. and L.A.J. O'Neill, *Targeting immunometabolism as an anti-inflammatory strategy*. Cell Research, 2020. **30**(4): p. 300-314.
 70. Gong, Y., et al., *Blockage of glycolysis by targeting PFKFB3 alleviates sepsis-related acute lung injury via suppressing inflammation and apoptosis of alveolar epithelial cells*. Biochem Biophys Res Commun, 2017. **491**(2): p. 522-529.
 71. Ramond, E., et al., *Pivotal Role of Mitochondria in Macrophage Response to Bacterial Pathogens*. Front Immunol, 2019. **10**: p. 2461.
 72. Dreschers, S., et al., *Impaired cellular energy metabolism in cord blood*

- macrophages contributes to abortive response toward inflammatory threats. Nat Commun*, 2019. **10**(1): p. 1685.
73. Lee, J.H., et al., *Intracellular ATP in balance of pro- and anti-inflammatory cytokines in adipose tissue with and without tissue expansion. Int J Obes (Lond)*, 2017. **41**(4): p. 645-651.
 74. Demine, S., P. Renard, and T. Arnould, *Mitochondrial Uncoupling: A Key Controller of Biological Processes in Physiology and Diseases. Cells*, 2019. **8**(8).
 75. Cadenas, S., *Mitochondrial uncoupling, ROS generation and cardioprotection. Biochim Biophys Acta Bioenerg*, 2018. **1859**(9): p. 940-950.
 76. Brennan, J.P., et al., *FCCP is cardioprotective at concentrations that cause mitochondrial oxidation without detectable depolarisation. Cardiovasc Res*, 2006. **72**(2): p. 322-30.
 77. Grasmick, K.A., et al., *Uncoupling of the Electron Transport Chain Compromises Mitochondrial Oxidative Phosphorylation and Exacerbates Stroke Outcomes. J Neuroinfect Dis*, 2018. **9**(4).
 78. Sugiyama, Y., et al., *Emodin, as a mitochondrial uncoupler, induces strong decreases in adenosine triphosphate (ATP) levels and proliferation of B16F10 cells, owing to their poor glycolytic reserve. Genes to Cells*, 2019. **24**(8): p. 569-584.
 79. Luo, Y., J.D. Bond, and V.M. Ingram, *Compromised mitochondrial function leads to increased cytosolic calcium and to activation of MAP kinases. Proc Natl Acad Sci U S A*, 1997. **94**(18): p. 9705-10.
 80. Nicholls, D.G., *The physiological regulation of uncoupling proteins. Biochim Biophys Acta*, 2006. **1757**(5-6): p. 459-66.
 81. Kizaki, T., et al., *Uncoupling protein 2 plays an important role in nitric oxide production of lipopolysaccharide-stimulated macrophages. Proc Natl Acad Sci U S A*, 2002. **99**(14): p. 9392-7.
 82. Haines, B. and P.A. Li, *Overexpression of mitochondrial uncoupling protein 2 inhibits inflammatory cytokines and activates cell survival factors after cerebral ischemia. PLoS One*, 2012. **7**(2): p. e31739.
 83. Bai, Y., et al., *Persistent nuclear factor-kappa B activation in Ucp2^{-/-} mice leads to enhanced nitric oxide and inflammatory cytokine production. J Biol Chem*, 2005. **280**(19): p. 19062-9.
 84. Axelrod, C.L., et al., *BAM15-mediated mitochondrial uncoupling protects against obesity and improves glycemic control. EMBO Mol Med*, 2020. **12**(7): p. e12088.
 85. Yan, J., S. Li, and S. Li, *The role of the liver in sepsis. Int Rev Immunol*, 2014. **33**(6): p. 498-510.
 86. Panpetch, W., et al., *Additional Candida albicans administration enhances the severity of dextran sulfate solution induced colitis mouse model through leaky gut-enhanced systemic inflammation and gut-dysbiosis but attenuated by Lactobacillus rhamnosus L34. Gut Microbes*, 2020. **11**(3): p. 465-480.
 87. Jaroonwichawan, T., et al., *Dysregulation of Lipid Metabolism in Macrophages Is Responsible for Severe Endotoxin Tolerance in FcγRIIB-Deficient Lupus Mice. Front Immunol*, 2020. **11**: p. 959.
 88. Vu, C.T.B., et al., *Alteration of macrophage immune phenotype in a murine*

- sepsis model is associated with susceptibility to secondary fungal infection.* Asian Pac J Allergy Immunol, 2019.
89. Vu, C.T.B., et al., *Blockade Of PD-1 Attenuated Postsepsis Aspergillosis Via The Activation of IFN-gamma and The Dampening of IL-10.* Shock, 2020. **53**(4): p. 514-524.
 90. Song, P., et al., *Hepatic recruitment of CD11b+Ly6C+ inflammatory monocytes promotes hepatic ischemia/reperfusion injury.* Int J Mol Med, 2018. **41**(2): p. 935-945.
 91. Mikula, M., et al., *Obesity increases histone H3 lysine 9 and 18 acetylation at Tnfa and Ccl2 genes in mouse liver.* Int J Mol Med, 2014. **34**(6): p. 1647-54.
 92. Zhang, N., et al., *An inducible nitric oxide synthase-luciferase reporter system for in vivo testing of anti-inflammatory compounds in transgenic mice.* J Immunol, 2003. **170**(12): p. 6307-19.
 93. Panpetch, W., et al., *Oral Candida administration in a Clostridium difficile mouse model worsens disease severity but is attenuated by Bifidobacterium.* PLoS One, 2019. **14**(1): p. e0210798.
 94. Issara-Amphorn, J., et al., *Syk Inhibitor Attenuates Polymicrobial Sepsis in FcγRIIb-Deficient Lupus Mouse Model, the Impact of Lupus Characteristics in Sepsis.* J Innate Immun, 2020. **12**(6): p. 461-479.
 95. Panpetch, W., et al., *Candida Administration Worsens Cecal Ligation and Puncture-Induced Sepsis in Obese Mice Through Gut Dysbiosis Enhanced Systemic Inflammation, Impact of Pathogen-Associated Molecules From Gut Translocation and Saturated Fatty Acid.* Front Immunol, 2020. **11**: p. 561652.
 96. Gray, L.R., S.C. Tompkins, and E.B. Taylor, *Regulation of pyruvate metabolism and human disease.* Cell Mol Life Sci, 2014. **71**(14): p. 2577-604.
 97. Amornphimoltham, P., et al., *Gut Leakage of Fungal-Derived Inflammatory Mediators: Part of a Gut-Liver-Kidney Axis in Bacterial Sepsis.* Dig Dis Sci, 2019. **64**(9): p. 2416-2428.
 98. Leelahavanichkul, A., et al., *Serum miRNA-122 in acute liver injury induced by kidney injury and sepsis in CD-1 mouse models.* Hepatol Res, 2015. **45**(13): p. 1341-52.
 99. Soto-Herederó, G., et al., *Glycolysis - a key player in the inflammatory response.* FEBS J, 2020. **287**(16): p. 3350-3369.
 100. Rogatzki, M.J., et al., *Lactate is always the end product of glycolysis.* Frontiers in Neuroscience, 2015. **9**.
 101. Walesky, C.M., et al., *Functional compensation precedes recovery of tissue mass following acute liver injury.* Nat Commun, 2020. **11**(1): p. 5785.
 102. Nishikawa, T., et al., *A switch in the source of ATP production and a loss in capacity to perform glycolysis are hallmarks of hepatocyte failure in advance liver disease.* J Hepatol, 2014. **60**(6): p. 1203-11.
 103. Sitia, G., et al., *Kupffer cells hasten resolution of liver immunopathology in mouse models of viral hepatitis.* PLoS Pathog, 2011. **7**(6): p. e1002061.
 104. Vollmar, B. and M.D. Menger, *The hepatic microcirculation: mechanistic contributions and therapeutic targets in liver injury and repair.* Physiol Rev, 2009. **89**(4): p. 1269-339.
 105. Garcia, D. and R.J. Shaw, *AMPK: Mechanisms of Cellular Energy Sensing and Restoration of Metabolic Balance.* Mol Cell, 2017. **66**(6): p. 789-800.

106. Carling, D., et al., *AMP-activated protein kinase: new regulation, new roles?* Biochem J, 2012. **445**(1): p. 11-27.
107. Busiello, R.A., S. Savarese, and A. Lombardi, *Mitochondrial uncoupling proteins and energy metabolism*. Front Physiol, 2015. **6**: p. 36.
108. Holmuhamedov, E.L., et al., *Mitochondrial ATP-sensitive K⁺ channels modulate cardiac mitochondrial function*. Am J Physiol, 1998. **275**(5): p. H1567-76.
109. Emre, Y., et al., *Role of uncoupling protein UCP2 in cell-mediated immunity: how macrophage-mediated insulinitis is accelerated in a model of autoimmune diabetes*. Proc Natl Acad Sci U S A, 2007. **104**(48): p. 19085-90.
110. Feng, J., et al., *Emerging roles and the regulation of aerobic glycolysis in hepatocellular carcinoma*. J Exp Clin Cancer Res, 2020. **39**(1): p. 126.
111. Tang, M., et al., *BAM15 attenuates transportation-induced apoptosis in iPS-differentiated retinal tissue*. Stem Cell Res Ther, 2019. **10**(1): p. 64.
112. Ishisaka, A., et al., *Mitochondrial dysfunction leads to deconjugation of quercetin glucuronides in inflammatory macrophages*. PLoS One, 2013. **8**(11): p. e80843.
113. Nomura, J., et al., *Intracellular ATP Decrease Mediates NLRP3 Inflammasome Activation upon Nigericin and Crystal Stimulation*. J Immunol, 2015. **195**(12): p. 5718-24.
114. McCall, C.E., et al., *Pyruvate dehydrogenase complex stimulation promotes immunometabolic homeostasis and sepsis survival*. JCI Insight, 2018. **3**(15).
115. Stacpoole, P.W., et al., *A controlled clinical trial of dichloroacetate for treatment of lactic acidosis in adults. The Dichloroacetate-Lactic Acidosis Study Group*. N Engl J Med, 1992. **327**(22): p. 1564-9.
116. Grondman, I., et al., *Frontline Science: Endotoxin-induced immunotolerance is associated with loss of monocyte metabolic plasticity and reduction of oxidative burst*. J Leukoc Biol, 2019. **106**(1): p. 11-25.
117. Ondee, T., et al., *Fc Gamma Receptor IIB Deficient Mice: A Lupus Model with Increased Endotoxin Tolerance-Related Sepsis Susceptibility*. Shock, 2017. **47**(6): p. 743-752.
118. Alasadi, A., et al., *Effect of mitochondrial uncouplers niclosamide ethanolamine (NEN) and oxyclozanide on hepatic metastasis of colon cancer*. Cell Death Dis, 2018. **9**(2): p. 215.
119. De Simone, R., et al., *The mitochondrial uncoupling protein-2 is a master regulator of both M1 and M2 microglial responses*. J Neurochem, 2015. **135**(1): p. 147-56.
120. Basu Ball, W., et al., *Uncoupling protein 2 negatively regulates mitochondrial reactive oxygen species generation and induces phosphatase-mediated anti-inflammatory response in experimental visceral leishmaniasis*. J Immunol, 2011. **187**(3): p. 1322-32.
121. Doi, K., *Role of kidney injury in sepsis*. J Intensive Care, 2016. **4**: p. 17.
122. Poston, J.T. and J.L. Koyner, *Sepsis associated acute kidney injury*. BMJ, 2019. **364**: p. k4891.
123. Schieber, A.M.P. and J.S. Ayres, *Thermoregulation as a disease tolerance defense strategy*. Pathogens and Disease, 2016. **74**(9).
124. Sag, D., et al., *Adenosine 5'-monophosphate-activated protein kinase promotes*

- macrophage polarization to an anti-inflammatory functional phenotype. J Immunol*, 2008. **181**(12): p. 8633-41.
125. Tai, Y., et al., *Mitochondrial uncoupler BAM15 inhibits artery constriction and potently activates AMPK in vascular smooth muscle cells. Acta Pharm Sin B*, 2018. **8**(6): p. 909-918.
 126. Escobar, D.A., et al., *Adenosine monophosphate-activated protein kinase activation protects against sepsis-induced organ injury and inflammation. J Surg Res*, 2015. **194**(1): p. 262-72.
 127. Zhang, M., et al., *Protective benefits of AMP-activated protein kinase in hepatic ischemia-reperfusion injury. Am J Transl Res*, 2017. **9**(3): p. 823-829.
 128. Zhao, W., et al., *SIRT3 Protects Against Acute Kidney Injury via AMPK/mTOR-Regulated Autophagy. Front Physiol*, 2018. **9**: p. 1526.
 129. Tong, X., K.A. Smith, and J.C. Pelling, *Apigenin, a chemopreventive bioflavonoid, induces AMP-activated protein kinase activation in human keratinocytes. Mol Carcinog*, 2012. **51**(3): p. 268-79.
 130. Zhao, X., et al., *Activation of AMPK attenuates neutrophil proinflammatory activity and decreases the severity of acute lung injury. Am J Physiol Lung Cell Mol Physiol*, 2008. **295**(3): p. L497-504.
 131. Yun, H., et al., *AMP-activated protein kinase mediates the antioxidant effects of resveratrol through regulation of the transcription factor FoxO1. Febs Journal*, 2014. **281**(19): p. 4421-4438.
 132. Alba, G., et al., *Stimulators of AMP-activated protein kinase inhibit the respiratory burst in human neutrophils. FEBS Lett*, 2004. **573**(1-3): p. 219-25.
 133. Ido, Y., D. Carling, and N. Ruderman, *Hyperglycemia-induced apoptosis in human umbilical vein endothelial cells - Inhibition by the AMP-activated protein kinase activation. Diabetes*, 2002. **51**(1): p. 159-167.
 134. Chung, K.W., et al., *The critical role played by endotoxin-induced liver autophagy in the maintenance of lipid metabolism during sepsis. Autophagy*, 2017. **13**(7): p. 1113-1129.
 135. Izadjoo, M., et al., *Medical applications of cold atmospheric plasma: state of the science. J Wound Care*, 2018. **27**(Sup9): p. S4-S10.
 136. Bernhardt, T., et al., *Plasma Medicine: Applications of Cold Atmospheric Pressure Plasma in Dermatology. Oxid Med Cell Longev*, 2019. **2019**: p. 3873928.
 137. Rehman, M.U., et al., *Comparison of free radicals formation induced by cold atmospheric plasma, ultrasound, and ionizing radiation. Arch Biochem Biophys*, 2016. **605**: p. 19-25.
 138. Davies, K.J., *The broad spectrum of responses to oxidants in proliferating cells: a new paradigm for oxidative stress. IUBMB Life*, 1999. **48**(1): p. 41-7.
 139. Jacobson, M.D., *Reactive oxygen species and programmed cell death. Trends Biochem Sci*, 1996. **21**(3): p. 83-6.
 140. Fridman, A.A., *Plasma chemistry*. 2008, Cambridge ; New York: Cambridge University Press. xlii, 978 p.
 141. Kalghatgi, S., et al., *Effects of non-thermal plasma on mammalian cells. PLoS One*, 2011. **6**(1): p. e16270.
 142. Zhou, Y., et al., *Free radical stress in chronic lymphocytic leukemia cells and its role in cellular sensitivity to ROS-generating anticancer agents. Blood*, 2003.

- 101(10):** p. 4098-104.
143. Dunnill, C., et al., *Reactive oxygen species (ROS) and wound healing: the functional role of ROS and emerging ROS-modulating technologies for augmentation of the healing process*. *Int Wound J*, 2017. **14(1)**: p. 89-96.
 144. Trachootham, D., J. Alexandre, and P. Huang, *Targeting cancer cells by ROS-mediated mechanisms: a radical therapeutic approach?* *Nat Rev Drug Discov*, 2009. **8(7)**: p. 579-91.
 145. Kvam, E., et al., *Nonthermal atmospheric plasma rapidly disinfects multidrug-resistant microbes by inducing cell surface damage*. *Antimicrob Agents Chemother*, 2012. **56(4)**: p. 2028-36.
 146. Schmidt, A. and S. Bekeschus, *Redox for Repair: Cold Physical Plasmas and Nrf2 Signaling Promoting Wound Healing*. *Antioxidants (Basel)*, 2018. **7(10)**.
 147. Haertel, B., et al., *Non-thermal atmospheric-pressure plasma possible application in wound healing*. *Biomol Ther (Seoul)*, 2014. **22(6)**: p. 477-90.
 148. Fathollah, S., et al., *Investigation on the effects of the atmospheric pressure plasma on wound healing in diabetic rats*. *Sci Rep*, 2016. **6**: p. 19144.
 149. Duchesne, C., et al., *Cold atmospheric plasma modulates endothelial nitric oxide synthase signalling and enhances burn wound neovascularisation*. *J Pathol*, 2019. **249(3)**: p. 368-380.
 150. Jeschke, M.G., et al., *Burn injury*. *Nature Reviews Disease Primers*, 2020. **6(1)**.
 151. Smolle, C., et al., *Recent trends in burn epidemiology worldwide: A systematic review*. *Burns*, 2017. **43(2)**: p. 249-257.
 152. Lachiewicz, A.M., et al., *Bacterial Infections After Burn Injuries: Impact of Multidrug Resistance*. *Clin Infect Dis*, 2017. **65(12)**: p. 2130-2136.
 153. Dai, T., et al., *Ultraviolet C irradiation: an alternative antimicrobial approach to localized infections?* *Expert Rev Anti Infect Ther*, 2012. **10(2)**: p. 185-95.
 154. Nicol, M.J., et al., *Antibacterial effects of low-temperature plasma generated by atmospheric-pressure plasma jet are mediated by reactive oxygen species*. *Sci Rep*, 2020. **10(1)**: p. 3066.
 155. Schmidt, A., et al., *A cold plasma jet accelerates wound healing in a murine model of full-thickness skin wounds*. *Exp Dermatol*, 2017. **26(2)**: p. 156-162.
 156. Kaushik, N.K., et al., *Preventing the Solid Cancer Progression via Release of Anticancer-Cytokines in Co-Culture with Cold Plasma-Stimulated Macrophages*. *Cancers (Basel)*, 2019. **11(6)**.
 157. Krzyszczyk, P., et al., *The Role of Macrophages in Acute and Chronic Wound Healing and Interventions to Promote Pro-wound Healing Phenotypes*. *Front Physiol*, 2018. **9**: p. 419.
 158. Cai, E.Z., et al., *Creation of consistent burn wounds: a rat model*. *Arch Plast Surg*, 2014. **41(4)**: p. 317-24.
 159. Kim, H.K., D. Missiakas, and O. Schneewind, *Mouse models for infectious diseases caused by Staphylococcus aureus*. *J Immunol Methods*, 2014. **410**: p. 88-99.
 160. Lu, X., et al., *Reactive species in non-equilibrium atmospheric-pressure plasmas: Generation, transport, and biological effects*. *Physics Reports-Review Section of Physics Letters*, 2016. **630**: p. 1-84.
 161. Jang, S.I., et al., *Effect of electrospun non-woven mats of dibutyril chitin/poly(lactic acid) blends on wound healing in hairless mice*. *Molecules*,

2012. **17**(3): p. 2992-3007.
162. Baron, P., et al., *Gut failure and translocation following burn and sepsis*. J Surg Res, 1994. **57**(1): p. 197-204.
163. Earley, Z.M., et al., *Burn Injury Alters the Intestinal Microbiome and Increases Gut Permeability and Bacterial Translocation*. PLoS One, 2015. **10**(7): p. e0129996.
164. Visitchanakun, P., et al., *Gut leakage enhances sepsis susceptibility in iron-overloaded beta-thalassemia mice through macrophage hyperinflammatory responses*. Am J Physiol Gastrointest Liver Physiol, 2020. **318**(5): p. G966-G979.
165. Panpetch, W., et al., *Candida Administration Worsens Uremia-Induced Gut Leakage in Bilateral Nephrectomy Mice, an Impact of Gut Fungi and Organismal Molecules in Uremia*. mSystems, 2021. **6**(1).
166. Kanazawa, S., et al., *bFGF regulates PI3-kinase-Rac1-JNK pathway and promotes fibroblast migration in wound healing*. PLoS One, 2010. **5**(8): p. e12228.
167. Brun, P., et al., *Helium generated cold plasma finely regulates activation of human fibroblast-like primary cells*. PLoS One, 2014. **9**(8): p. e104397.
168. Udornpornpitak, K., et al., *Lipopolysaccharide-Enhanced Responses against Aryl Hydrocarbon Receptor in FcγRIIb-Deficient Macrophages, a Profound Impact of an Environmental Toxin on a Lupus-Like Mouse Model*. 2021. **22**(8): p. 4199.
169. Issara-Amphorn, J., et al., *The Synergy of Endotoxin and (1→3)-beta-D-Glucan, from Gut Translocation, Worsens Sepsis Severity in a Lupus Model of Fcγ Receptor IIb-Deficient Mice*. J Innate Immun, 2018. **10**(3): p. 189-201.
170. Church, D., et al., *Burn wound infections*. Clin Microbiol Rev, 2006. **19**(2): p. 403-34.
171. Herndon, D.N. and S.T. Zeigler, *Bacterial translocation after thermal injury*. Crit Care Med, 1993. **21**(2 Suppl): p. S50-4.
172. Bae, S., et al., *In vitro antibacterial effects of non-thermal atmospheric plasma irradiation on Staphylococcus pseudintermedius and Pseudomonas aeruginosa*. Pol J Vet Sci, 2020. **23**(1): p. 13-19.
173. Bainbridge, P., *Wound healing and the role of fibroblasts*. J Wound Care, 2013. **22**(8): p. 407-8, 410-12.
174. Sung, S.J., et al., *Sterilization effect of atmospheric pressure non-thermal air plasma on dental instruments*. J Adv Prosthodont, 2013. **5**(1): p. 2-8.
175. Kalghatgi, S.U., et al., *Mechanism of blood coagulation by nonthermal atmospheric pressure dielectric barrier discharge plasma*. Ieee Transactions on Plasma Science, 2007. **35**(5): p. 1559-1566.
176. Gilmore, B.F., et al., *Cold Plasmas for Biofilm Control: Opportunities and Challenges*. Trends Biotechnol, 2018. **36**(6): p. 627-638.
177. Kubinova, S., et al., *Non-thermal air plasma promotes the healing of acute skin wounds in rats*. Sci Rep, 2017. **7**: p. 45183.
178. Wolff, C.M., et al., *Combination Treatment with Cold Physical Plasma and Pulsed Electric Fields Augments ROS Production and Cytotoxicity in Lymphoma*. Cancers (Basel), 2020. **12**(4).

179. Boeckmann, L., et al., *Cold Atmospheric Pressure Plasma in Wound Healing and Cancer Treatment*. Applied Sciences-Basel, 2020. **10**(19).
180. Gloire, G., S. Legrand-Poels, and J. Piette, *NF-kappaB activation by reactive oxygen species: fifteen years later*. *Biochem Pharmacol*, 2006. **72**(11): p. 1493-505.
181. Morgan, M.J. and Z.G. Liu, *Crosstalk of reactive oxygen species and NF-kappaB signaling*. *Cell Res*, 2011. **21**(1): p. 103-15.
182. Levrard, S., et al., *Peroxyntirite is a potent inhibitor of NF-kappaB activation triggered by inflammatory stimuli in cardiac and endothelial cell lines*. *J Biol Chem*, 2005. **280**(41): p. 34878-87.
183. Ogino, T., et al., *Oxidative modification of IkappaB by monochloramine inhibits tumor necrosis factor alpha-induced NF-kappaB activation*. *Biochim Biophys Acta*, 2005. **1746**(2): p. 135-42.
184. Sindrilaru, A., et al., *An unrestrained proinflammatory M1 macrophage population induced by iron impairs wound healing in humans and mice*. *J Clin Invest*, 2011. **121**(3): p. 985-97.
185. Bekeschus, S., et al., *Plasma-treated medium tunes the inflammatory profile in murine bone marrow-derived macrophages*. *Clinical Plasma Medicine*, 2018. **11**: p. 1-9.
186. Jonkers, J., et al., *On the differences between ionizing helium and argon plasmas at atmospheric pressure*. 2002. **12**(1): p. 30.
187. Addis, R., et al., *Fibroblast Proliferation and Migration in Wound Healing by Phytochemicals: Evidence for a Novel Synergic Outcome*. *Int J Med Sci*, 2020. **17**(8): p. 1030-1042.
188. Weltmann, K.D. and T. von Woedtke, *Plasma medicine-current state of research and medical application*. *Plasma Physics and Controlled Fusion*, 2017. **59**(1).
189. Arturson, G., *Pathophysiology of the burn wound*. *Ann Chir Gynaecol*, 1980. **69**(5): p. 178-90.
190. Gomez, R., et al., *Causes of mortality by autopsy findings of combat casualties and civilian patients admitted to a burn unit*. *J Am Coll Surg*, 2009. **208**(3): p. 348-54.
191. Ballard, J., et al., *Positive fungal cultures in burn patients: a multicenter review*. *J Burn Care Res*, 2008. **29**(1): p. 213-21.
192. Abdullahi, A., S. Amini-Nik, and M.G. Jeschke, *Animal models in burn research*. *Cell Mol Life Sci*, 2014. **71**(17): p. 3241-55.
193. van de Goot, F., et al., *Acute Inflammation is Persistent Locally in Burn Wounds: A Pivotal Role for Complement and C-Reactive Protein*. *Journal of Burn Care & Research*, 2009. **30**(2): p. 274-280.
194. Lee, M.S., et al., *meso-Dihydroguaiaretic acid inhibits hepatic lipid accumulation by activating AMP-activated protein kinase in human HepG2 cells*. *Biol Pharm Bull*, 2011. **34**(10): p. 1628-30.
195. Korneev, K.V., *[Mouse Models of Sepsis and Septic Shock]*. *Mol Biol (Mosk)*, 2019. **53**(5): p. 799-814.
196. Thomas, R.C., et al., *Exploring LPS-induced sepsis in rats and mice as a model to study potential protective effects of the nociceptin/orphanin FQ system*. *Peptides*, 2014. **61**: p. 56-60.



จุฬาลงกรณ์มหาวิทยาลัย
CHULALONGKORN UNIVERSITY



จุฬาลงกรณ์มหาวิทยาลัย
CHULALONGKORN UNIVERSITY

VITA

NAME DANG PHI CONG
DATE OF BIRTH 13 Aug 1993
PLACE OF BIRTH Vietnam
INSTITUTIONS ATTENDED Chulalongkorn university
HOME ADDRESS CU-iHouse, 268, Chula soi 9, Pathumwan, Wangmai, Bangkok, 10330
AWARD RECEIVED The 100th Anniversary Chulalongkorn University for Doctoral Scholarship

